Issue No. 35
March 2007

IGACtivities Newsletter

of the International Global Atmospheric Chemistry Project

In this Issue:

A Note from the IGAC Co-chairs: Phil Rasch and Kathy Law

This newsletter provides an introduction to satellite-based instruments in use for assessing tropospheric constituent distributions, and it highlights how these satellite observations have contributed to rapid developments in our understanding of tropospheric chemistry. Examples include the quantification of emissions, improved estimates of radiative forcing, observation of long-range transport on regional to continental scales, and air quality characterization. Increasing concern over changes taking place in the Earth system due to human activities makes it critical that we understand how these data can be used to understand the Earth system. We hope that this summary can provide a glimpse into the many available opportunities for exploiting these data.

The use of satellite remote sensing, especially for tropospheric applications, is a fairly new field. Like the very first picture of Earth taken from space, the images from these instruments provide, at a glance, an unprecedented and inspiring world-view. They are both illustrative of specific events (e.g. pollution sources, fires, and transport pathways) and useful for quantitative studies (e.g. inversions for source emission estimates). However, for quantitative applications, there is a significant learning curve to using the data with appreciation of its strengths and limitations, especially when trying to compare or integrate the data with models or in-situ measurements. We have only recently learned how satellite data contributes to a cross-scale integrated observing capability, yet such integration is critical: Whilst satellite data provides much-needed information about the global distribution and temporal evolution of atmospheric constituents, other types of data are required to build a more complete picture about processes influencing composition changes and interactions with climate and biogeochemistry. Routine vertical profile data (e.g. from aircraft) and ground-based data are thus also an invaluable source of information.

While this is a very exciting time for our community, there is a very real possibility that we could be left without, or with a significantly reduced number of, satellite data products in a few years' time. Many of the current missions are maturing or are already past their design lifetimes. Others have just been launched, but given the long lead time for new mission development and the dearth of new missions in the pipeline, there is not a comprehensive plan for maintaining capability for observations of atmospheric composition. Unfortunately, a lack of funding has inhibited the development of new instruments for the near future. To quote the recent NRC Decadal Survey recommendation: "The U.S. government, working in concert with the private sector, academe, the public, and its international partners, should renew its investment in Earth observing systems and restore its leadership in Earth science and applications." The September, 2004 report of IGOS Integrated Global Atmospheric Chemistry Observation System (IGACO) similarly emphasizes the need for continuous data sets from both ground- and satellite-based instruments. Given the rapidly changing atmospheric composition, this is a critical time to support that consensus, and we at IGAC urge the national funding agencies to consider the carefully-formulated recommendations of such committees.

Finally, we note that Kathy Law has taken over from Sandro Fuzzi as the European co-Chair of IGAC from January 2007. Kathy obtained her PhD in Atmospheric Chemistry at the University of Cambridge, UK, where she worked as a research scientist up to 2002 before taking up a position at CNRS as Director of Research at the Service d'Aéronomie/IPSL (Institut Pierre Simon Laplace), UPMC (Université Pierre et Marie Curie), Paris, France. Her current research interests include long-range transport of pollutants (co-lead of the IGAC POLARCAT task) and the West African monsoon (as part of the IGAC AMMA task).

GLOBAL CHANGE IGBP
A Core Project of the Internations Geosphere-Biosphere Programme

CACGP
In Cooperation with IAMAS Commission on Atmospheric Chemistry and Global Pollution

Satellite Observations of Tropospheric Trace Gases and Aerosols

An Emerging and Compelling Component of the Science of Earth Observation and Global Change

Introduction

Contributed by **Randall Martin** (Randall.Martin@dal.ca) *Sir James Dunn Building, Room 129, Department of Physics and Atmospheric Science, Dalhousie University, Halifax, NS, B3H 3J5, Canada, and Harvard-Smithsonian Center for Astrophysics, and* **John P. Burrows** (burrows@iup.physik.uni-bremen.de) *Institute of Environmental Physics and Remote Sensing IUP/IFE University of Bremen - FB1 Postfach 330440 28334 Bremen Germany*

The last fifteen years have been of pivotal significance for the emerging science of Earth Observation and in particular for the determination from space of key atmospheric trace constituents in the troposphere and boundary layer. Although the stratosphere, mesosphere, and thermosphere had been previously probed successfully from space, it had been questioned whether valuable information about the amounts and distributions of tropospheric trace gases and aerosol could be retrieved. For the remote sensing community, accurate information about the lower troposphere had some similarities with the search for the holy grail. However in the last decade a suite of both passive and active remote sounding instrumentation, capable of providing information on tropospheric constituents, has been successfully deployed in space.

These new observations are contributing to rapid developments in scientific understanding of the global complexities of and feedback within tropospheric chemistry, especially the transport of pollution to and the emissions from remote regions that are otherwise rarely observed. Noteworthy applications include quantification of emissions, improved estimates of radiative forcing, observation of long-range transport on regional to continental scales, and air quality characterization.

The following sections provide a summary of the major satellite instruments for remote sensing of tropospheric trace gases and aerosols. In addition, several other noteworthy instruments are discussed herein. Many of these instruments have complementary capability to

provide information on meteorological parameters, cloud parameters, stratospheric or mesospheric dynamics and chemistry. While these are essential contributions, these capabilities are well described elsewhere and will be omitted here due to space constraints and in light of IGAC's focus on tropospheric chemistry.

Remote sensing instruments do not directly measure atmospheric composition. Rather, atmospheric composition is "retrieved" through an inversion technique from observed radiances leaving the top of the atmosphere. Such retrievals can be rather direct but also often require external information on geophysical fields, as summarized in the following sections. Integral to the success of modern remote sensing has been the development of a variety of mathematical approaches and elegant numerical techniques to extract physical parameters by accounting for atmospheric radiative transfer.

Table 1 summarizes the capabilities of some of the important satellite instruments of relevance for remote sensing of tropospheric trace gases and aerosols. Included are instruments currently in orbit or planned for launch in the near future. More detailed discussion on each is presented in this newsletter. Table 2 lists additional satellite instruments whose data have been applied successfully for remote sounding of the tropospheric constituents. These instruments and their data products are not the focus of this newsletter, but links to more extensive information are provided for the interested reader. Acronyms are defined in Table 3.

Many of the instruments that yield tropospheric information on trace constituents fly in near-polar, sun-synchronous, low earth orbits, LEO. For low and mid latitudes, this results in observations at a constant local time, and global coverage is achieved in 0.5 or more days. At high latitudes such orbits have a relatively high sampling frequency. Asynchronous LEO satellites observe different local times at the same location but generally do not yield representative information, as a result of sparse sampling in conjunction with the high intrinsic variability of tropospheric gas and aerosol chemical composition and cloud cover. Solar occultation instruments in sun synchronous orbits typically measure between 60-80° latitudes, whereas those in asynchronous orbits yield 14 sunset and sunrise measurements around the globe per day.

Figure 1 shows different geometries used for atmospheric remote sensing. Many of the instruments used for tropospheric research are nadir viewing, and thus yield the total atmospheric column modulated by the physics of radiative transfer. However several instruments utilize the limb viewing geometry to infer vertical profiles into the upper troposphere. The majority of instruments employ passive techniques, observing either solar backscatter or thermal emission. Solar backscatter measurements are the most common to date, in part due to their sensitivity to the lower troposphere, especially at visible and near infrared wavelengths where Rayleigh scattering is weak. Measurements of thermal emission have the advantage of yielding both daytime and nighttime observations, and can

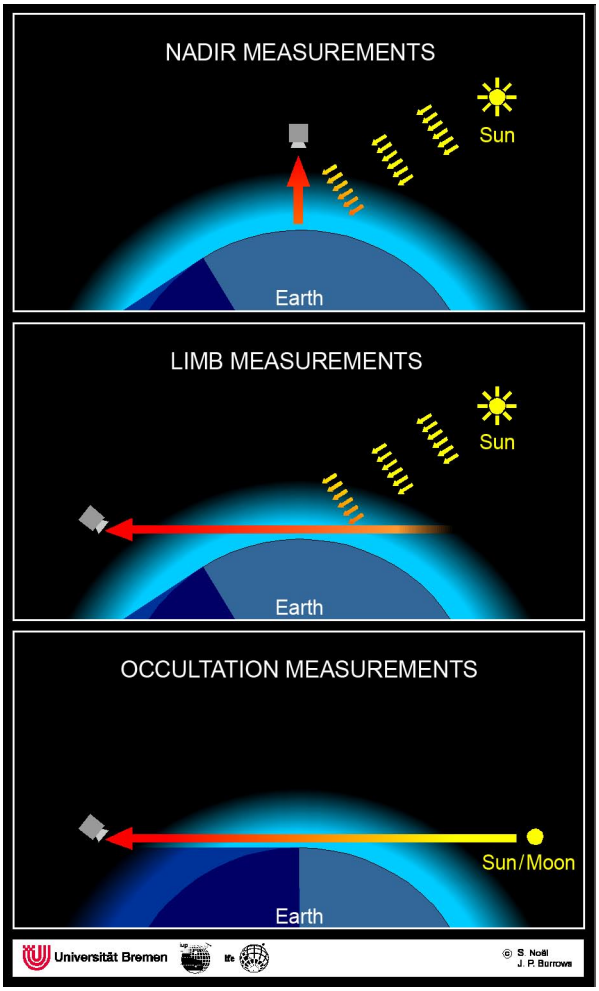

Figure 1. Various viewing geometries are used to measure atmospheric composition. The nadir geometry observes the entire atmospheric column. For passive sensors, vertical resolution is generally achieved using the limb or occultation measurements. (Image courtesy Stefan Noel and John Burrows, University of Bremen).

provide useful information on the vertical profile within the troposphere. However the lack of thermal contrast results in low sensitivity to the lowermost troposphere. In the ultraviolet the strong increase in Rayleigh scattering by air molecules also reduces sensitivity. Very recently, active LIDAR (light detection and ranging; analogous to radar) measurements have been deployed on satellites to yield relatively high resolution vertical profiles of aerosol parameters.

Satellite remote sensing of tropospheric trace gases inadvertently began in 1978 with the deployment of the TOMS instrument onboard the Nimbus 7 satellite and, later, the SAGE-1 instrument onboard the Applications Explorer Mission 2. Although the TOMS and SAGE instruments were aimed at determining global knowledge of stratospheric ozone and aerosols, it was later recognized by NASA scientists that these instruments also yield information about the troposphere. TOMS observes solar backscatter though a single monochromater at ultraviolet wavelengths where ozone has strong absorption features. Despite the design of TOMS for total column ozone,

considerable information exists about tropospheric ozone, volcanic SO_2, and aerosols that absorb ultraviolet radiation. Several approaches have been developed to extract tropospheric ozone columns from TOMS total ozone columns, with the highest confidence at low latitudes where the stratospheric ozone column is least variable and more readily separable. Highlights from TOMS include the first observation of volcanic SO_2 clouds and the discovery of a maximum in tropospheric ozone columns over the tropical Atlantic. The TOMS successors, SAGE-I and SAGE-II, have similarly provided a unique record of upper tropospheric ozone and aerosol.

Also deployed in the 1970's for other purposes, the AVHRR and GOES instruments were designed for monitoring of surface and meteorological fields. Both instruments have been applied to infer aerosol information, particularly

Table 1: Satellite instruments yielding tropospheric composition[a,b]

Instrument	Platform	Meas. Period	Typical Res. (km)	Global coverage (days)[c]	Spectral Range (μm)	Trop O_3	SO_2	Aer Ind	Trop NO_2	HCHO	BrO	H_2O	CO	CH_4	HNO_3	AOT	Aer prop.	CO_2	Aer prof.
TOMS	Nimbus 7, ADEOS, Earth Probe	1978-1992 1996-1997 1996-	38x38 nadir	~ 1	6 λ[d] 0.31-0.36	1 (low-lat)	1	1											
GOME	ERS-2	1995-2003	320x40 nadir	3	0.23-0.79	2-3	1	1	1	1	1	1							
IMG	ADEOS	1996-1997	8x8 nadir	variable	3.3-16.7	2-4							1.5-2.2	0.7-1.5	0.8-1.8				
MOPITT	Terra	2000-	22x22 nadir	3.5	4.7								1.5-2						
MISR	Terra	2000-	18x18e 9 angles	7	4 λ 0.45-0.87											1	1		
MODIS	Terra Aqua	2000- 2002-	10x10e nadir	2	36 λ 0.41-14.2											1	1		
SCIA-MACHY	Envisat	2002-	60x30 nadir	6	0.23-2.3	2-3	1	1	1	1	1	1	1	1				1	
ACE-FTS	SCISAT-1	2003-	4 limb	n/a	2-13	X			X			X	X	X	X				
MLS	Aura	2004-	3-4.5 limb	n/a	Micro-wave	<150 hPa							<150 hPa		X				
OMI	Aura	2004-	13x24 nadir	1	0.27-0.50	2-3	1	1	1	1	1					1	1		
TES	Aura	2004-	5x8 nadir 2 limb	n/a	3.3-15.4	2						5	2						
PARASOL	PARASOL	2004-	16x18	1	9 λ 0.44-1.0											1	1		
CALIOP	CALIPSO	2006-	40x40	n/a	0.53, 1.06														120-360m
GOME-2	MetOp	2006-	80x40	1	0.24-0.79	2-3	1	1	1	1	1	1							
IASI	MetOp	2006-	12x12	0.5	3.6-15.5	2-3						10		1	1			1	
OCO	OCO	2008?	5x5	1	0.76, 1.6, 2.1													1	

[a]Additional species are available as described in the individual sections

[b]The number of independent degrees of freedom is given for each nadir measurement. A value of 1 indicates a tropospheric column. X denotes a partial tropospheric column.

[c]Value given for clear-sky conditions. Clouds impede the retrieval.

[d]Number of discrete wavelengths

[e]Radiances for MISR and MODIS are acquired at between 205 m and 1.1 km, depending on channel. Resolutions reported here are for the Standard operational aerosol products

over water.

More recently, the OSIRIS instrument, launched onboard Odin on February 23, 2002, has been providing information on upper tropospheric trace gases through observations of limb scatter. While the primary goal for OSIRIS is to measure ozone, its optic spectrograph and infrared imager are also being used to produce concentration maps of aerosols and nitrogen dioxide. OSIRIS also provides daily, monthly, and annual height profile maps of ozone for a given area.

In an early endeavor to measure tropospheric chemical composition from space, the MAPS instrument was deployed onboard the Space Shuttle in 1981, 1984 and again in 1994, making the first successful measurements of carbon monoxide in the upper troposphere.

GOME, which is a smaller scale version of the SCIAMACHY instrument, was launched aboard the ESA ERS-2 in April 1995. This instrument was designed primarily to provide the research community with global knowledge of stratospheric ozone and related species, but it was also designed to investigate the potential of nadir remote sounding of backscattered ultraviolet and visible radiation for the retrieval of tropospheric trace gases. GOME observations have turned out to provide a wealth of additional insight about the troposphere. The broad spectral coverage of GOME from ultraviolet to near infrared wavelengths, coupled with spectroscopic inversions, provided the additional capability for remote sensing of several key species in tropospheric chemistry: O_3, NO_2, HCHO, BrO, SO_2, and H_2O. Most species have strong signals in the lower troposphere, as evident from their spatial patterns. Highlights of GOME include insight into emissions of nitrogen oxides, volatile organic compounds, polar bromine, and volcanic sulfur.

The IMG instrument onboard ADEOS, which flew in 1996, is the first high-resolution nadir infrared tropospheric sounder. IMG observations have recently been exploited to provide information about O_3, CO, CH_4, and HNO_3. These measurements of thermal emission yield 1-4 degrees of freedom for each species, providing insight into their vertical distribution.

The launch of the Terra satellite in December 1999 significantly expanded scientific perspective about the scale of tropospheric pollution. The MOPITT instrument is a nadir-viewing gas correlation radiometer operating in the 4.7 μm band of carbon monoxide. Highlights of the MOPITT observations include insight into the long-range transport of pollution, the impact of frontal systems on CO transport, and improved estimates of CO emissions. The AIRS instrument onboard Aqua has also been used to retrieve CO.

Similarly, the MODIS and MISR instruments (both initially launched in late 1999 on NASA's Terra satellite) provide unprecedented information about aerosol abundance and properties at high spatial resolution. Spatial resolution is of particular relevance for aerosol remote sensing in order to minimize contamination by clouds and to capture spatial variability, especially over land. MODIS and MISR have provided considerable insight into the global distribution of aerosols, their long range transport, and increasingly about aerosol optical properties. The MISR instrument includes nine fixed push-broom cameras pointed at angles varying from +70°, through nadir, to -70°. A strength of MISR is the ability to retrieve aerosol optical thickness even over bright surfaces such as deserts. The MODIS instrument uses a scanning mirror which allows global coverage in two days. A second MODIS instrument also is deployed onboard Aqua (2002 launch). Aqua is currently the lead satellite of NASA's "A-train", a series of 6 satellites that orbit within 30 minutes of each other. The other 5 satellites are CloudSat, CALIPSO, PARASOL, Aura, and OCO. The SeaWifs instrument has also proven useful for determination of aerosol spatial distribution.

The European Space Agency's Envisat satellite (2002 launch) carries MERIS, a nadir sounding spectrometer which, like MODIS, retrieves information on ocean color, land surface, and aerosols and clouds. This instrument is yielding exciting measurements of aerosol distributions over land and ocean.

The SCIAMACHY instrument, also launched onboard Envisat in 2002, measures back-scattered solar radiation upwelling from the atmosphere, alternately in nadir and limb viewing geometry. This limb-nadir matching is expected to improve the separation of a tropospheric column from the total atmospheric column. SCIAMACHY has the most comprehensive tropospheric coverage of chemical species of any single satellite instrument. SCIAMACHY provides the capability for retrieval at ultraviolet through infrared wavelengths with a typical spatial resolution of 30 x 60 km. This enables retrieval of all the species observed by GOME at higher resolution, and in addition CHOCHO, CO, CH_4, and CO_2. A highlight from SCIAMACHY is insight into the tropical emissions of CH_4 and the first global dry column distributions of CO_2 over land.

The MIPAS instrument on Envisat makes measurements of the atmospheric infrared emission in the upper troposphere. These have been used to make unique observations, such as of O_3, CO, PAN, H_2O, and HNO_3. Also on board is the AATSR instrument, which is a follow-on to the ATSR-2 instrument that has been operational on the ERS-2 satellite since 1995. While the ATSR-2 and AATSR were primarily designed to look at sea surface temperature they are also providing unique insight for aerosol physics via multi angle measurements.

ACE-FTS has been providing insight into the upper tropospheric distribution of trace gases since its launch onboard SCISAT-1 in 2003. The ACE-FTS is a high resolution infrared Fourier transform spectrometer, which makes solar occultation measurements. Profiles of numerous molecules are retrieved including O_3, CO, CH_4, NO, NO_2, HNO_3, and methanol. Measurement of the distribution of trace gases from biomass burning in the free troposphere has been a scientific highlight.

The launch of Aura in 2004 into the A-train began a period of unprecedented coverage of tropospheric trace gases from three separate instruments: MLS, OMI, and TES.

Table 2: Additional satellite instruments with significant capability for tropospheric retrievals of trace constituents

Instrument	Platform	Measurement Period	Viewing Geometry	Reference
GOES	NOAA Geostationary	1975-	nadir	http://www.goes.noaa.gov/
AVHRR	NOAA polar orbiter	1979-	nadir	http://edc.usgs.gov/products/satellite/avhrr.html
SAGE I	Applications Explorer Mission 2	1979-1981	limb	http://www-sage1.larc.nasa.gov/
SAGE II	ERBS	1984-2005	limb	http://www-sage2.larc.nasa.gov/
SAGE III	Meteor-3M	2002-2005	limb	http://www-sage3.larc.nasa.gov/
MAPS	Space Shuttle	1984, 1994	nadir	http://www.nasa.gov/centers/langley/news/factsheets/MAPS.html
ATMOS	Space Shuttle	1985, 1992, 1993, 1994	limb	http://remus.jpl.nasa.gov/atmos/
ATSR-2, AATSR	ERS-2 Envisat	1991-	nadir	http://www.atsr.rl.ac.uk/
LITE	Space Shuttle	1994	nadir	http://www-lite.larc.nasa.gov/
SeaWifs	SeaStar	1997-	nadir	http://oceancolor.gsfc.nasa.gov/SeaWiFS/
OSIRIS	Odin	2001-	limb	http://osirus.usask.ca/
AIRS	Aqua	2002-	nadir	http://airs.jpl.nasa.gov/
MIPAS	Envisat	2002-	limb	http://envisat.esa.int/instruments/mipas/
MERIS	Envisat	2002-	nadir	http://envisat.esa.int/instruments/meris/
GLAS	ICESat	2003-	nadir	http://glas.gsfc.nasa.gov/
OMPS	NPOESS	2008?	nadir	http://www.ipo.noaa.gov/
GOSAT-FTS	GOSAT	2008?	nadir	http://www.jaxa.jp/missions/projects/sat/eos/gosat/index_e.html

Table 3. Selected list of acronyms

AATSR	Advanced Along-Track Scanning Radiometer
ACE-FTS	Atmospheric Chemistry Experiment Fourier Transform Spectrometer
ADEOS	Advanced Earth Observing Satellite
AIRS	Atmospheric Infrared Sounder
ATMOS	Atmospheric Trace Molecule Spectroscopy Experiment
ATSR	Along-Track Scanning Radiometer
ATOVS	Advanced TIROS Operational Vertical Sounder
AVHRR	Advanced Very High Resolution Radiometer
CALIOP	Cloud-Aerosol LIdar with Orthogonal Polarization
CALIPSO	Cloud-Aerosol Lidar and Infrared Pathfinder Satellite Observation
CEOS	Committee on Earth Observation Satellites
ERBS	Earth Radiation Budget Satellite
ERS-2	European Remote-Sensing Satellite-2
ESA	European Space Agency
GLAS	Geoscience Laser Altimeter System
GOES	Geostationary Operational Environmental Satellites
GOME	Global Ozone Monitoring Experiment
IASI	Infrared Atmospheric Sounding Interferometer
ICESat	Ice, Cloud and land Elevation Satellite
IGOS	Integrated Gobal Observation Strategy
IGACO	Integrated Global Atmospheric Chemistry Observations
IMG	Interferometric Monitor for Greenhouse gases
JAXA	Japan Aerospace Exploration Agency
LITE	Lidar In-space Technology Experiment
MAPS	Mapping of Atmospheric Pollution from Space
MERIS	MEdium Resolution Imaging Spectrometer
MIPAS	Michelson Interferometer for Passive Atmospheric Sounding
MISR	Multiangle Imaging SpectroRadiometer
MLS	Microwave Limb Sounder
MODIS	Moderate Resolution Imaging Spectroradiometer
MOPITT	Measurements Of Pollution In The Troposphere
NASA	National Aeronautics and Space Administration
NOAA	National Oceanic and Atmospheric Administration
NPOESS	National Polar-orbiting Operational Environmental Satellite System
OCO	Orbiting Carbon Observatory
OMI	Ozone Monitoring Instrument
OMPS	Ozone Mapping and Profiler Suite
OSIRIS	Optical Spectrograph and Infrared Imager System
PARASOL	Polarization & Anisotropy of Reflectances for Atmospheric Sciences coupled with Observations from a Lidar
SCIAMACHY	SCanning Imaging Absorption SpectroMeter for Atmospheric CHartographY
SAGE II	Stratospheric Aerosol and Gas Experiment II
TES	Tropospheric Emission Spectrometer
TIROS	Television Infrared Observation Satellite
TOMS	Total Ozone Mapping Spectrometer
UARS	Upper Atmosphere Research Satellite

MLS is a limb sounder that operates in the microwave to measure thermal emission during both day and night. Profiles of O_3, CO, and H_2O are being retrieved from MLS from the stratosphere into the upper troposphere. OMI is a nadir viewing imaging spectrometer that measures solar backscatter at ultraviolet and visible wavelengths with spatial resolution as high as 13 x 24 km and daily global coverage. This high resolution enables observation of more cloud-free scenes than previous backscatter measurements, along with increased retrieval precision. OMI and MLS observations can be combined to infer the distribution of tropospheric ozone. TES is a Fourier transform spectrometer observing thermal emission with both nadir and limb capability. The nadir version features a particularly high spatial resolution of 5 x 8 km, and is being applied to retrieve O_3 and CO with up to 2 degrees of freedom in the vertical.

The POLDER instrument was deployed on both the ADEOS-I and ADEOS-II satellites. The variant PARASOL flies in the A-train. These instruments offer the unique capability of measuring polarization, which yields additional insight into aerosol optical properties beyond aerosol optical thickness.

The first LIDAR system to operate in space was the LITE experiment, which flew for 9 days on the space shuttle. The same team has developed CALIOP, which is a nadir-pointing lidar that was launched in April, 2006 into the A-train. CALIOP offers unprecedented global vertical profiles of aerosol extinction at a vertical resolution of 120-360m, providing an exciting complement to the other satellite instruments. The GLAS instrument on board the ICESat satellite is primarily designed to to measure ice-sheet topography and associated temporal changes, but also measures cloud and atmospheric properties.

The first of the MetOp satellite series was launched by EUMETSAT and ESA in October 2006. This will be the first operational meteorological platform to have instrumentation dedicated to making trace gas measurements. The series will consist of three satellites to be deployed over the next 14 years, each containing two instruments for remote sensing of tropospheric chemistry: GOME-2 and IASI. GOME-2 is an improved version of GOME, featuring a typical spatial resolution of (40-80) x 40 km. IASI contains a nadir-viewing Fourier transform spectrometer to measure thermal emission. Retrievals will include O_3, CO, CH_4, HNO_3, and CO_2 at a spatial resolution of up to 12 km in diameter.

OCO will complete the A-train when launched in 2008. It will carry three high resolution grating spectrometers designed to measure the absorption of reflected sunlight by CO_2 and O_2, to infer CO_2 column abundance with a precision of 0.3%. GOSAT, which is planned to be launched by JAXA around the same time will make measurements of the dry columns of CO_2 and CH_4.

These satellite instruments represent the emergence of global observations of atmospheric chemistry. However, noteworthy challenges remain such as described by the Committee on Earth Observing Satellites, IGOS-IGACO and the National Research Council's Decadal Survey. More complete characterization of aerosol optical properties is necessary to quantify their climatic impact. Observations at higher temporal resolution are required for air quality characterization and monitoring of environmental disasters. Improved vertical resolution is desirable for both trace gases and aerosols. Higher spatial resolution is necessary to improve retrievals in the presence of clouds.

Since the pioneering decisions to fly atmospheric chemistry instrumentation aboard ERS-2 Envisat platforms of ESA and the Terra and Aura platforms of NASA were made at the end of the 1980's, the number of new instruments planned for atmospheric chemistry has been limited. Recently the NPOESS program that was designed for global environmental monitoring has been significantly descoped with respect to measurements of atmospheric composition.

The atmospheric chemistry community has realized for some time that research applications such as air quality, where large diurnal variation and high intrinsic variability are an issue, require high spatial and temporal sampling at mid and low latitudes. These are most readily and practically achieved using remote sounding instrumentation deployed in geostationary orbit, GEO, similar to the systems developed for meteorological parameters. Combinations of LEO and GEO, as called for in the IGOS-IGACO strategy and the NRC Decadal Survey, and the opportunity of utilizing synergistically different observations will provide the next leap forward in the remote sensing of tropospheric composition. Satellite instruments in mid-Earth orbits (MEO) could provide alternative temporal sampling. Over the longer term, global measurements could be obtained from an L-1 orbit at the stationary point between the Earth and the Sun.

As a result of the intrinsic non linearity and multiple feedbacks within the system comprising the Sun, the Earth and its atmosphere, improved measurements of the changing global composition of trace constituents are required to test our understanding of the response of the Earth-atmosphere system to global climate change and to assess the accuracy of our current predictive capability. Measurements from space have an integral role to play in this future. Given the rapid changes in the atmospheric composition resulting from anthropogenically forced climate change, there is pressing need for new instrumentation in optimal combinations of orbits, representing a challenge to agencies and scientists.

TOMS/Nimbus 7, TOMS/ ADEOS, and TOMS/Earth Probe

Contributed by **Richard McPeters** (mcpeters@wrabbit.gsfc.nasa.gov), *and* **Ronald Cohen** *Code 916, NASA Goddard Space Flight Center, Greenbelt, MD 20771 USA*

The Total Ozone Mapping Spectrometer (TOMS) instrument was launched onboard the Nimbus 7 satellite in 1978, the Earth Probe satellite in 1996, and the ADEOS satellite in 1997.

Scientific Questions

The TOMS instrument provides information about ozone distribution, the distributions of ultraviolet-absorbing aerosols (including ash plumes) in the troposphere, sulfur dioxide concentrations following large volcanic eruptions, and the flux of ultraviolet radiation reaching the Earth's surface. While the original Nimbus 7 TOMS (launched in 1978) was designed for mapping total column ozone on a global basis, continuing analysis showed that much additional information could be derived. TOMS data have been used to monitor the decline in global (i.e. stratospheric) ozone, but TOMS is best known for its images of the developing Antarctic ozone hole each year. Although tropospheric ozone cannot be directly measured by TOMS, information on its distribution can be obtained by subtracting stratospheric ozone derived from another instrument (from SAGE or MLS for example) or by another technique such as on-cloud versus off-cloud subtraction.

Sulfur dioxide has a unique signature in the ultraviolet that is different from ozone. SO_2 retrieved by TOMS can be used for monitoring volcanic eruptions. The amount of ultraviolet radiation reaching the Earth's surface can be estimated using a radiative transfer model constrained by the TOMS measured ozone along with cloud cover data from a long wavelength TOMS channel.

Instrument Description

TOMS provides information on Earth's total column ozone by measuring the backscattered Earth radiance in the six 1 nm bands in the ultraviolet from 308 nm to 360 nm. The experiment uses a single monochromator and scanning mirror to sample the backscattered solar ultraviolet radiation at 35 sample points at 3-degree intervals along a line perpendicular to the orbital track. This sampling provides near-global coverage on a daily basis.

The Earth Probe TOMS instrument was launched in July of 1996 into a 500 km sun synchronous orbit. EP TOMS and its data products are described in the User's Guide [1]. The Earth Probe orbit was raised to 730 km in December of 1997 in order to provide more complete coverage after the failure of ADEOS, which also carried a TOMS instrument. Instrument degradation began to affect TOMS accuracy beginning in 2000. In this period TOMS derived ozone had an uncorrected latitude-dependent error of about 4%. The transmitter on Earth Probe failed in December of 2006.

Scientific Highlight – TOMS

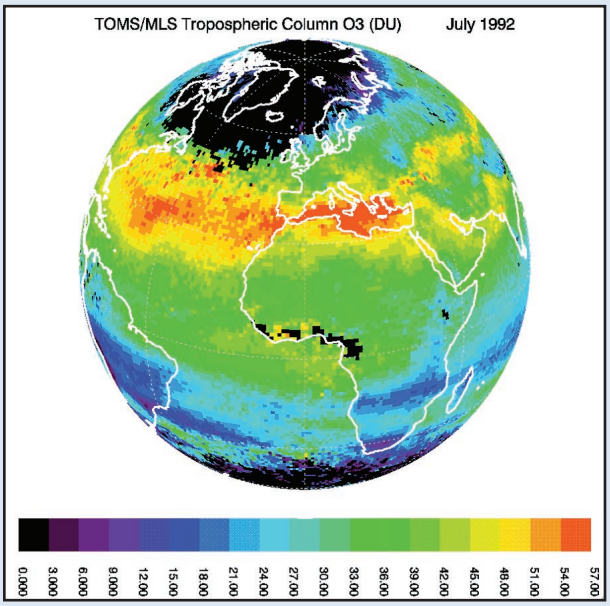

Figure 2. Tropospheric ozone columns inferred as a residual of TOMS total ozone columns and UARS MLS stratospheric ozone columns.

Table 4. Overview of TOMS tropospheric chemistry data products.

Retrieved quantity	Horizontal[a] resolution (km)	Vertical resolution	Typical accuracy	Typical precision	Reference(s) of retrieval algorithm	Validation reference(s)
Total column ozone	1° x 1.25°	na	2%	1%	see ATBD	[2] McPeters et al., 1996
Tropospheric ozone	1° x 1.25°	na	20% (or 3DU)	5%	[3] Ziemke et al., 1998	[3] Ziemke et al., 1998
Aerosol index	1° x 1.25°	na	na[b]	0.5 N value	[4] Torres et al., 1998	[4] Torres et al., 1998
SO_2	1° x 1.25°	na	8 DU	3 DU	see ATBD	[5] Krueger, 1983

[a] resolution of level-2 data is 38 x 38 km at nadir; resolution of grid products is 1° latitude x 1.25° longitude

[b] accuracy undefined for an "index"

Retrieval Description

Current TOMS data were processed with the Version 8 algorithm that has been developed by NASA Goddard's Ozone Processing Team to address errors associated with extreme viewing conditions. This algorithm is described in detail in the algorithm theoretical basis document (ATBD) which is available online from the TOMS web site. The basic algorithm uses just 2 wavelengths (317.5 and 331.2 nm under most conditions, and 331.2 and 360 nm for high ozone and high solar zenith angle conditions). The longer of the two wavelengths is used to derive the surface reflectivity (or cloud fraction). Once the surface reflectivity has been established the shorter wavelength, which is heavily absorbed by ozone, may be used to derive total ozone. The algorithm also calculates the "aerosol index" (AI) from the difference in surface reflectivity derived from the 331.2 and 360 nm measurements. The AI primarily provides a measure of absorption of UV radiation by smoke and desert dust. A very simple algorithm using the four shortest TOMS wavelengths is used to separate SO_2 from ozone. See the ATBD for details.

Data accessibility

Data from all the TOMS instruments are freely available from the TOMS web site: http://toms.gsfc.nasa.gov

Complete data can also be obtained on DVD from the GES DISC at Goddard: http://daac.gsfc.nasa.gov/data/dataset/TOMS

References

[1] McPeters,R.D., P.K. Bhartia, A.J. Krueger, J.R. Herman, C.G. Wellemeyer, C.J. Seftor, G. Jaross, O. Torres, L. Moy, G. Labow, W. Byerly, S.L. Taylor, T. Swissler, and R.P. Cebula, Earth Probe Total Ozone Mapping Spectrometer (TOMS) Data Products User's Guide, *NASA/TP-1998-206895,* November 1998.

[2] McPeters, R.D. and G.J. Labow, An assessment of the accuracy of 14.5 years of Nimbus 7 TOMS version 7 ozone data by comparison with the Dobson network, *Geophys. Res. Lett., 23,* 3695-3698, 1996.

[3] Ziemke, J., S. Chandra, and P.K. Bhartia, Two new methods for deriving tropospheric column ozone from TOMS measurements, *J. Geophys. Res., 103,* 22115-22127, 1998.

[4] Torres, O., P.K. Bhartia, J. Herman, Z. Ahmad, and J. Gleason, Derivation of aerosol properties from satellite measurements of backscattered ultraviolet radiation: Theoretical basis, *J. Geophys. Res., 103,* 17099-17110, 1998.

[5] Krueger, A. J., Sighting of El Chichon Sulfur Dioxide Clouds With the Nimbus 7 Total Ozone Mapping Spectrometer, *Science, 220,* 1377–1378, 1983.

GOME-1 / ERS-2

Contributed by **John P. Burrows** (burrows@iup.physik.uni-bremen.de) *Institute of Environmental Physics and Remote Sensing IUP/IFE University of Bremen - FB1 Postfach 330440 28334 Bremen Germany*

The Global Ozone Monitoring Experiment, GOME-1, was developed as a spin off from the SCIAMACHY Project. The instrument SCIA-mini was proposed in response to the ESA call in December 1988 for Instruments to measure Atmospheric Constituents aboard the second European Research Satellite ERS-2. SCIA-mini was selected for this opportunity then subsequently descoped, losing its limb viewing capability, to become GOME-1, making ultraviolet, visible, and near infrared nadir measurements of the backscattered solar radiation. ERS-2, which was launched on the 20th of April 1995 into a sun synchronous orbit in descending mode, having an equator crossing time of 10:30 a.m. GOME-1 made global measurements from July 1995 to June 2003, when the tape recorder on ERS-2 failed. Currently GOME-1 is functioning well and about 40% coverage of its data is obtained using the ERS-2 direct broadcast and a network of receivers. It is planned to continue GOME-1 for at least one year overlap with the recently launched GOME-2 on Metop-A.

Scientific Questions

As its name implies GOME was intended to provide information about the global distribution and variability of the most important atmospheric trace gas ozone, O_3, and builds on the heritage of the development of the DOAS (Differential Optical Absorption Spectroscopy) in Europe and the TOMS and SBUV instruments, developed by NASA. Absorption in the ultraviolet and visible spectral regions yields information about O_3 in the mesosphere, stratosphere and troposphere. GOME-1 provided the first opportunity to investigate the retrieval of tropospheric and stratospheric trace gases other than O_3 and sulfur dioxide, SO_2, which absorb in the ultraviolet, visible, and near infrared red. In this context the observations of nitrogen dioxide, NO_2, formaldehyde, HCHO, Bromine Oxide, BrO, and Chlorine dioxide, OClO, have been significant. In order to achieve these measurement goals, it is also necessary to retrieve information about surface spectral reflectance, aerosol and cloud, which represent GOME's ancillary objectives. The daily observation of extra terrestrial solar irradiance, which is necessary for retrieval of trace gaseous absorption in regions where the Fraunhofer structure varies, provides in addition long-term knowledge about the variability of the solar output from ~230 to 793nm.

Current Targeted Tropospheric Constituents:

Trace gases (O_3, nitrogen dioxide, NO_2, Formaldehyde, HCHO, water vapor, H_2O, Sulphur dioxide, SO_2, and Bromine Oxide, BrO, Iodine Monoxide, IO), and aerosol and cloud parameters.

Tropospheric Scientific Applications:

Weekly, monthly, seasonal and annual variability of the targeted trace gases.

The study of tropospheric pollution from fossil fuel combustion, changes in land use, biomass burning and the interaction with biospheric emissions.

Instrument Description

The GOME instrument comprises a telescope, spectrometer, and thermal and electrical sub system. Upwelling radiation from the atmosphere is collected by the scan mirror directed, via an off axis parabolic mirror, through the entrance slit of the spectrometer and then towards a dispersing prism. A small fraction of the light, polarized parallel to the direction of the entrance slit, leaves the appropriate face of the prism, forming a second spectrum, which is then focused onto the polarization monitoring device, PMD. The majority of the light forms an intermediate spectrum in the instrument. Light is reflected and directed by a prism to channels 1 and 2, which measure in the ultraviolet from ~230 nm to 400 nm. The light at longer wavelengths is reflected and transmitted by a dichroic mirror to channels 3 and 4 measuring from 400 to 793nm. The PMD comprises three detectors, which make measurements from 300 to ~800nm, corresponding to the spectral ranges of channels 2, 3 and 4 of the spectrometer. The spatial resolution of a ground scene is variable but is typically 40x320 km^2.

Retrieval Description

The measurements of GOME-1 yield level 0 data. These are manipulated, using the level 0 to 1 processor and the instrument calibration, to produce the geophysical products at level 1: solar irradiance and TOA radiance and are provided by ESA. Total column ozone and related data products are provided by ESA and by scientific institutions. In addition scientific institutions have developed tropospheric data products, some of which will be operationalized within the framework of the GMES activities at ESA and the EU.

Data accessibility

Data from GOME of relevance to tropospheric research are at the following web sites and links:

http://earth.esa.int/

http://iup.physik.uni-bremen.de/gome/

http://www.accent-network.org/portal/integration-tasks/satellite-observations-at2

http://troposat.iup.uni-heidelberg.de/AT2/Data_available/Data_available.htm

Table 5. Overview of GOME tropospheric chemistry data products.

Retrieved quantity or Data Product [Unit]	Nadir Horizontal resolution[a] along x across track (km x km)	Vertical resolution	Threshold i.e. S/N =1 and Accuracy[b]	References: Retrieval, Validation and Model Comparison
Ozone: Total Column, Profile, and Tropical Tropospheric Column	Column: 90% of time: 40x320 10% of time: 40x80 Profile: 40x320 or 200x960	Total Column Profile (5km min.) Tropos. Column	n.a.: 1% n.a.: 5% n.a.: ~(20-40)%	[1, 2, 3, 10,11,12, 13, 14, 18, 30, 31,32, 33, 38, 45, 46, 55, 59, 64, 65, 68, 69]
SO_2 [molecules/cm^2]	40x320	Column	~$5x10^{15}$: 20-40%	[4,5,61]
Tropospheric NO_2 [molecules/cm^2]	40x320 40x80	Column	$1x10^{15}$: 20-40%	[1, 2, 3, 23, 24, 25, 28, 29, 30, 44, 45, 46, 50, 51, 52, 53, 54, 58, 59, 61, 62, 63, 66, 73, 74, 75, 76, 77, 78]
HCHO [molecules/cm^2]	40 x 320	Column	$4x10^{15}$: 20-40%	[1, 2, 15, 16, 21, 26, 41, 42, 46, 60]
BrO [molecules/cm^2]	40 x 320	Column	$1x10^{13}$: 20-40%	[1, 2, 3, 6, 7, 8, 9, 55, 56, 57, 58, 70]
H_2O, Water Vapour [molecules/cm^2]	40x320	Column	n.a.: < 10%	[19, 20, 37, 38, 70, 72]
Aerosol Index	40 x 320	Column	n.a.: < 5%	[17, 22, 65]

[a]GOME scans a swath of either 960 km or 240 km, recording 3 grounds scenes in forward scan and one in back scan. This implies global coverage in 3 days or 9 days respectively. The scan strategy of GOME-1 was selected to provide 9 out of 10 days' measurements with a ground scene of 40x320 along track(km) x across track (km) and 1 out of 10 days at a higher spatial resolution of 40kmx80km in order to investigate seasonal higher spatial resolution features in the targeted species. The PMD are read out simultaneously and have a spatial resolution of 40kmx20km.

[b]The threshold represents the value of the data product for an effective S/N = 1. The accuracy refers to typical values for columns or profile ~3x the threshold and higher. The basic measurement of GOME-1 is a slant column, SC, which have a precision that is determined by the random error of the number of photons captured by the spectrometer and instrument noise. The accuracy of the SC depends on the knowledge of the relevant molecular absorption cross sections and scattering parameters and other sources of systematic error. The SCs are converted to total columns or tropospheric columns, by determining the relevant air mass factor. This quantity is, in its simplest form, determined by the geometry of the solar and azimuthal scattering angles, but in addition depends on: i) the shape of the vertical profile of the species, ii) cloud and aerosol optical parameters, and iii) the surface spectral reflectance. For species having a significant stratospheric abundance the accuracy of the tropospheric column depends further on the knowledge of the stratospheric column. For many data products, the accuracy is determined by uncertainties in the above sources of error in the retrieval algorithm, rather than the instrument error.

Scientific Highlight – GOME-1

In addition to its role in providing knowledge about stratospheric ozone and its changing behavior, GOME-1 yielded the first global measurements of the total column and tropospheric columns of NO_2, HCHO, and BrO as well as the first measurements of SO_2 from surface-sourced pollution. The retrieval of tropospheric O_3 columns outside the tropics and sub tropics remains very challenging as a result of the intrinsic variability of the tropopause. Table 1 contains a listing of the products of GOME and the relevant validation and scientific references. The observations of clouds of tropospheric BrO at high latitude in spring and early summer indicate the release from sea ice by complex but natural phenomena. The identification of global tropospheric BrO indicates global sources of Bromine from the release of organic bromine compounds. The GOME data products have provided unique insight into the changing emissions from pollution, biomass burning, the biosphere and soils. In addition the importance of halogens in the troposphere from the sea ice regions has been established.

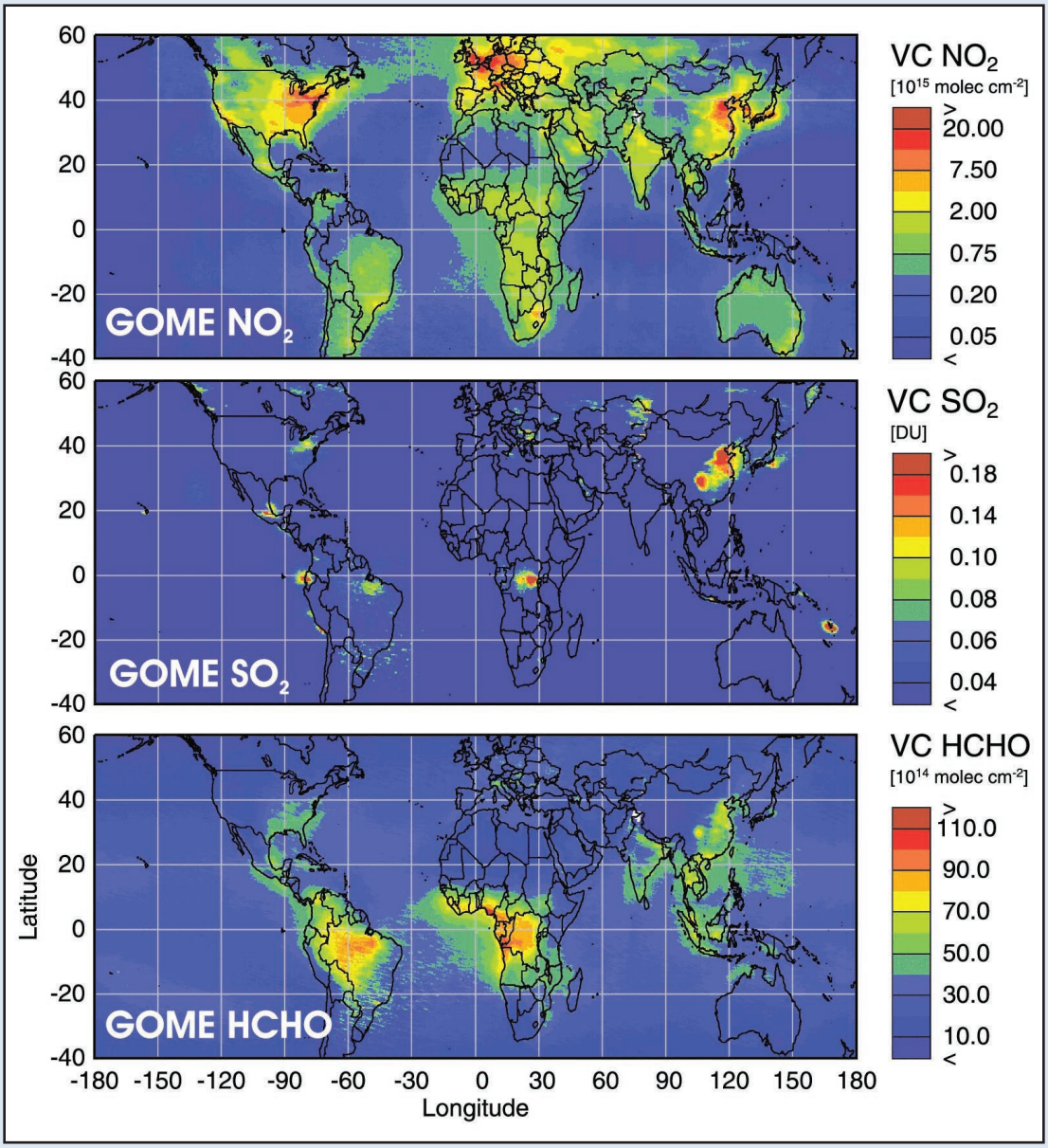

Figure 3. The tropospheric column amounts of NO_2, SO_2 and HCHO determined for the years 1996 to 2002 (Richter, Wittrock and Burrows IUP/IFE-UB). For NO_2, anthropogenic pollution, biomass burning regions and emission of NO_x from the soil are visible. Lightning-produced NO_x is also observed, some of it being emitted to the upper troposphere where it is much longer lived than in the lower troposphere. The outflow of NO_x from the continents is clearly visible. The SO_2 sources are volcanic eruptions and pollution from the combustion of lignite or from metal smelting. Oxidation of biogenic and anthropogenic emissions, in particular the non-methane hydrocarbons, isoprene and the terpenes, and that within or resulting from biomass and biofuel burning, are the main source for HCHO.

Acknowledgments

ESA funded the space and ground segment for GOME-1 and some validation. Research institutions at universities and national laboratories and their relevant national funding agencies (e.g. DFG, BMBF, DLR, NIVR, SRON etc.) as well as the EU through its framework research programs, have supported a large part of the validation and data exploitation of the GOME-1 observations.

References

[1] Burrows, J.P., et al., 1999, *J. Atmospheric Sciences, 56,* 151-175.
[2] Burrows, J. P., 1999, in Developments in Atmospheric Sciences 24: Approaches to Scaling Trace Gas Fluxes in Ecosystems, Ed A. F. Bouwman Elservier Amsterdam pp 315-347. ISBN: 0-444-82934-2.
[3] ESA Publication WPP-108 GOME Geophysical Validation Campaign, published by ESA 1996.
[4] Eisinger, M., and J. P. Burrows, 1998a, *Earth Observation Quarterly 58*, 16-18.
[5] Eisinger, M. and J. P. Burrows, 1998b, *Geophys. Res. Lett., 25,* 4177-4180.
[6] Hegels, E. et al., 1998, *Geophys. Res. Lett. 25,* 3127-3130.
[7] Richter, A. et al., 1998, *Geophy. Res. Lett. 25,* 2683-2686.
[8] Wagner, T., and U. Platt, 1998, *Nature, 395,* 486–490.
[9] Chance, K., 1998, *Geophys. Res. Lett. 25,* 3335-3338.
[10] Hoogen, R. et al., 1998, *Earth Observation Quarterly 58,* 9-10.
[11] Burrows, J. P. et al., 1998, XVIII Quadrennial Ozone Sympoisum 1996 L'Aquila Italy Atmospheric Ozone: Proceedings of the Quadrennial Ozone Symposium 1996 Italy 12-21 September 1996, Eds R. D. Bojkov and G. Visconti, 657-660.
[12] Hoogen, R. et al., 1998, *Proceedings of SPIE, Vol. 3495,* 367-378.
[13] Munro, R. et al., 1998, *Nature 392,* 168-171, doi:10.1038/32392.
[14] Hoogen, R. et al., 1998, *Earth Observation Quarterly 58,* 9-10.
[15] Ladstätter-Weißenmayer, A. and J. P. Burrows, 1998, *Earth Observation Quarterly 58,* 28-30.
[16] Thomas, W. et al., 1998, *Geophys. Res. Lett.,* doi:10.1029/98GL01087, 25(9), 1317-1320.
[17] Gleason, J. F. et al., 1998, *J. Geophys. Res., 103* (D24), 31,969–31,978.
[18] Hoogen, R. et al., 1999, *J. Geophys. Res., 104* (D7), 8263-8280, doi:10.1029/1998JD100093.
[19] Noel, S., et al.,1999, *Geophys. Res. Lett., 26* (13), 1841-1844.
[20] Maurellis, A. N. et al., 2000, *Geophys. Res. Lett., 27,* 903–906.
[21] Chance, K. et al., 2000, *Geophys. Res. Lett., 27* (21), 3461-3464, doi:10.1029/2000GL011857.
[22] Veefkind, J.P. et al., 2000, *Remote Sensing of Environment, 74* (3) 377-386, doi:10.1016/S0034-4257(00)00106-1.
[23] Lauer, A. et al., 2001, *Atmospheric Chemistry and Physics, 2,* 67-78.
[24] Velders, G. J. M. et al., 2001, *J. Geophys. Res., 106* (D12), 12643-12660.
[25] Leue, C. et al., 2001, *J. Geophys. Res., 106,* 5493-5505.
[26] Palmer et al., 2001, *J. Geophys. Res., 106,* 14539-14550.
[27] Koelemeijer, R. B. A. et al., 2001, *J. Geophys. Res., 106,* pp. 3475–3490.
[28] Richter, A. and J.P. Burrows, 2002, *Adv. Space Res., 29* (11), 1673-1683.
[29] Martin, R.V. et al., 2002, *J. Geophys. Res., 107,* 4437, doi:10.1029/2001JD001027.
[30] Heland, J. et al., 2002, *Geophys. Res. Lett., 29,* 44-1 to 44-4, doi:10.1029/2002GL015528.
[31] Bramstedt, K. et al., 2002, *Adv. Space Res., 29* (11), 1637-1642.
[32] Bramstedt, K. et al., 2002, *Atmospheric Chemistry and Physics, 3,* 1409-1419.
[33] Tellmann, S. et al., 2002, "GOME satellite detection of ozone over snow/ice covered surface in the presence of broken cloud", *Proceedings of SPIE, 4539,* Ed.: K. Schäfer et al., ISBN 0-8194-4263-X.
[34] Müller, R.W. et al., 2002, Adv. Space Res., 29(11), 1655-1660.
[35] Richter, A. et al., 2002, Adv. Space Res., 29(11), 1667-1672.
[36] Roozendael, M. van et al., 2002, *Adv. Space Res., 29* (11), 1661-1666.
[37] Noël, S., et al., 2002, *Adv. Space Res., 29* (11), 1697-1702.
[38] Lang, R. et al., 2002, *J. Geophys. Res., 107* (D16), 4323, doi:10.1029/2001JD001453.
[39] Koelemeijer, R. B. A. et al., 2002, *J. Geophys. Res., 107* (D12), 6017, doi:10.1029/2001JD000840.
[40] Mueller, M. D. et al., 2003, *J. Geophys. Res., 108* (D16), p. 4497, doi:10.1029/2002JD002784.
[41] Palmer, P. I. et al., 2003, *J. Geophys. Res., 108* (D6), p.4180, doi:10.1029/2002JD002153.
[42] Abbot et al., 2003, *Geophys. Res.. Lett., 30* (17), 1886.
[43] Lang, R. et al., 2003, *Atmos. Chem. Phys., 3,* 145–160.
[44] Edwards, D. P. et al., 2002, *J. Geophys. Res., 108* (D8), 4237, doi:10.1029/2002JD002927.
[45] Stohl, A. et al., 2003, *Atmos. Chem. Phys. Discuss., 3,* 2101-2141.
[46] Ladstätter-Weißenmayer, A. et al., 2003, *Atmos. Chem. Phys. Discuss., 3,* 3051-3094.
[47] Koelemeijer, R. B. A. et al., 2003, *J. Geophys.Res., 108* (D2), doi:10.1029/2002JD002429.
[48] Ladstätter-Weißenmayer, A. et al., 2004, *Atmos. Chem. Phys., 4,* pp. 903-909.
[49] Bracher, A. et al., 2004, *Journal of Geophysical Research, 109,* D20308, 2004, doi:10.1029/2004JD004677.
[50] Boersma, K. F., et al. 2004, *J. Gephys. Res., 109,* D04311, doi:10.1029/2003JD003962.
[51] Martin R,V. et al. 2004, *J. Geophys. Res., 109,* D24307, doi:10.1029/2004JD004869.
[52] Kunhikrishnan, T. et al., 2004, *Atmospheric Environment, 38,* 581-596.
[53] Kunhikrishnan T. et al., 2004, *Geophys. Res. Lett., 31,* L08110, doi: 10.1029/2003GL019269.
[54] Konovalov, I.B. et al., 2004, *Atmos. Chem. Phys., 5,* 169-190.
[55] Afe, O. T. et al., 2004, *Geophys. Res.Lett., 31,* L24113, doi:10.1029/2004GL020994.
[56] Kaleschke, L. et al., 2004, *Geophys. Res. Lett., 31,* L16114, doi:10.1029/2004GL020655.
[57] Lang, R. and M. G. Lawrence, 2004, *Atmos. Chem. Phys. Discuss., 4,* 7917–7984.
[58] de Beek, R. et al., 2004, *Adv. Space Res. 34,* 727-733.
[59] Liu, X. et al., 2005, *J. Geophys. Res., 110,* D20307, doi:10.1029/2005JD006240.
[60] Meyer-Arnek, J. et al., 2005, *Faraday Discussions, 130,* 387, doi:10.1039/b502106p.
[61] Konovalov, I. B. et al., 2005, *Atmos. Chem. Phys., 6,* 1747-1770.
[62] Richter, A. et al., 2005, *Nature, 437,* 129-132, doi:10.1038/Nature04092.
[63] Jaeglé, L. et al. 2005, *Faraday Discuss.,* 407-423.
[64] Boersma et al., 2005, *Atmos. Chem. Phys., 5,* 2311-2331.
[65] Choi et al., 2005, *Geophys. Res. Lett., 32,* L02805, doi:10.1029/2004GL021436.
[66] Khokhar, M. F. et al., 2005, *Adv. Space Res. 36,* 879-887.
[67] de Graaf, M. et al., 2005, *J. Geophy. Res., 110,* doi:10.1029/2004JD005178.

[68] Coldewey-Egbers, M. et al., 2004, *Atmos. Chem. Phys., 5,* 1015-1025.
[69] Weber, M. et al., 2004, *Atmos. Chem. Phys., 5,* 1341-1355.
[70] Wagner, T. et al., 2005a, *J. Geophys. Res., 110,* D15104, doi:10.1029/2005JD005972.
[71] Wagner, T. et al., 2005b, *J. Geophys. Res., 111,* D12102, doi:10.1029/2005JD006523.
[72] Liu, X. et al., 2006, *J. Geophys. Res., 111,* D02308, doi:10.1029/2005JD006564.
[73] Ladstätter-Weißenmayer, A. et al., 2006, *Atmos. Chem. Phys. Discuss., 6,* 9273-9296.
[74] Ordóñez, C. et al., 2006, *J. Geophys. Res., 111,* D05310, doi:10.1029/2005JD006305.
[75] Kunhikrishnan, T. et al., 2006, *J. Geophys. Res., 111,* D15301, doi:10.1029/2005JD006036.
[76] Ma, J. et al. 2006, Atmospheric Environment, 40, 593–604.
[77] Toenges-Schuller, N. et al., 2006, *J. Geophys. Res., 111,* D05312, doi:10.1029/2005JD006068.
[78] Kim, S.-W. et al., 2006, *Geophys. Res. Lett., 33,* L22812, doi:10.1029/2006GL027749.
[79] Rozanov, V.V. et al., 2006, *Remote Sensing of Environment, 102* (1-2), 186-1.

IMG / ADEOS

Contributed by **Cathy Clerbaux** (ccl@aero.jussieu.fr), **Solène Turquety** (turquety@aero.jussieu.fr), *and* **Juliette Hadji-Lazaro** (juliette.hadji-lazaro@aero.jussieu.fr), *Service d'Aéronomie, IPSL, Universite Pierre et Marie Curie, Boîte 102, 4, place Jussieu, 75252 Paris Cedex 05, France, and* **Pierre-Françoise Coheur** *and* **Catherine Wespes,** *Université Libre de Bruxelles, CP 160/09, avenue F. D. Roosevelt 50, 1050 Bruxelles, Belgium.*

IMG was launched as part of the Japanese ADEOS payload in August 1996. The ADEOS satellite ceased to collect and transmit data in June 1997 due to a power failure in its solar panel.

Scientific Questions

The Interferometric Monitor for Greenhouse gases (IMG) instrument was the first high-resolution nadir infrared tropospheric sounder allowing the simultaneous measurement from space of a series of trace gases relevant for climate and chemistry studies: H_2O, CO_2, N_2O, CH_4, O_3, CO, CFCs, and HNO_3.

Instrument Description

IMG used a nadir-viewing Fourier transform interferometer that recorded the thermal emission of the Earth-atmosphere system between 600 and 3030 cm^{-1}, with a maximum optical path difference of 10 cm (i.e. 0.1 cm^{-1} unapodized spectral resolution) [1].

ADEOS was a sun-synchronous (equator local crossing time at descending node at 10:30 a.m.), ground track repeat, polar-orbiting satellite. The instrument performed a global coverage of the Earth, making 14 1/4 orbits per day with a series of six successive measurements separated by 86 km (every 10 s) along the track. The footprint on the ground was 8 km × 8 km, in three spectral bands, corresponding to three different detectors and three geographically adjacent footprints. Due to the huge data flow rate, the operational mode of IMG was set to 4 days operation/10 days halt alternation, except for one specific period from 1 to 10 April 1997 for which 10 consecutive days are available.

Table 6. Overview of IMG tropospheric chemistry data products.

Retrieved quantity	Horizontal[a] resolution (km)	Vertical[b] resolution	Typical accuracy	References
CO	IMG pixel	8 km DOFs: 1.5-2.2	5-15%	[3] Turquety et al., 2004 [4] Barret et al., 2005
Total ozone	IMG pixel	Column	5%	[3] Turquety et al., 2004
Trop. ozone	IMG pixel	5 km DOFs : 2-4	20%	[5] Coheur et al., 2005
Methane	IMG pixel	10 km DOFs : 0.7-1.5	5%	[6] Clerbaux et al., 2003 [3] Turquety et al., 2004
CFC12, CFC11	IMG pixel	Column	10%	[5] Coheur et al., 2003
Total HNO_3	IMG pixel	Column	25%	[8] Wespes et al., 2007
Trop. HNO_3	IMG pixel	10 km DOFs : 0.7-1.8	60%	[8] Wespes et al., 2007
$H_2{}^{16}O$	IMG pixel	4 km DOFs : 2.5-5.5	10 %	[12] Herbin et al., 2007
$H_2{}^{18}O$, HDO	IMG pixel	8 km DOFs : 1-3	15-25 %	[12] Herbin et al., 2007

[a] 8 x 8 km, every 86 km along the track
[b] DOFs=degrees of Freedom (number of independent information on the vertical). DOFs depend on the surface temperature of the location: higher values are for tropical conditions, lower values for polar latitudes.

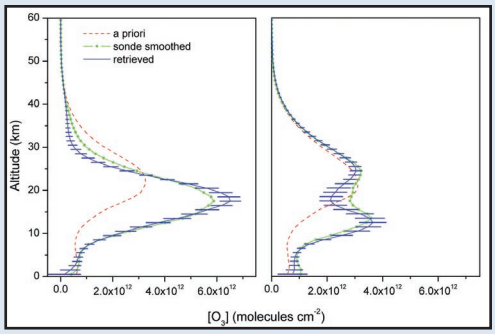

Figure 4. Examples of O_3 profile retrievals from IMG and comparison with coincident sonde measurements, at Ny-Alesund, in January (left) and April (right) 1997. The a priori profile used for the retrieval is also indicated (dashed line). A good agreement between the IMG remote sensor and the ozone sondes is obtained from the ground to the stratosphere. (Adapted from Coheur et al., 2005 [5])

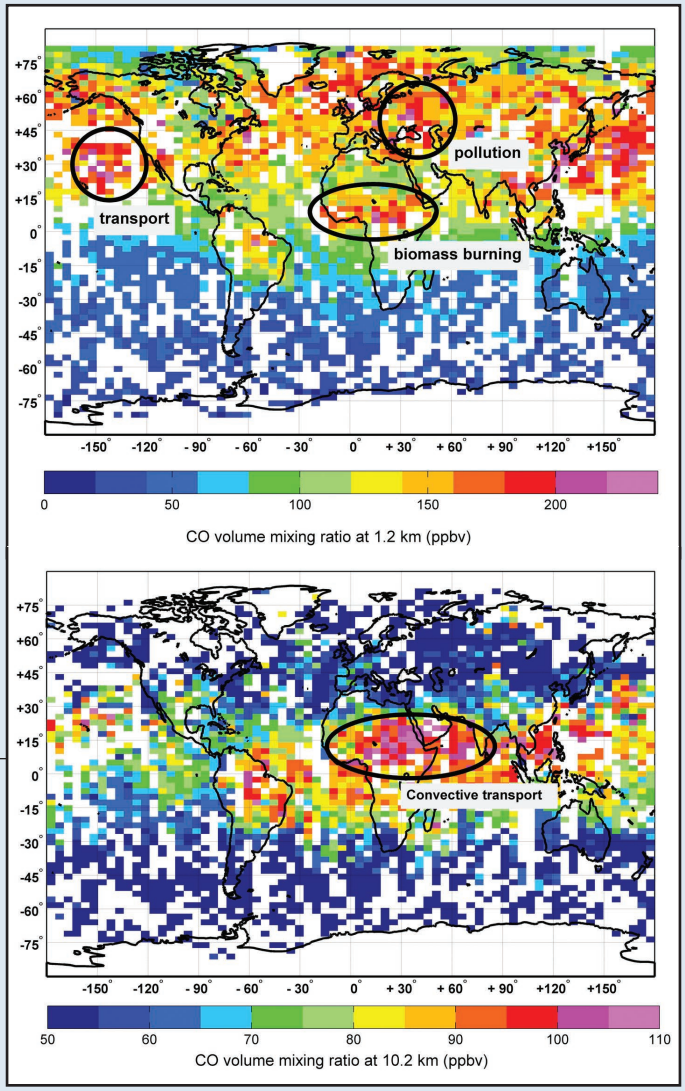

Figure 5. Distributions of CO in the boundary layer (1.2 km, top plot) and in the upper troposphere (10.2 km, bottom plot) retrieved from IMG in April 1997. Both the sources and the transport of pollution plumes are identified. (Adapted from Barret et al., 2005 [4])

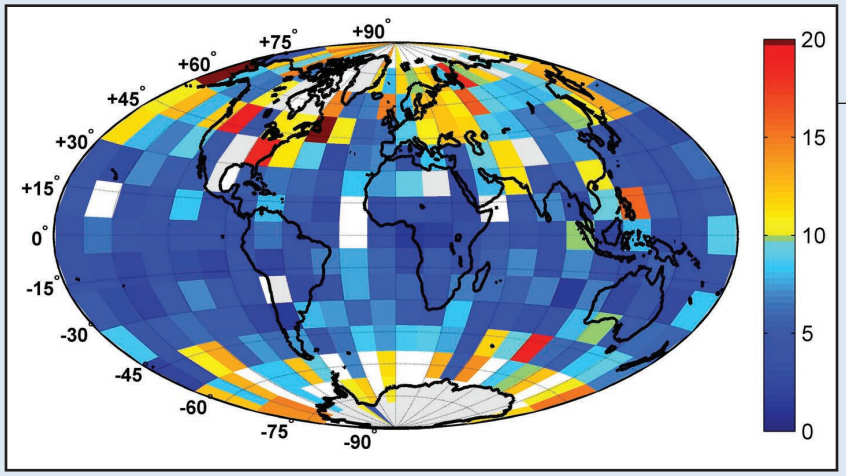

Figure 6. HNO_3 tropospheric columns (0-10 km, in 10^{15} molecules cm^{-3}) retrieved from IMG in April 1997. (Adapted from Wespes et al., 2007 [8])

Retrieval Description

Level 1C radiance spectra and Level 2 retrieved products were distributed by IMGDIS/ERSDAC.

The Level 1C data are calibrated radiance spectra, unapodized, and cloud contaminated. The official Level 2 data are not quantitative and their use is not recommended.

Other retrieval algorithms, developed for nadir-looking infrared sounders, were used to retrieve products from the IMG radiances; e.g. CO columns were retrieved using TES, MOPITT and IASI retrieval codes [2].

Data accessibility

IMG data are available from the IMG Science Team. A set of 20 000 cloud-filtered radiance spectra [9] is available from Service d'Aéronomie (ccl@aero.jussieu.fr).

Acknowledgments

The authors are grateful to Ryoichi Imasu and the IMG team for providing the Level 1 data.

References

[1] Kobayashi, H., Shimota, A., Kondo, K., Okumura, E., Kameda, Y., Shimoda, H., and Ogawa, T., 1999, Development and evaluation of the interferometric monitor for greenhouse gases: a high throughput Fourier-transform infrared radiometer for nadir Earth observation, *Appl. Opt., 38,* 6801–6807.

[2] Clerbaux, C., J. Hadji-Lazaro, S. Payan, C. Camy-Peyret, J. Wang, D. Edwards and M. Luo, 2002, Retrieval of CO from nadir remote-sensing measurements in the infrared by use of four different inversion algorithms, *Appl. Optics, 41,* 33, 7068-7078.

[3] Turquety, S., J. Hadji-Lazaro, C. Clerbaux, D. A. Hauglustaine, S. A. Clough, V. Cassé, P. Schlüssel and G. Mégie, 2004, Operational trace gas retrieval algorithm for the Infrared Atmospheric Sounding Interferometer, *J. Geophys. Res., 109,* D21301, doi:10.1029/2004JD004821.

[4] Barret, B., S. Turquety, D. Hurtmans, C. Clerbaux, J. Hadji-Lazaro, I. Bey, M. Auvray and P.-F Coheur, 2005, Global carbon monoxide vertical distributions from space borne high-resolution FTIR nadir measurements, *Atmospheric Chem. and Phys.,* 5, 2901-2914.

[5] Coheur, P.-F., B. Barret, S. Turquety, D. Hurtmans, J. Hadji-Lazaro and C. Clerbaux, 2005, Retrieval and characterization of ozone vertical profiles from a thermal infrared nadir sounder, *J. Geophys. Res., 110,* D24303, doi:10.1029/2005JD005845.

[6] Clerbaux, C., J. Hadji-Lazaro, S. Turquety, G. Mégie, and P.-F. Coheur, 2003, Trace gas measurements from infrared satellite for chemistry and climate applications, *Atmos. Chem. Phys., 3,* 1495-1508.

[7] Coheur, P.-F., C. Clerbaux and R. Colin, 2003, Spectroscopic measurements of halocarbons and hydrohalocarbons by satellite-borne remote sensors, *J. Geophys. Res, 108* (D4), doi:10.1029/2002JD002649.

[8] Wespes, C., D. Hurtmans, H. Herbin, B. Barret, S. Turquety, J. Hadji Lazaro, C. Clerbaux and P.-F. Coheur, 2007, Satellite measurements of nitric acid global distributions in the troposphere and the stratosphere, *J. Geophys. Res.,* in press.

[9] Hadji-Lazaro, J., C. Clerbaux, P. Couvert, P. Chazette and C. Boonne, 2001, Cloud filter for CO retrieval from IMG infrared spectra using ECMWF temperatures and POLDER cloud data, *Geophys. Res. Lett., 28* (12), 2397-2400.

[10] Clerbaux, C., J. Hadji-Lazaro, D. Hauglustaine, G. Mégie, B. Khattatov and J.-F. Lamarque, 2001, Assimilation of carbon monoxide measured from satellite in a three-dimensional chemistry-transport model, *J. Geophys. Res, 106* (D14), 15,385-15,394.

[11] Turquety, S., J. Hadji-Lazaro and C. Clerbaux, 2002, First satellite ozone distributions retrieved from nadir high-resolution infrared spectra, *Geophys. Res. Lett., 29* (24), 2198, doi:10.1029/2002GL016431.

[12] H. Herbin, D. Hurtmans, C. Wespes, S. Turquety, J. Hadji-Lazaro, C. Clerbaux, and P.F. Coheur, Simultaneous retrievals of $H_2{}^{16}O$, $H_2{}^{18}O$ and HOD vertical profiles in the troposphere from high spectral resolution nadir IR measurements, *Atmos. Chem. Phys. Disc.,* submitted.

MOPITT / Terra

Contributed by **James R. Drummond** (james.drummond@utoronto.ca), *Department of Physics, University of Toronto, 60 St. George Street, Toronto, Ontario, M5S 1A7 Canada, and* **David P. Edwards** (edwards@ucar.edu), *National Center for Atmospheric Research, Atmospheric Chemistry Division, 2450 Mitchell Lane, Boulder, CO 80301 USA.*

The Measurement of Pollution in the Troposphere (MOPITT) instrument was launched on NASA's Terra satellite on 19th December 1999. In the 6½ years that it has been in orbit, it has made well over a billion measurements of carbon monoxide in the troposphere. The Terra mission has recently been extended to 10 years of operations.

Scientific Questions

MOPITT is designed to produce global maps of vertically-resolved carbon monoxide. These data can be used to

Table 7. Overview of MOPITT tropospheric chemistry data products.

Retrieved quantity	Horizontal resolution (km)	Vertical resolution	Typical accuracy	Typical precision	Reference(s) of retrieval algorithm	Validation reference(s)
CO	22 x 22	1.5-2	10%	10%	[2] Deeter et al., (2003)	[3] Emmons et al. (2004)

Scientific Highlights – MOPITT

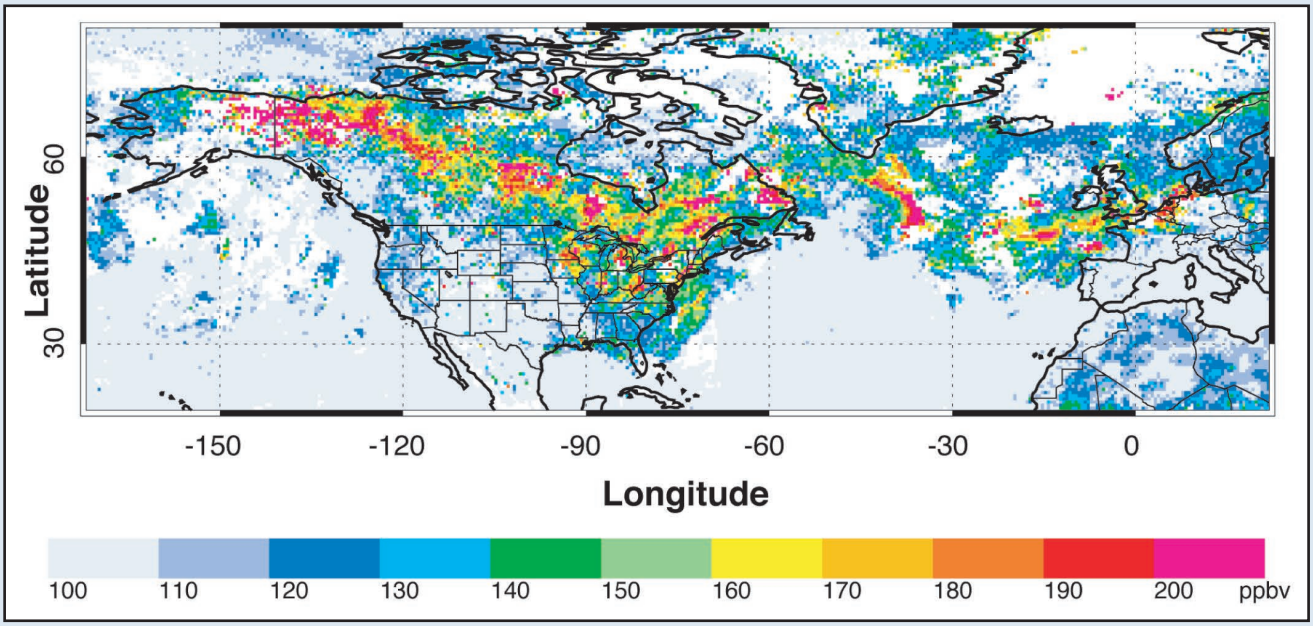

Figure 7. MOPITT 700 hPa CO mixing ratio for the period 15-23 July, 2004, during the INTEX-NA field campaign. The intense wildfires in Alaska produced plumes of pollution that can be traced across North America and the Atlantic Ocean.

Long-Range Transport of Pollution: MOPITT data have been used extensively to examine the impact of localized emissions on larger scale air quality. This is illustrated in Figure 7 which shows the MOPITT 700 hPa CO mixing ratio for the period 15-23 July, 2004, during the INTEX-NA field campaign. The intense wildfires in Alaska produced plumes of pollution that can be traced across North America and the Atlantic Ocean. (e.g., Pfister, G., et al., 2005 [4])

Development of Data Assimilation Techniques: MOPITT data has motivated several important advances in data assimilation of satellite trace gas measurements into chemical transport models [5].

Improvement of Emissions Using Inverse Modeling: A major advance in emission studies has been the use of MOPITT measurements and inverse modeling to constrain surface CO fluxes and to assess the accuracy of the current inventories [6].

Investigation of Vertical Transport In the Troposphere: MOPITT CO retrievals can distinguish vertical structure in the tropospheric profile, particularly in the tropics. This characteristic can be employed to study vertical transport phenomena such as convection, illustrated in Figure 8 [7, 1].

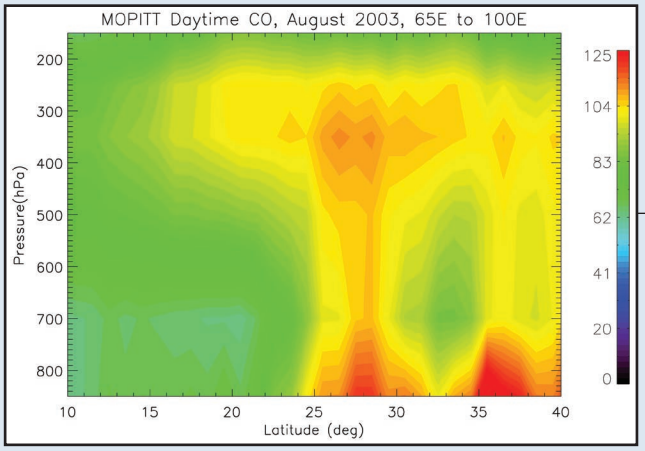

Figure 8. Cross-Section from 5°N to 35°N averaged over 65°-100°E (essentially across the Indian sub-continent) showing daytime high CO mixing ratios(in ppbv) in the mid-troposphere caused by uplift and transport by the monsoon circulation.

Scientific Highlights, cont. – MOPITT

Small-Scale Dynamic Features related to Meteorology: The swath of MOPITT enables a single "snapshot" of dynamic features related to air flow and meteorology. "Fronts" of CO have been observed at several locations. ([8], Figure 9).

Investigations of Tropospheric Chemistry: The integration of satellite retrievals of CO from MOPITT with other data has provided a powerful method for investigating the production of tropospheric ozone and investigating its spatial and temporal distribution [9,10].

Quantifying Seasonal and Inter-Annual Pollutant Variability: The multi-year MOPITT dataset forms the foundation of a long-term observational data record that will be used to investigate the links between chemistry, climate, and other components of the Earth system [11].

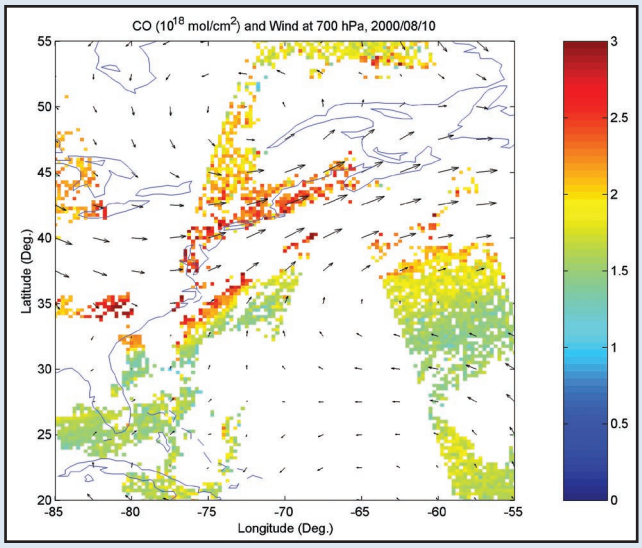

Figure 9. Snapshot of CO off of the East Coast of the US on 10th August, 2000 showing a distinct "front" in CO concentration.

answer such questions as:

- What is the distribution of carbon monoxide over the planet?
- How does it change with time?
- What are the major influences on the distribution?
- How do local sources affect the local environment?
- Where are the major source regions?
- What is the impact on regional and global scale air quality?
- How are these parameters changing over time?

Instrument Description

MOPITT is a thermal nadir-viewing gas correlation radiometer operating in the 4.7μm band of carbon monoxide. It uses a cell of the target gas to filter out the relevant signal from the total upwelling radiation. By setting these correlation cells at different pressures, the signal can be obtained from different heights in the atmosphere allowing MOPITT to obtain some altitude resolution. A cooler failure one year into the mission has degraded this ability somewhat, but MOPITT still produces significant altitude-dependent information.

MOPITT uses side-scanning to tile a complete swath about 650km wide as it traverses the planet. Combined with Terra's 705km altitude, 10:30am crossing time, sun-synchronous orbit, this gives complete global coverage in 16 days, and practically complete coverage (gaps in data due to orbital coverage are much less than gaps due to clouds, etc.) in about 3-4 days. The MOPITT pixel is 22km x 22km at nadir with a 29 pixel wide swath. MOPITT data are reported at 7 pressure levels plus the total column amount, although there is a considerable correlation between levels with about 1.5-2 independent pieces of information [1].

MOPITT data have been extensively validated and are considered to be within the target accuracy and precision of 10% over much of the planet. Quality control flags in the data are used to aid the user in accessing appropriate data for their purposes.

Retrieval Description

MOPITT cannot see through clouds and therefore all data from cloudy pixels, (defined as >5% of cloud in the pixel) are discarded. The cloud mask for this is either internally generated from examination of the radiances or it is taken from the MODIS cloud mask, also from the Terra satellite and therefore contemporaneous.

Input data to the MOPITT retrieval, which is an optimal estimation retrieval [2], are: the MOPITT radiances; MOPITT instrument state; a single a priori CO profile for the globe; the temperature profile from NCEP; the MODIS cloud mask; and spectroscopic information from the HITRAN database.

The outputs from the retrieval are: the CO mixing ratio on 7 levels and the total column amount; the averaging kernels of the retrieval; and the covariance matrix describing the errors.

Data accessibility

The MOPITT data are archived at the Langley Distributed Active Archive Center (DAAC) and are freely available at http://eosweb.larc.nasa.gov/PRODOCS/mopitt/table_mopitt.html. Quick-look monthly maps are available at: http://www.eos.ucar.edu/mopitt/data/plots/mapsv3_mon.html

Acknowledgments

The MOPITT instrument was financed by the Canadian Space Agency and built by COMDEV of Cambridge, Ontario. The Terra mission and the data processing at the National Center for Atmospheric Research were funded by NASA. Funding for science activities in Canada was provided by the Natural Sciences and Engineering Research Council (NSERC). The authors wish to thank Ms. Liu and Dr. Kar for assistance in preparing this paper and the MOPITT science team for their support of the overall program.

References

[1] Deeter M. N., L. K. Emmons, D. P. Edwards, J. C. Gille, and James R. Drummond, 2004, Vertical resolution and information content of CO profiles retrieved by MOPITT, *Geophys. Res. Lett., 31,* L15112, doi:10.1029/ 2004GL020235.

[2] Deeter, M. N., et al., 2003, Operational carbon monoxide retrieval algorithm and selected results for the MOPITT instrument, *J. Geophys. Res., 108,* No. D14, 4399 10.1029/2002JD003186.

[3] Emmons, L. K., et al., 2004, Validation of Measurements of Pollution in the Troposphere (MOPITT) CO retrievals with aircraft in situ profiles, *J. Geophys. Res., 109,* No. D3, D03309, 10.1029/2003JD004101.

[4] Pfister G., et al., 2005, Quantifying CO emissions from the 2004 Alaskan wildfires using MOPITT CO data, *Geophys. Res. Lett., 32,* L11809, doi:10.1029/2005GL022995.

[5] Lamarque, J.-F., et al., 2004, Application of a bias estimator for the improved assimilation of Measurements of Pollution in the Troposphere (MOPITT) carbon monoxide retrievals, *J. Geophys. Res., 109,* No. D16, D16304 10.1029/2003JD004466.

[6] Petron G., et al., 2004, Monthly CO surface sources inventory based on the 2000-2001 MOPITT satellite data, *Geophys. Res. Lett., 31,* L21107, doi:10.1029/2004GL020560.

[7] Kar J., et al., 2004, Evidence of Vertical Transport of Carbon Monoxide From Measurements of Pollution in the Troposphere (MOPITT), *Geophys. Res. Lett. 31,* L23105, doi:10.1029/2004GL021128.

[8] Liu, J., et al., 2006, Large horizontal gradients in atmospheric CO at the synoptic scale as seen by spaceborne Measurements of Pollution in the Troposphere, *J. Geophys. Res., 111,* D02306, doi:10.1029/2005JD006076.

[9] Edwards, D.P., et al., 2003, Tropospheric Ozone Over the Tropical Atlantic: A Satellite Perspective, *J. Geophys. Res., 108* (D8), 4237, doi:10.1029/2002JD002927.

[10] Bremer, H., et al., 2004, The Spatial and Temporal Variation of MOPITT CO in Africa and South America: A Comparison With SHADOZ Ozone and MODIS Aerosol, *J. Geophys. Res., 109,* No. D12, D12304 10.1029/2003JD004234.

[11] Edwards, D.P., et al., 2004, Observations of carbon monoxide and aerosols from the Terra satellite: Northern Hemisphere variability, *J. Geophys. Res.-Atmospheres, 109,* D24202,doi:10.1029/2004JD004727.

MISR / Terra

Contributed by **Ralph Kahn** (ralph.kahn@jpl.nasa.gov), *Jet Propulsion Laboratory, MS 169-237, 4800 Oak Grove Dr. Pasadena CA 91109 USA, and* **The MISR Team**

In mid-December 1999, the NASA Earth Observing System's Terra satellite, carrying the Multi-angle Imaging SpectroRadiometer (MISR) instrument, was launched into a sun-synchronous, near-polar orbit with a 16-day repeat cycle. MISR data acquisition began on February 24, 2000; the nominal mission is six years, but as of 2006,

Table 8. Overview of MISR tropospheric chemistry data products.

Retrieved quantity	Horizontal resolution (km)	Vertical resolution	Typical accuracy	Typical precision	References of retrieval algorithm	Validation references
MISR AOT	17.6 km	Total Column	Better than 0.05 ±20% AOT†	Between 0.025 and 0.05†	Martonchik et al., [1] 1998; [2] 2002; [3] Diner et al., 2005; [4] Kahn et al., 2001	[5] Kahn et al., 2005; [6] Abdou et al, 2005; [7] Kalashnikova & Kahn, 2006; [8] Chen et al., 2006; [5] Kahn, Gaitley, et al., 2005
MISR Aerosol properties (Angstrom exponent, single scatter albedo, size, sphericity)	17.6 km	Column Average	Currently being assessed†	Over dark surface, with AOT>~0.15: 3-5 groupings based on particle size distribution, 2-4 groupings of SSA, at least two shape groupings†	[9] Kahn et al., 1997; [10] 1998; and refs. above	See refs. above
MISR Stereo-Derived Plume Height	1.1 km	About 20 steps over the troposphere	~ 0.5 to 1.0 km	~ 0.5 km	[11] Moroney et al., 2002	[12] Muller et al., 2002; Naud et al., [13] 2002; [14] 2004

†Depends on conditions: surface brightness & variability, AOT & aerosol type, cloud situation, etc.; see references. Particle microphysical properties are difficult to retrieve when mid-visible AOT is lower than about 0.15 over dark surfaces. Coincident column-average property validation data are also difficult to obtain. Values presented are for good, but not ideal, cloud-free viewing conditions.

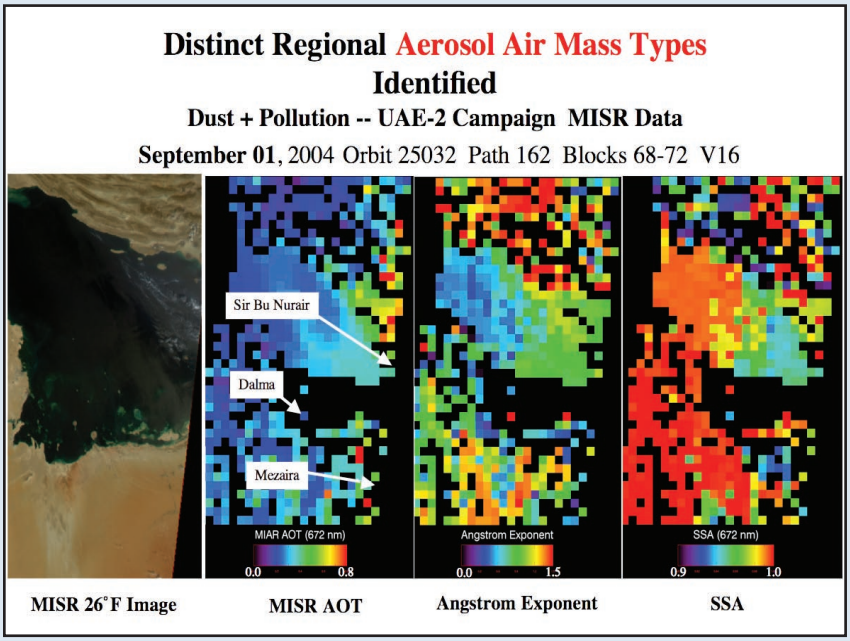

Figure 10. An example of MISR aerosol air mass type identification, based on particle microphysical properties retrieved from space. The first panel shows the MISR true-color image of a 400 km wide swath crossing Iran, the Arabian Gulf, and south to the United Arab Emirates and Bahrain, taken on September 01, 2004, Orbit 25032, Path 162, Blocks 68-72. Subsequent panels give the MISR-retrieved aerosol optical depth, aerosol angstrom exponent, and red-band single-scattering albedo, respectively, for the same region. Differences, especially in single-scattering albedo and angstrom exponent, for five distinct aerosol air masses stand out. These are associated with different mixtures of desert dust and pollution in the aerosol column. The results are being validated with coincident AERONET sun photometer and in situ measurements made as part of the UAE2 field campaign. (From Kahn et al., 2007 [15])

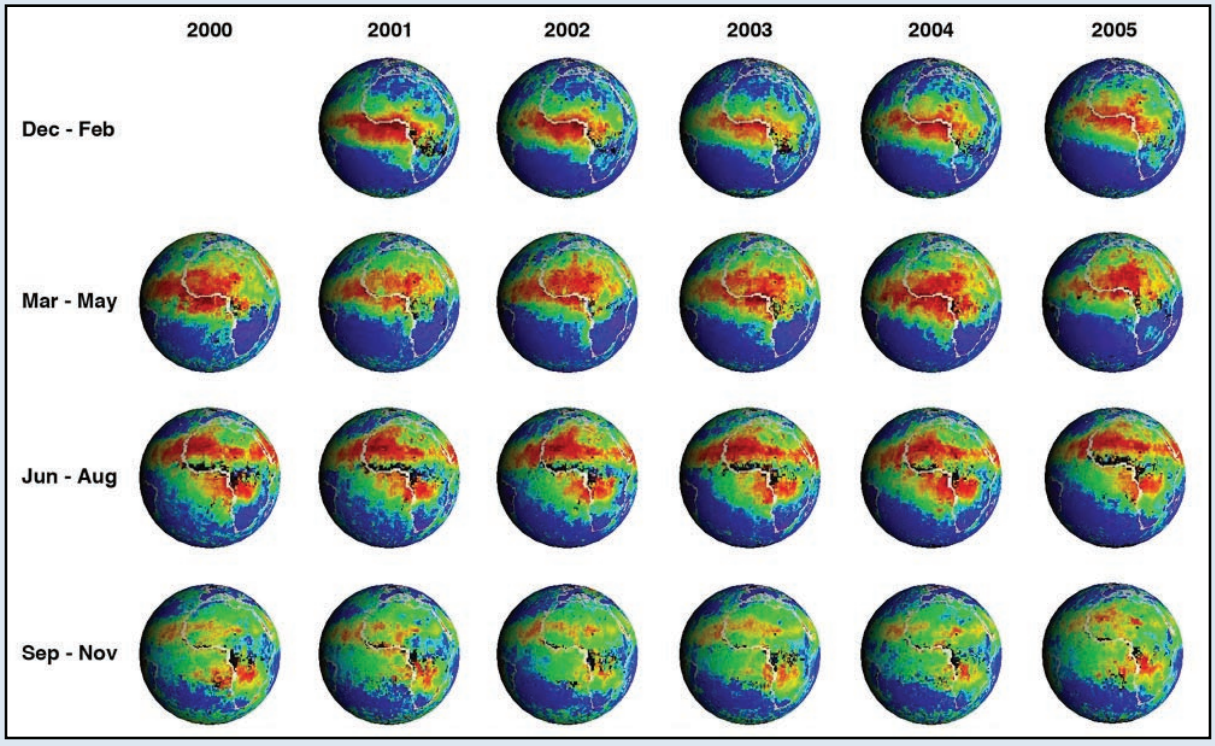

Figure 11. Six years of MISR global aerosol optical depth showing seasonal and inter-annual variations. Additional observations include particle size and shape.

the instrument and spacecraft are estimated to have an additional six to twelve years of operational life.

Scientific Questions

The major scientific goals of MISR are to study the properties of clouds, Earth's surface, and aerosols. MISR strengths include the ability to retrieve aerosol optical thickness even over bright surfaces such as deserts, to distinguish spherical from non-spherical particles based on differences in single-scattering phase function, to provide some information about particle size and single-scattering albedo, and to extract the heights of discrete aerosol plumes and clouds.

Instrument Description

The instrument images Earth with nine cameras pointed at angles varying from +70˚, through nadir, to -70˚ in the along-track direction, in a fixed-position, push-broom configuration, each having four line-array CCDs covering spectral bands centered at 446, 558, 672, and 867 nm, and having spectral widths between 20 and 40 nm, giving a total of 36 channels. MISR's swath width is about 400 km, and its highest spatial sampling is 275 m at all angles. The standard acquisition mode provides full resolution data in all four nadir-viewing channels and the red-band channels at the other eight angles; the remaining 24 channels are reported at 1.1 km. With Local Mode acquisitions, specially planned in advance, all 36 channels are reported at full resolution for close to the entire swath width and 300 km along-track. Global coverage is obtained about once per week at mid-to-low latitudes, and every two days near the poles.

Retrieval Description

The MISR Standard Aerosol Retrieval Algorithm is documented by references in Table 8. The algorithm operates on patches of 16 x 16 1.1 km pixels. It initially selects pixels that meet a series of criteria, which include tests against cloudiness, topographic complexity, and shallow water. The algorithm then determines whether the scene is suitable for a coupled surface-atmosphere (over land) or dark water retrieval. The coupled algorithm assumes the angular shape of the surface radiance is nearly independent of wavelength, and uses the spatial variation of surface brightness in the angular signature to separate surface from atmospheric contributions. Both surface spectral bidirectional reflectance distribution function (BRDF) and aerosol quantities are self-consistently retrieved. Over water, the surface is modeled as dark and Fresnel-reflecting, assuming climatological wind speeds. Over land or water, the atmospheric path radiance is compared to simulated MISR radiances, appropriate to the sun and viewing geometry, for a range of optical depths and a range of assumed aerosol components and mixtures. Chi-squared tests determine which subset of aerosol mixtures in the database meet a set of acceptance criteria; the subset defines the solution space and uncertainty for that retrieval. This algorithm runs automatically on the entire MISR data set.

Plume heights are derived from stereographic feature matching, a geometric process independent of radiometric calibration. Research Retrieval algorithms for aerosol properties and plume heights can provide greater precision, but can be run only on selected individual cases and can not be archived in the operational data stream. For aerosol optical depth and properties, the research algorithm can also provide higher horizontal resolution and a much larger space of candidate aerosol mixtures and components; the research height algorithm offers greater vertical resolution and greater sensitivity to thin hazes.

Data accessibility

All data, documentation, and data handling tools are distributed through the NASA Langley Atmospheric Sciences Data Center: http://eosweb. larc.nasa.gov/PRODOCS/misr/table_misr.html

Assistance with this archive is provided by ASDC User Services: larc@eos.nasa.gov

References

[1] Martonchik, J.V., D.J. Diner, R. Kahn, M.M. Verstraete, B. Pinty, H.R. Gordon, and T.P. Ackerman, 1998, Techniques for the Retrieval of aerosol properties over land ocean using multiangle data, *IEEE Trans. Geosci. Remt. Sensing 36,* 1212-1227.

[2] Martonchik, J.V., D.J. Diner, K.A. Crean, and M.A. Bull, 2002. Regional aerosol retrieval results from MISR, *IEEE Transact. Geosci. Remt. Sens. 40,* 1520-1531.

[3] Diner, D.J., J.V. Martonchik, R.A. Kahn, B. Pinty, N. Gobron, D.L. Nelson, and B.N. Holben, 2005, Using angular and spectral shape similarity constraints to improve MISR aerosol and surface retrievals over land, *Rem. Sens. Environ. 94,* 155-171.

[4] Kahn, R., P. Banerjee, and D. McDonald, 2001, The Sensitivity of Multiangle Imaging to Natural Mixtures of Aerosols Over Ocean, *J. Geophys. Res., 106,* 18219-18238.

[5] Kahn, R., B. Gaitley, J. Martonchik, D. Diner, K. Crean, and B. Holben, 2005, MISR global aerosol optical depth validation based on two years of coincident AERONET observations, *J. Geophys. Res.,* doi:10:1029/2004JD004706.

[6] Abdou, W.A., D.J. Diner, J.V. Martonchik, C.J. Bruegge, R.A. Kahn, B.J. Gaitley, K.A. Crean, L.A. Remer, and B. Holben, 2005, Comparison of coincident MISR and MODIS aerosol optical depths over land and ocean scenes containing AERONET sites, *J. Geophys. Res.,* doi:10.1029/2004JD004693.

[7] Kalashnikova, O.V. and R.A. Kahn, 2006, The ability of multi-angle remote sensing observations to identify and distinguish mineral dust types: Part 2. Sensitivity data analysis, *J. Geophys. Res., 111,* D11207, doi:10.1029/2005JD006756.

[8] Chen, W-T., R. Kahn, W-H. Li, and J. Seinfeld, 2006, Sensitivity of multi-angle imaging to optical and microphysical properties of biomass burning particles, *J. Geophys. Res.,* submitted.

[9] Kahn, R., P. Banerjee, D. McDonald, and D. Diner, 1998, Sensitivity of Multiangle imaging to Aerosol Optical Depth, and to Pure-Particle Size Distribution and Composition Over Ocean, *J. Geophys. Res., 103,* 32,195-32,213.

[10] Kahn, R., R. West, D. McDonald, B. Rheingans, and M.I. Mishchenko, 1997, Sensitivity of Multi-angle remote sensing observations to aerosol sphericity, *J. Geophys. Res., 102,* 16861-16870.

[11] Moroney, C., R. Davies, and J-P. Muller, 2002, MISR stereoscopic image matchers: Techniques and results, *IEEE Trans. Geosci. Remt. Sens. 40,* 1547-1559.

[12] Muller, J-P, A. Mandanayake, C. Moroney, R. Davies, D.J. Diner, and S. Paradise, 2002, Operational retrieval of cloud-top heights using MISR data, *IEEE Trans. Geosci. Remt. Sens. 40,* 1532-1546.

[13] Naud, C., J-P. Muller, and E.E. Clothiaux, 2002, Comparison of cloud top heights derived from MISR stereo and MODIS CO_2-slicing. *Geophys. Res. Lett. 29,* (10),1029/2002 GL015460.

[14] Naud, C., J. Muller, M. Haeffelin, Y. Morille, and A. Delaval, 2004, Assessment of MISR and MODIS cloud top heights through inter-comparison with a back-scattering lidar at SIRTA, *Geophys. Res. Lett., 31,* L04114, doi:10.1029/2003GL018976.

[15] R. Kahn et al., Desert Dust and Pollution Aerosol Air Mass Mapping From Space-based Multi-angle Imaging, *J. Geophys. Res.,* 2007, to be submitted

MODIS / Terra & Aqua

Contributed by **Lorraine Remer** (Lorraine.A.Remer@nasa.gov) *Laboratory for Atmospheres, NASA Goddard Space Flight Center, Code 913 Greenbelt, MD 20771 USA*

MODIS/Terra was launched December 1999 and began data collection in February 2000.

MODIS/Aqua was launched May 2002 and began data collection in July 2002.

Both satellites are in sun-synchronous near-polar orbit. Terra is descending with equator crossing time of 1030. Aqua is ascending with equator crossing time of 1330. The designed lifetime is for 6 year missions, but Terra just underwent a Senior review with the result of a 5 year extension to the mission.

Scientific Questions

The MODIS instrument was designed to:

- help build a global aerosol climatology,
- better quantify aerosol contributions to global change and climate,
- and contribute to our understanding of aerosol impacts on air quality and human health

Instrument Description

MODIS has 36 channels with varying spatial resolution of 250 m, 500 m and 1000m, depending on the channel. The channels span the spectral range from 410 nm to 14200 nm, and bandwidth varies from channel to channel. MODIS uses a scanning mirror to observe a 2330 km cross track swath, which allows full global coverage in 2 days.

Retrieval Description

There are two independent aerosol retrieval algorithms applied to MODIS data. One is for retrievals over ocean and the other over land. The following descriptions apply to data available as Collection 004 or 005.

The over-ocean algorithm assumes a rough ocean surface with constant wind speed of 6 m/s and all channels with no suspended pigments except for the 550 nm channel where the water-leaving radiance is 0.005. The algorithm matches the measured reflectance in six channels (550, 660, 870, 1240, 1630 and 2130 nm) to Look-Up Table values and returns: the aerosol optical thickness at 550 nm; an aerosol model consisting of one well-defined fine mode and one well-defined coarse mode; and the ratio between the two modes. This in effect provides the optical thickness and information about the aerosol size. The size parameter is reported in several forms: spectral aerosol optical thickness, Angstrom Exponent, effective particle radius and fine mode fraction. Although there are different forms of the size parameter, they all derive from the selection of aerosol model and therefore are not independent pieces of information.

The over-land algorithm makes independent retrievals in two channels: 470 nm and 660 nm, then interpolates between them to also report a value at 550 nm. The land

Table 9. Overview of MODIS tropospheric chemistry data products.

Retrieved quantity	Horizontal resolution (km)	Vertical resolution	Typical accuracy	Typical precision	References of retrieval algorithm	Validation references
Aerosol optical depth (unitless)	10 or 1 degree	column	(ocean) ±0.03±5%AOD (land) ±0.05±15%AOD		[1] Remer et al. (2005) [2] Kaufman et al. (1997) [3] Tanré et al. (1997)	[1] Remer et al. (2005) [4] Ichoku et al. (2005)
Ratio fine mode aod to total aod (fine mode fraction) over ocean	10 or 1 degree	column	±0.25		[1] Remer et al. (2005) [3] Tanré et al. (1997)	[5] Kleidman et al. (2005)
Effective radius over ocean	10 or 1 degree	column	±30%		[1] Remer et al. (2005) [3] Tanré et al. (1997)	[6] Remer et al., (2002) [1] Remer et al. (2005)

Scientific Highlight – MODIS

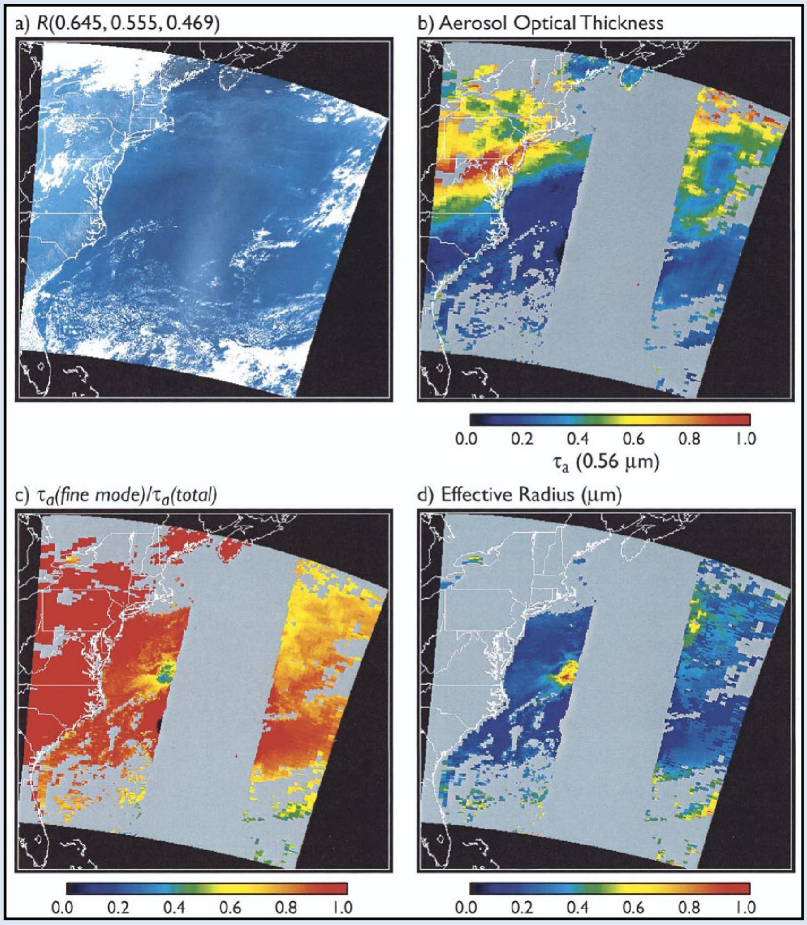

Figure 12. Aerosol optical properties over the Eastern United States on May 4, 2001. Panel (a) is a true color composite of one MODIS granule, showing cloud cover over northern New York, central Florida, and the nearby Atlantic Ocean. Panels (b) and (d) show the aerosol optical thickness at 0.56 μm and the effective radius derived for this scene, showing pollution along the Ohio Valley and transport to the north Atlantic. Panel (c) shows the ratio of fine to total aerosol optical thickness. Gray areas denote areas where no retrieval is possible due to sun-glint, bright land, and clouds. (From King et al., 2003 [7])

algorithm assumes that surface reflectance in each of the visible channels (470 and 660 nm) can be estimated from the top of atmosphere value of reflectance at 2130 nm using empirical relationships. Multi-modal aerosol models are assumed based on geography and season. A dust model is offered as an alternative choice. The land algorithm provides aerosol optical depth in 3 visible channels, an Angstrom Exponent calculated from those channels and a very qualitative fine mode fraction.

The retrieval over land is not as accurate as the retrieval over ocean.

Data accessibility

The Collection 004 data can be obtained from the Goddard DAAC.

MODIS-Terra data are available at:

http://eosdata.gsfc.nasa.gov/daac-bin/MODIS/Data_order.pl?PRINT=1

MODIS-Aqua data are available at:

http://eosdata.gsfc.nasa.gov/daac-bin/MODIS/Data_order.pl?PRINT=1&AQUA_DATA=1

The Collection 005 data can be obtained from the AADS Web site:

http://aadsweb.nascom.nasa.gov/

For all documentation, for disclaimers and updates, for information concerning the differences between Collections 004 and 005, go to the MODIS Atmospheres web site:

http://modis-atmos.gsfc.nasa.gov/

The Spotlight section in the right hand column gives the latest news.

References

[1] Remer, L. A., Kaufman, Y. J., Tanré, D., Mattoo, S., Chu, D. A., Martins, J. V., Li, R.-R., Ichoku, C., Levy, R. C., Kleidman, R. G., Eck, T. F., Vermote, E. and Holben, B. N., 2005, The MODIS aerosol algorithm, products and validation., *J. Atmos. Sci., 62* (4), 947-973.

[2] Kaufman, Y.J., D. Tanré, L.A. Remer, E. Vermote, A. Chu and B.N. Holben, 1997, Operational remote sensing of tropospheric aerosol over land from EOS moderate resolution imaging spectroradiometer. *J. Geophys. Res., 102,* 17051-17067.

[3] Tanré, D., Y.J. Kaufman, M. Herman and S. Mattoo, 1997, Remote sensing of aerosol properties over oceans using the MODIS/EOS spectral radiances. *J. Geophys. Res., 102,* 16971-16988.

[4] Ichoku, C., Remer, L. A. and Eck, T. F., 2005, Quantitative evaluation and intercomparison of morning and afternoon MODIS aerosol measurements from the Terra and Aqua satellites, *J. Geophys. Res., 110,* D10S03, doi:10.1029/2004JD004987.

[5] Kleidman, R. G., O'Neill, N. T., Remer, L. A., Kaufman, Y. J., Eck, T. F., Tanré, D., Dubovik, O. and Holben, B. N., 2005, Comparison of MODIS and AERONET remote sensing retrievals of aerosol fine mode fraction over ocean., *J. Geophys. Res., 110,* D22205, doi:22210.21029/22005/JD005760.

[6] Remer, L.A., D. Tanré, Y.J. Kaufman, C. Ichoku, S. Mattoo, R. Levy, D.A. Chu, B.N. Holben, O. Dubovik, A. Smirnov, J.V. Martins, R.-R. Li and Z. Ahmad, 2002, Validation of MODIS aerosol retrieval over ocean. *Geophys. Res. Lett., 29,* 10.1029/2001GL013204.

[7] King, M. D., Menzel, W. P., Kaufman, Y. J., Tanré, D., Gao, B.-C., Platnick, S., Ackerman, S. A., Remer, L. A., Pincus, R. and Hubanks, P. A., 2003, Cloud and aerosol properties, precipitable water, and profiles of temperature and humidity from MODIS., *IEEE Trans. Geosci. Remote Sens., 41,* 442-458.

SCIAMACHY / ENVISAT

Contributed by **John P. Burrows** (burrows@iup.physik.uni-bremen.de) *Institute of Environmental Physics and Remote Sensing IUP/IFE University of Bremen - FB1 Postfach 330440 28334 Bremen Germany*

The SCIAMACHY (Scanning Imaging Absorption spetroMeter for Atmospheric CHartographY) proposal was submitted in response to an ESA open call in July 1988 for instrumentation to fly on its Polar Platform. After peer review, SCIAMACHY was selected for flight, prior to GOME-1. The ESA Polar Platform, renamed ENVISAT and comprising ten experiments, was launched on 28 February 2002 into a sun synchronous polar low earth orbit, LEO, having an equator crossing time of 10.00am in descending node. Global coverage of the alternate limb and nadir observations is achieved in 6 days at the equator and more rapidly at higher altitudes. Solar occultation measurements and calibration are made in the northern hemisphere on every orbit and lunar occultation in the southern hemisphere, when viewing is possible. After a commissioning period, routine measurements from SCIAMACHY began at the end of July 2002.

Scientific Questions

As a result of both natural phenomena and anthropogenic activity, the composition of the atmospheric trace constituents is changing and impacting on the conditions at the earth's surface. The SCIAMACHY project was initiated to improve our knowledge of the physical and chemical processes, which determine the composition and behavior of the atmosphere. SCIAMACHY observations yield a three dimensional view of atmospheric constituents and parameters, which absorb or emit in the solar spectral region, from the earth's surface to approximately 100 km.

Current Targeted Tropospheric Constituents:

Trace gases (Ozone, O_3, Nitrous oxide, N_2O, Nitrogen Dioxide NO_2, Carbon Monoxide, CO, Formaldehyde, HCHO, Sulfur Dioxide, SO_2, Glyoxal, CHO.CHO, Carbon Dioxide, CO_2, Methane, CH_4, and water vapor, H_2O and Bromine Oxide, BrO) aerosol, cloud parameters and surface spectral reflectance.

Scientific Highlights – SCIAMACHY

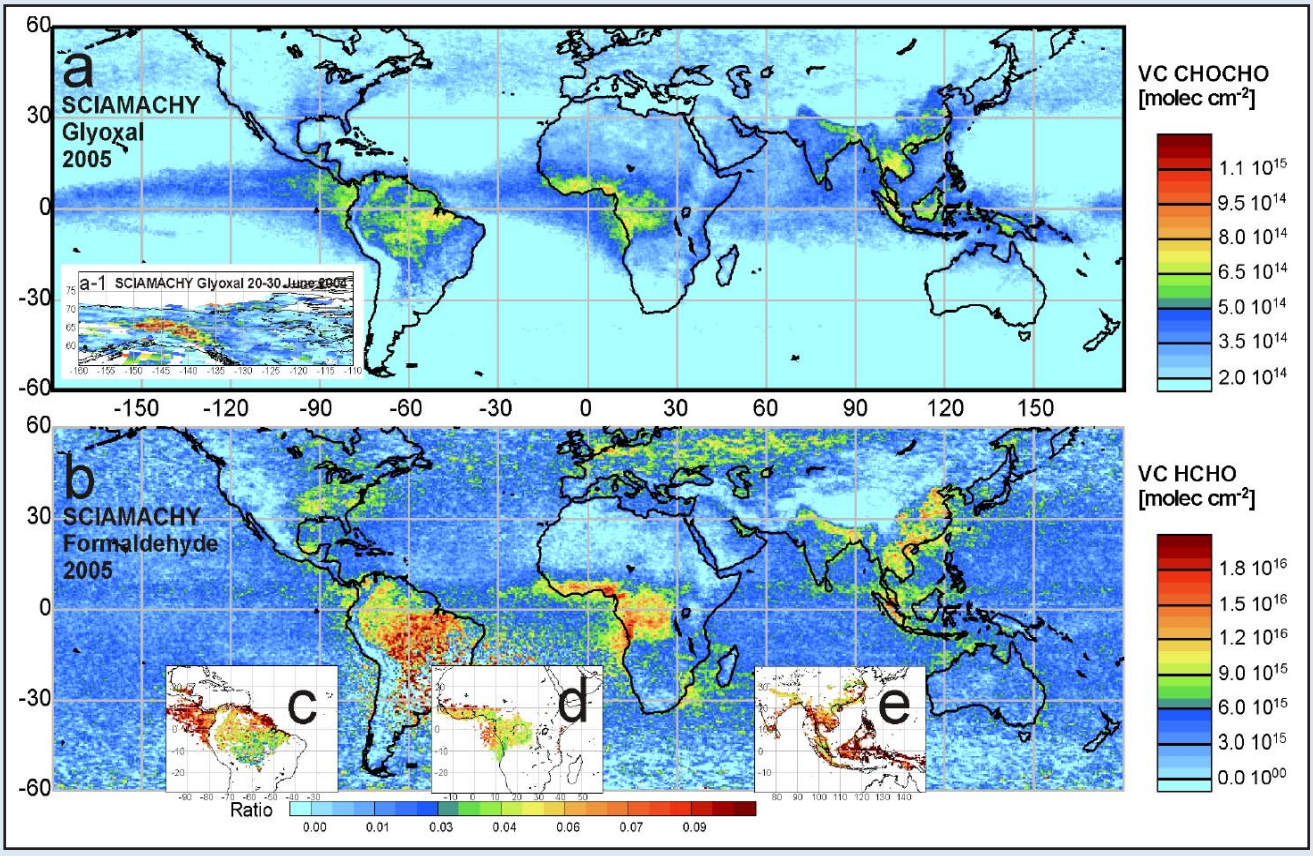

Figure 13. Annual mean composite maps derived from SCIAMACHY (Courtesy of F. Wittrock, A. Richter and J Burrows University of Bremen), of a) global glyoxal CHO.CHO, a1) CHO.CHO over Alaska during biomass burning in 2005, b) formaldehyde HCHO, derived from SCIAMACHY observations in 2005. The maps (c) to (e) show the ratio between measured CHOCHO and HCHO.

Scientific Highlights, cont. – SCIAMACHY

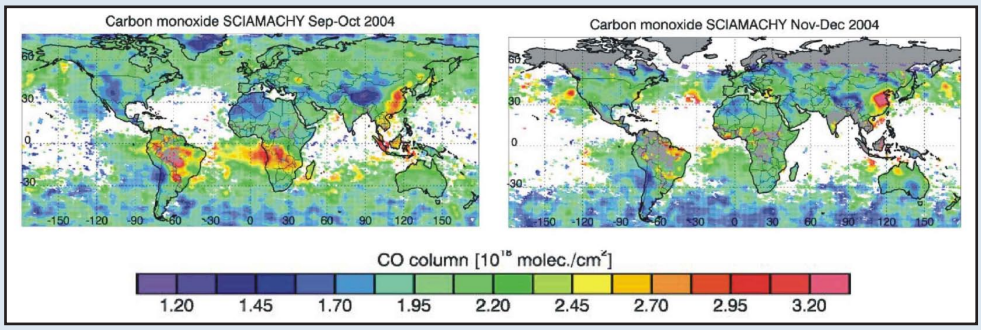

Figure 14. Bimonthly composites of CO observed form SCIAMACHY after cloud screening and data quality checking (courtesy of M. Buchwitz, I. Khlystova, and J. P. Burrows, University of Bremen). CO from pollution and biomass burning is transported around the globe in both hemispheres.

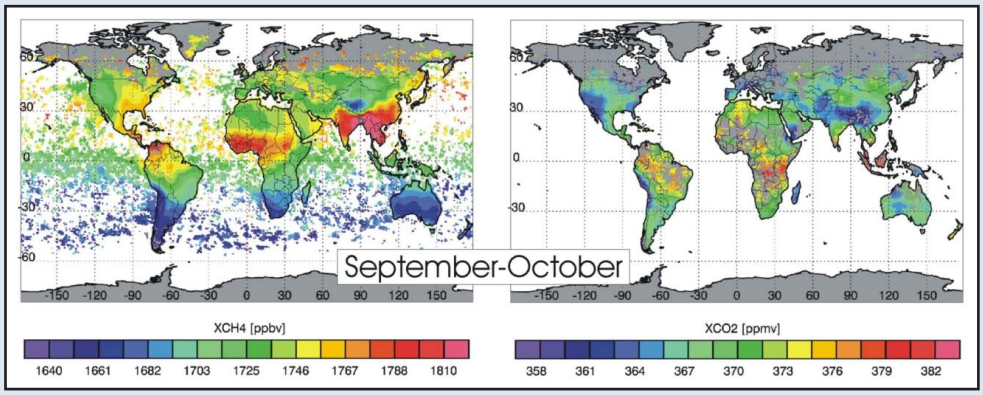

Figure 15. The bimonthly composite of the dry columns of methane and carbon dioxide in 2003 (courtesy of Buchwitz, Schneising and Burrows University of Bremen) is presented. The release of methane from the biosphere at high latitudes and low latitudes is visible. Similarly the uptake of carbon dioxide by the biosphere, in particular the boreal forests, is dramatic in the growing season. Emission of carbon dioxide is also observed from biomass burning.

For tropospheric research applications, SCIAMACHY has extended the visible and near infrared observations of GOME-1 and makes higher spatial resolution measurements. Improved accuracy of tropopsheric constituents with significant stratospheric amounts is achieved using the matched limb nadir observations. The combination of GOME and SCIAMACHY has been used to determine the changes of NO_2 and SO_2 amount and emissions over the last decade, 1995-2005. The remarkable increase in emissions over parts of Asia and significant decreases over parts of Europe and America have been identified. NO_2 resulting from fossil fuel combustion and biomass burning (even from shipping) and from lightning has been observed and interpreted. Recently the control of NO_x emissions by its removal from power plant emissions during summer in the Ohio valley in the U.S.A. could be quantified using SCIAMACHY and GOME- data records. The observations of Formaldehyde, HCHO, which results from fossil fuel combustion, biomass burning, the oxidation of methane and biogenic emissions of volatile organic compounds has been used to estimate emissions. Recently Glyoxal, CHO.CHO, has been observed using SCIAMACHY observations. CHO.CHO is produced in the oxidation of non-methane hydrocarbons. SCIAMACHY is the first instrument to successfully utilize short wave infrared measurements for the retrieval of the columns of CO. The first measurements of the total dry column of the greenhouse gases CO_2 and CH_4 from space have also been retrieved. SCIAMACHY has demonstrated that the global measurement of greenhouse gases from space provides unique information of value for global change research. The CH_4 measurements indicate unforeseen sources of CH_4 in wetlands.

Tropospheric Scientific Applications:

a) The Transport and Transformation of atmospheric pollution in the troposphere.

b) The global distribution and variability of the greenhouse gases

Instrument Description

SCIAMACHY measures the back-scattered solar radiation upwelling from the top of atmosphere, TOA, alternately in nadir and limb viewing geometry. In addition it measures solar and lunar occultation and the extra terrestrial solar irradiance. The instrument comprises a telescope, a calibration unit, spectrometer and electronic and thermal sub systems. Eight channels, comprising gratings optics and a linear diode array detector, measure contiguously the spectrum between 214 and 1750 nm at resolutions between 0.2 and 1.4 nm, and on two spectral bands around 2.0 µm and 2.3 µm, having a spectral resolution of 0.2 nm. In addition there are seven broad band polarisation monitoring detectors, PMD, which measure the TOA radiance polarized parallel to the entrance slit of the instrument, at selected broad bands of wavelength between 0.3 and 2.4µm. In Limb viewing, the instrument scans from the surface to approximately 95 km. At each tangent height, four measurements of the radiance are made. The spectral channels observe with a horizontal dimension of 240 km and a vertical sampling

Table 10. Overview of SCIAMACHY tropospheric chemistry data products.

Retrieved quantity or Data Product [Unit]	Nadir Horizontal resolution[a] along x across track (km x km)	Vertical resolution	Threshold i.e. S/N =1 and Accuracy[b]	References: Retrieval Precision, Validation and Model Comparison
O_3 Total Column Profile O_3 Tropical Tropospheric column Ozone [DU]	30x60 30x30 30x60 30x30	Total Column Tropospheric Column	n.a.: 1% na.: ~(20-40)%	[1,4, 20, 23, 32]
SO_2 [molecules/cm^2]	30x60 30x60	Column	~5x10^{15} : 20-40%	[1,4]
Tropospheric NO_2 [molecules/cm^2]	30x60 30x30	Column	1x10^{15}: 20-40%	[11, 23, 32, 33, 34, 35, 36]
HCHO [molecules/cm^2]	30x60	Column	8x10^{15}: 20-40%	[37]
CHO,CHO [molecules/cm^2]	30x60	Column	2x10^{14}: 20-40%	[37]
BrO [molecules/cm^2]	30x60	Column	1x10^{13}: 20-40%	[12, 13, 38]
CO [molecules/cm^2]	30x120	Column	2x10^{17}:10-20%	[6, 7, 15, 16, 17, 19, 24, 26, 27, 40, 41, 44, 48]
CO_2, XCO_2 [molecules/cm^2, mixing ratio]	30x60, 30x120	Column, Dry Column Mixing ratio	n.a.: 2% n.a.: 2%	[6, 7, 15, 16, 18, 19, 27, 39, 40, 45, 46, 47]
CH_4 , XCH_4 [molecules/cm^2, mixing ratio]	30x60, 30x120	Column Dry Column Mixing Ratio	n.a.: 1-2% n.a.: 1-2%	[6, 7, 15, 16, 18, 19, 25, 26, 27, 40, 42, 43]
Water Vapor [molecules/cm^2]	30x30 30x60	Column	n.a.:<10%	[6, 10, 22]
Aerosol	30x30 30x60	Column	See reference	[49, 50]

[a] During every orbit, SCIAMACHY (references 1-5), after a solar occultation, makes alternate nadir and limb measurements. This strategy is selected to provide simultaneous stratospheric and mesospheric profiles of species for the nadir observations: the limb state being matched to the nadir state, which comprises many individual ground scenes. Similar to GOME-1 the nadir swath is 960 km, yielding global coverage of limb and nadir observations in 6 days. The spatial resolution, however, surpasses that of GOME-1, at ~30km (along track) x 15km (across track). As a result of data rate limitations the majority of measurements have ground scenes of 30x30 km x km or 30x60 km x km. For the SWIR array channels (Ch#7 1940-2040 nm & Ch#8 2265-2380 nm) the spatial resolution is 30x120 km x km. The instrument and its modes of operation are described in references 1-5.

[b] The threshold represents the value of the data product for an effective S/N = 1. The accuracy refers to typical values for columns or profile ~3x the threshold and higher. Refer to note b) of the GOME-1 table for more details of the origin or error. Outside the 400 nm -1600 nm band the instrumental read-out noise as well as shot noise is significant. As a result of a detector error at around 360 nm, the threshold values for HCHO detection and BrO detection are somewhat poorer than GOME-1 although at high spatial resolution. The radiative transfer code SCIATRAN [6, 8, 34] and some other codes have been extensively used in the determination of air mass factor or their equivalent.

of 2.6 km, the tangent height steps being 3 km. The PMD are read out more rapidly and have a horizontal sampling of ~40 km and vertical sampling of 2.6 km. For nadir viewing, the ground scene of the detector array varies between 30x15 to 30x120 km^2 whereas simultaneously the PMD observe a ground scene of 32 x 7 km^2.

Data accessibility

SCIAMACHY data products of relevance for atmospheric research, or links to SCIAMACHY data products, can be found at:

http://earth.esa.int/

http://www/iup.physik.uni-bremen.de/sciamachy/

http://www.accent-network.org/portal/integration-tasks/satellite-observations-at2

http://troposat.iup.uni-heidelberg.de/AT2/Data_available/Data_available.htm

Acknowledgments

SCIAMACHY is a national contribution to ESA, funded by Germany, The Netherlands and Belgium. ESA is responsible for ENVISAT. Thanks to the large team of scientists and engineers that are maintaining and exploiting SCIAMACHY data for scientific research and the development of services related to chemical weather and climate change.

References

[1] Burrows J. P., et al., 1995, *Acta Atronautica 35* (7) 445-451.
[2] Noel, S. et al., 1998, *SPIE, 3498*, 94-104.
[3] Noel, S. et al., 1999, *Earth, 24* (5), 427-434.
[4] Bovensmann, H. et al., 1999, *Atmospheric Sciences, 56,* 127-150.
[5] Noel, S. et al., 2002, *Adv. Space Res., 26* (12), 1949-1954.
[6] Buchwitz, M. et al., 1999, SPIE, 3495,171-186.
[7] Buchwitz, M. et al., 2000, *J. Geophys. Res., 105* (D12, 15,231-15246, doi:10.1026/2000JD900191.
[8] Rozanov, V.V. et al., 2002, *Adv. Space Research, 29,* 11, 1831-1835.
[9] Kokhanovsky, A. A. et al., 2003, *J. Geophys. Res., 108* (D1), 4008, doi:10.1029/2001JD001543.
[10] Noel, S., M. Buchwitz, J.P. Burrows, 2004, *Atmos. Chem. Phys., 4, 111-125.*
[11] Heue, K.-H. et al., 2005, *Atmos. Chem. Phys., 5,* 1039-1051.
[12] Afe, O. T. et al., 2004, *Geophys. Res. Lett., 31,* L24113, doi:10.1029/2004GL020994.
[13] Kaleschke, L. et al., 2004, *Geophys. Res. Lett., 31,* L16114, doi:10.1029/2004GL020655.
[14] de Beek, R. et al., 2004, *Advances in Space Research, 34,* 734-738.
[15] Buchwitz, M. et al., 2004a, *Advances in Space Research, 34,* 809-814, doi:10.1016/j.asr.2003.05.054.
[16] Buchwitz, M. et al., 2004b, J.P. Burrows, *SPIE 5235,* 375-388.
[17] Buchwitz M. et al., 2004c, *Atmos. Chem. Phys., 4,* 1954-1960.
[18] Buchwitz, M. et al., 2004d, *Atmos. Chem. Phys. Discuss., 4,* 7217-7279, and 2005a, *Atmos. Chem. Phys., 5,* 941-962.
[19] Buchwitz M. et al 2005b, Proceedings of ENVISAT Symposium 2004, 6.-10.9.2004, Salzburg, Austria, Special Publication SP-572 (CD-ROM) from ESA publications division.
[20] Bracher, A. et al., 2005, *Atmospheric Chemistry and Physics, 5,* 2357-2368.
[21] Eskes, H. J. et al., 2005, *Atmospheric Chemistry and Physics Discussions, 5,* 4429-4475.
[22] Noël, S. et al., 2005, *Atmos. Chem. Phys., 5,* 1835-1841.
[23] Richter, A. et al., 2005, *Nature, 437,* 129-132, doi: 10.1038/Nature04092.
[24] Buchwitz M. et al, 2005, *Atmos. Chem. Phys. Discuss., 5,* 3313-3329.
[25] Frankenberg C., J. F. Meirink, M. van Weele, U. Platt, T. Wagner, 2005, *Science, 13* May 2005, 308(5724), 1010 – 10140.
[26] A.G. Straume et al., 2005, *Advances in Space Research, 36* (5), 821-827.
[27] Dils, B. et al., 2006, *Atmospheric Chemistry and Physics, 6,* 1953-1976.
[28] Kokhanovsky, A. A. et al., 2005a, *Adv. Space Res., 36,* 789-799.
[29] Kokhanovsky, A. A. et al., 2005b, *Atmos. Chem. Phys., 6,* 1905-1911.
[30] Rozanov A. et al., 2005, *Adv. Space Res., 36* (5), 1015-1019, doi:10.1016/j.asr.2005.03.012.
[31] Sinnhuber, B.-M. et al., 2005, *Geophys. Res. Lett., 32,* L20810, doi:10.1029/2005GL023839.
[32] Sierk, B. et al., 2006, *Environmental Monitoring and Assessment,* doi:10.1007/s10661-005-9049-9.
[33] Martin, R. V. et al., 2006, *J. Geophys. Res., 111,* D15308, doi:10.1029/2005JD006680.
[34] van der A, R. J. et al., 2006, *J. Geophys. Res., 111,* D12317, doi:10.1029/2005JD006594.
[35] Sussmann, R. et al., 2006, *Atmospheric Chemistry and Physics, 5,* 2657-2677.
[36] Kim, S.-W. et al., 2006, *Geophys. Res. Lett., 33,* L22812, doi:10.1029/2006GL027749.
[37] Wittrock, F. et al., 2006, *Geophys. Res. Lett., 33,* L16804, doi:10.1029/2006GL026310.
[38] Sheode, N. et al., 2006, *Atmos. Chem. Phys. Discuss., 6,* 6431-6466, 2006.
[39] Bösch, H. et al., 2006, *J. Geophys. Res. 111,* D23302, doi:10.1029/2006JD007080.
[40] Buchwitz, M. et al., 2006, *Atmos. Chem. Phys., 6,* 2727-2751.
[41] de Laat, A. T. J. et al., 2006, *Geophys. Res. Lett., 33,* L07807,doi:10.1029/2005GL025530.
[42] Frankenberg, C. et al., 2006, *J. Geophys. Res., 111,* D07303, doi:10.1029/2005JD006235.
[43] Houweling S. et al., 2006, *Geophys. Res. Lett., 33,* L15821, doi:10.1029/2006GL026162.
[44] Gloudemans, A. M. S. et al., 2006, *Geophys. Res. Lett., 33,* L16807,doi:10.1029/2006GL026804.
[45] Barkley, M. P. et al., 2006a, *Geophys. Res. Lett., 33,* L20805, doi:10.1029/2006GL026807.
[46] Barkley, M. P. et al., 2006b, *Atmos. Chem. Phys., 6,* 4483-4498.
[47] Barkley, M. P. et al., 2006c, *Atmos. Chem. Phys., 6,* 3517-3534.
[48] Buchwitz, M. et al., 2007, *Atmos. Chem. Phys. Discuss., 7,* 405-428.
[49] von Hoyningen-Huene, W. et al., 2006, *Atmos. Chem. Phys. Discuss., 6,* 673-699.
[50] de Graaf, M. and P. Stammes, 2005, *Atmos. Chem. Phys. Discuss., 5,* 2385-2394.

ACE-FTS / SCISAT-1

Contributed by **Peter Bernath** (bernath@uwaterloo.ca), *Department of Chemistry, University of Waterloo, Waterloo, Ontario N2L 3G1, Canada.*

The Atmospheric Chemistry Experiment Fourier Transform Spectrometer (ACE-FTS) was launched onboard SCISAT-1 by NASA using a Pegasus XL rocket on 12 August 2003 for a nominal 2-year mission.

Scientific Questions

The primary goals of the ACE mission are to:

- understand the chemical and dynamical processes that control the distribution of ozone in the stratosphere and upper troposphere, particularly in the Arctic;
- explore the relationship between atmospheric chemistry and climate change;
- study the effects of biomass burning in the free troposphere; and
- measure aerosols and clouds to reduce the uncertainties in their effects on the global energy balance.

Instrument Description

The ACE-FTS is a high resolution (0.02 cm^{-1}) infrared Fourier transform spectrometer (FTS) operating from 2 to 13 microns (750-4400 cm^{-1}), measuring the vertical distribution of trace gases, particles and temperature by solar occultation [1]. During sunrise and sunset, the FTS measures sequences of atmospheric absorption spectra in the limb viewing geometry with different slant paths and tangent heights; when these spectra are analyzed, the results are inverted into vertical profiles of atmospheric constituents. Aerosols and clouds are monitored using the extinction of solar radiation at 1.02 and 0.525 microns as measured by two filtered imagers. The vertical resolution is about 3 - 4 km from about 5 km up to about 100 km.

A high inclination (74°), circular low earth orbit (650 km) gives ACE coverage of tropical, mid latitude and polar regions. This orbit provides about 30 occultations per day (15 sunrises and 15 sunsets) and the orbit was designed to repeat on an annual basis.

The ACE-FTS and imagers were built by ABB-Bomem in Quebec City, Quebec and the satellite bus was made by Bristol Aerospace in Winnipeg, Manitoba. ACE is the first mission in the Canadian Space Agency's small science satellite (SCISAT) program.

Table 11. Overview of ACE-FTS tropospheric chemistry data products.

Retrieved quantity	Horizontal resolution	Vertical resolution	Typical accuracy	Typical precision estimate (single-profile)*	Reference(s) of retrieval algorithm	Validation reference(s)
H_2O	3.5 km	3.5 km	(cal/val in progress)	4 %	[2] Boone et al. (2005)s	Validation of version 2.2 is underway.
O_3	3.5 km	3.5 km		4 %		
N_2O	3.5 km	3.5 km		4 %		
CO	3.5 km	3.5 km		6 %		
CH_4	3.5 km	3.5 km		4 %		
NO	3.5 km	3.5 km		15 %		
NO_2	3.5 km	3.5 km		7 %		
HNO_3	3.5 km	3.5 km		4 %		
HF	3.5 km	3.5 km		10 %		
HCl	3.5 km	3.5 km		10 %		
N_2O_5	3.5 km	3.5 km		20 %		
$ClONO_2$	3.5 km	3.5 km		15 %		
CCl_2F_2	3.5 km	3.5 km		4 %		
CCl_3F	3.5 km	3.5 km		4 %		
COF_2	3.5 km	3.5 km		15 %		
CHF_2Cl	3.5 km	3.5 km		10 %		
HDO	3.5 km	3.5 km		4 %		
SF_6	3.5 km	3.5 km		12 %		
OCS	3.5 km	3.5 km		12 %		
HCN	3.5 km	3.5 km		12 %		
CF_4	3.5 km	3.5 km		10 %		
CH_3Cl	3.5 km	3.5 km		50 %		
C_2H_6	3.5 km	3.5 km		12 %		

* Estimates exclude extreme cases where signal is weak.

Scientific Highlight – ACE-FTS

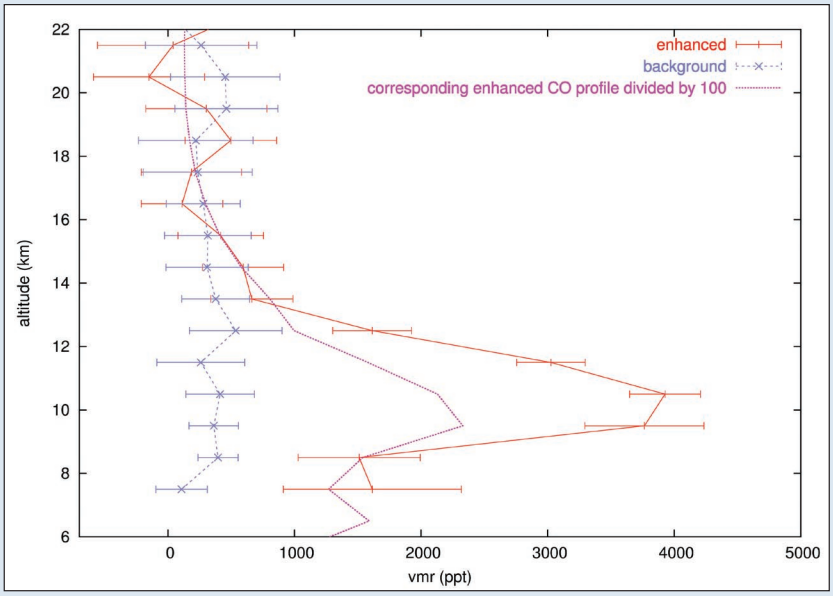

Figure 16. Enhanced methanol profile retrieved from a biomass burning plume from the sunset occultation ss6153 measured on 3 October 2004 at 30.2°S and 56.9°E. The CO profile retrieved for the same occultation is plotted for comparison as well as an example of background profile of methanol retrieved during the same time period and in the same latitude band [3].

Retrieval Description

The ACE instruments are "self calibrating" because reference spectra of the sun (I0) are recorded outside the earth's atmosphere. To be more specific, the observed atmospheric spectra (I) are divided by the appropriate reference solar spectrum and the resulting atmospheric transmission spectra (I/I0) are analyzed using Beer's law and a global fit approach [2]. The ACE level 2 data products are atmospheric height profiles of various constituents plus temperature and pressure, all reported on an interpolated 1 km grid. The vertical profiles are also provided on the measurement grid. The measurement grid is determined by the vertical sampling of the atmosphere, which varies from about 2 km to 6 km (in the absence of refraction) as a function of the beta angle of the orbit. The vertical resolution, however, is limited by the input field of view of 1.25 mrad of the FTS or about 4 km. The horizontal resolution along the field of view varies with height but is typically 500 km.

Version 1.0 of the ACE-FTS level 2 data has been generated at the University of Waterloo. This data set consists of concentration profiles of 18 molecules: H_2O, O_3, N_2O, CO, CH_4, NO, NO_2, HNO_3, HF, HCl, N_2O5, $ClONO_2$, CCl_2F_2, CCl_3F, COF_2, CHF_2Cl, HDO, SF_6, plus p and T, interpolated on a 1 km grid for sunrises from February through October 2004. Aerosol and cloud properties are being retrieved by individual research groups. Version 1.0 was intended primarily for validation exercises, but was also used for preliminary scientific investigations. A special issue of Geophysics Research Letters (http://www.agu.org/journals/ss/ACECHEM1/) was devoted to the first ACE results based on version 1.0 retrievals. The current version is 2.2 for the ACE-FTS processing and now includes the additional molecules HCN, CH_3Cl, CF_4, C_2H_2, C_2H_6, ClO and N_2 (for diagnostic purposes) in the routine processing. Version 1.0 processing for the Imagers is also available and the imager data product is atmospheric extinction at the two imager wavelengths of 525 nm and 1.02 microns.

Data accessibility

Version 1.0 of the ACE-FTS Level 2 data is freely available and more information is provided on the web site http://www.ace.uwaterloo.ca. The current version of the FTS data (Version 2.2) is available to science team members and will be released when validated. ACE is a third party ESA mission and data can also be obtained through ESA: http://earth.esa.int/missions/thirdpartymission/scisatace.html.

References

[1] P.F. Bernath et al., 2005, *Geophys. Res. Lett., 32,* L15S01, doi:10.1029/2005GL022386.

[2] C.D. Boone, R. Nassar, K.A. Walker, Y. Rochon, S.D. McLeod, C.P. Rinsland, P.F. Bernath, 2005, *Applied Optics, 44,* 7218.

[3] G. Dufour, C. D. Boone, C. P. Rinsland and P. F. Bernath, 2006, *Atmospheric Chemistry and Physics, 6,* 3463.

MLS / Aura

Contributed by **Lucien Froidevaux** (Lucien.Froidevaux@jpl.nasa.gov) *Jet Propulsion Laboratory, M/S 183-701, 4800 Oak Grove Drive, Pasadena, CA 91109 USA, and MLS team, Jet Propulsion Laboratory, Caltech, Pasadena*

The Earth Observing System (EOS) Microwave Limb Sounder (MLS) on the Aura satellite, launched July 15 2004, is a follow-up to the Upper Atmosphere Research Satellite (UARS) MLS. The satellite is in a 98.2° inclination (near-polar) orbit at about 705 km altitude, with 100 minute orbital period and 16 day repeat cycle.

Scientific Questions

The MLS is designed to address the following issues:

- How is stratospheric ozone and its chemistry changing

Table 12. Overview of MLS tropospheric chemistry data products.

Retrieved quantity (upper troposphere)[a]	Horizontal resolution (km)	Vertical resolution	Typical accuracy	Typical precision estimate (single-profile)	Reference(s) of retrieval algorithm	Validation reference(s)
O_3	165 km(al-t; along-track); 15 orbits/day	3 km		25 ppbv	[2], [3]	[4]
CO	300 km(al-t)	4.5 km		20 ppbv	[2], [3]	[4], [5]
H_2O	see O_3	3 km		15%	[2], [3]	[4], [6]

[a]Upper tropospheric retrievals are at pressures of 316, 215, and 147 hPa, but the tropopause can occur at pressures higher than some of these pressures (in particular at high latitudes).

Scientific Highlight – MLS

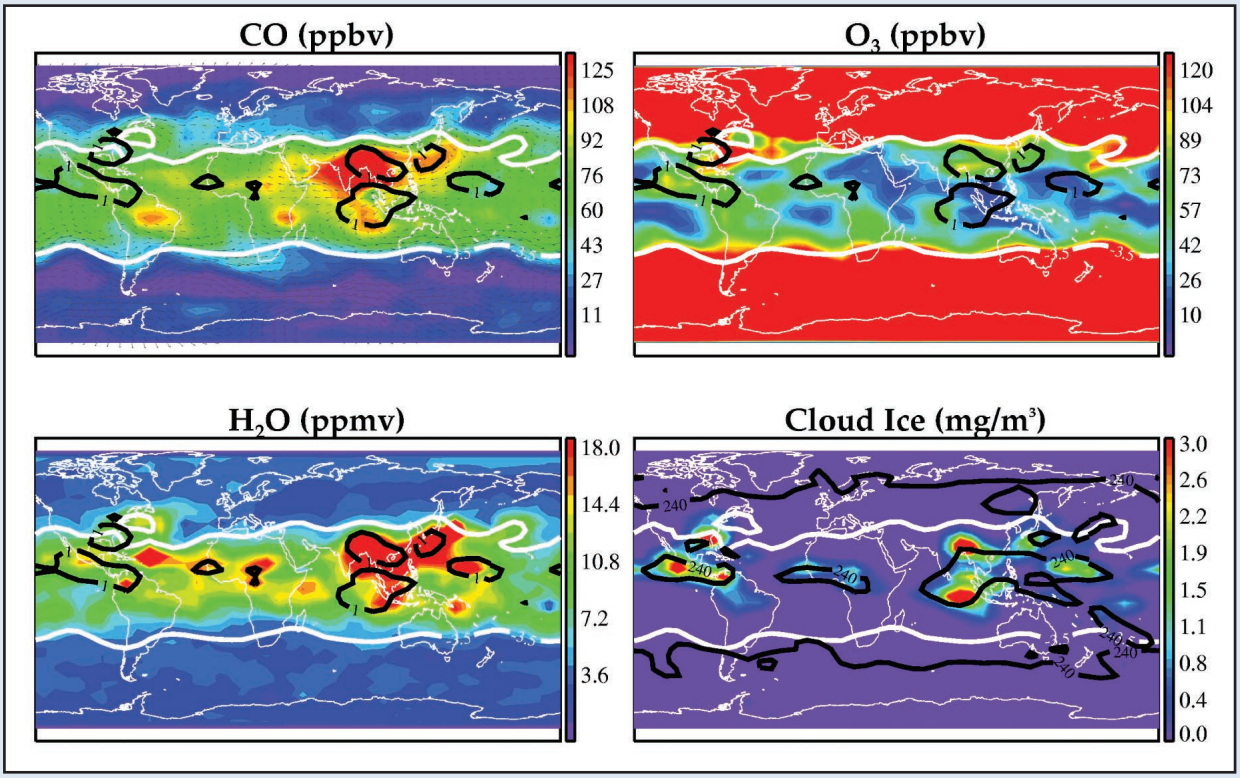

Figure 17. MLS version 1.5 retrievals for CO, O, H_2O, and cloud ice water content at 147 hPa, from 28-31 August 2004. CO and ozone data are cloud-filtered according to MLS detection of ice from thick clouds (see [4], [7]). White contours indicate tropopause location (based on GMAO potential vorticity). Black contours show Outgoing Longwave Radiation (GMAO), with minima indicating convection regions, often coincident with high H_2O and cloud ice. High CO over the Tibetan plateau is from lofted Asian pollution ([5]).

towards an expected recovery?

- How does atmospheric composition affect climate?
- How do upper tropospheric measurements enhance our understanding of global pollution in the troposphere?

While tropospheric measurements are not the primary focus of MLS on Aura, questions 2 and 3 above have upper tropospheric measurement goals. The MLS measurements of H_2O and ice water content (+ temperature) are relevant for question 2, with height-resolved cloud ice data very useful for constraints on GCMs. Question 3 is applicable to MLS upper tropospheric CO and O_3 data, which can help track polluted air masses in the global troposphere. Measurements of upper tropospheric enhancements of HCN and CH_3CN (often related to biomass burning), and volcanic SO_2 are goals for future retrieval versions.

Instrument Description

MLS measures many atmospheric chemical species (see Table 12), cloud ice, temperature and geopotential height. The instrument performs continuous vertical scans (every

25 s, day and night) of the Earth's limb ahead of the Aura satellite and measures thermal emission of millimeter and submillimeter spectral lines. There are 5 radiometers operating at ambient temperature at frequencies near 118, 190, 240, 640, and 2500 GHz, the latter via a 2nd antenna. There are various spectrometers, mainly 25-channel spectrometers with a bandwidth of 1300 MHz and resolution varying from 6 to 96 MHz, with digital autocorrelator (DAC) spectrometers giving finer spectral resolution for mesospheric measurements and 'wide' (0.5 GHz width) filters helping to extend some measurements into the upper troposphere. MLS mass, power, and data rate are 455 kg, 535 W, and 100 kb/s, respectively. The MLS design lifetime is 5 years. See [1] for an overview of MLS.

Retrieval Description

MLS profiles are retrieved roughly every 165 km along-track, with 240 profiles per orbit; see the Table for product-specific resolution and precision. Accuracies are still being determined and only a few published validation references exist so far (i.e. see Table). For Version 1.5 data, the most useful upper tropospheric O_3 and CO data are for 100-147 hPa at low latitudes with some improvements in the upcoming version 2 data at higher pressures; high biases (20 to 100%) and significant scatter exist at 215 hPa. 100-315 hPa H_2O values are within ~5-25% of AIRS data. MLS information also exists for HNO_3, N_2O, and HCl in the upper troposphere, mostly for low latitudes, although signal-to-noise for single-profile measurements is fairly low, and these retrievals are still largely considered to be part of research development. In addition to expected improvements in the above products (e.g., better accuracy, resolution, vertical range), HCN and CH_3CN in the upper troposphere are retrieval goals for a future data version. Note, however, that these will only be viable when there are large enhancements over background conditions on a scale observable by MLS. SO_2 files with data on occasional volcanic enhancements of this gas in the upper troposphere (and stratosphere) are expected in the second public release (version 2.2) of MLS data.

Assumptions made in retrieval(s): Profiles are piece-wise continuous; the vertical retrieval grid is currently 6 points per decade change in pressure; along-track gradients are taken into account. Upcoming version 2.2 data will have a retrieval grid with 12 points per decade change in pressure for H_2O and temperature in the lower stratosphere and upper troposphere.

Data from other sources that (could/does) improve retrieval: Improvements in knowledge of spectroscopy and spectral continuum.

Data accessibility

MLS data version 1.5 is available for 2004-2006 from the NASA Goddard Space Flight Center Earth Distributed Active Archive Center (DAAC) at http://disc.gsfc.nasa.gov/data/dataset/MLS . Data users need to read [4] for data issues and screening recommendations. The version 2.2 MLS data set reprocessing and "forward processing" is planned starting in late 2006 and should become publicly available by early 2007.

References

[1] Waters, J.W., et al., 2006, The Earth Observing System Microwave Limb Sounder (EOS MLS) on the Aura satellite, *IEEE Trans. Geosci. Remote Sensing, 44* (5), 1075-1092.

[2] Livesey, N.J., et al., 2006, Retrieval algorithms for the EOS Microwave Limb Sounder (MLS) instrument, *IEEE Trans. Geosci. Remote Sensing, 44* (5), 1144-1155.

[3] Read, W.G., et al., 2006, The clear-sky unpolarized forward model for the EOS Microwave Limb Sounder (MLS), *IEEE Trans. Geosci. Remote Sensing, 44* (5), 1367-1379.

[4] Livesey, N.J., et al., 2005, EOS MLS Version 1.5 Level 2 data quality and description document, JPL D-32381. Available at MLS website (http://mls.jpl.nasa.gov); see website for updates on data issues.

[5] Filipiak, M.J., et al., 2005, Carbon monoxide measured by the EOS Microwave Limb Sounder on Aura: First Results, Geophys. Res. Lett., 14, L14825, doi:1029/2005GL022765.

[6] Froidevaux, L., et al., 2006, Early validation analyses of atmospheric profiles from EOS MLS on the Aura satellite, *IEEE Trans. Geosci. Remote Sensing, 44* (5), 1106-1121.

[7] Wu, D.L., et al., 2006, EOS MLS cloud ice measurements and cloudy-sky radiative transfer model, *IEEE Trans. Geosci. Remote Sensing, 44* (5), 1156-1165.

[8] Li, J.-L., et al., 2005, Comparisons of EOS MLS cloud ice measurements with ECMWF analyses and GCM simulations: initial results, *Geophys. Res. Lett., 32,* L18710, doi:10.1029/2005GL023788.

OMI / Aura

Contributed by **Pieternel F. Levelt,** (levelt@knmi.nl), *KNMI, P.O. Box 201, 3730 AE De Bilt, The Netherlands,* **Pawan K. Bhartia,** (pawan.k.bhartia@nasa.gov) *NASA-GSFC, Mail Code 613.3, Greenbelt MD 20771, USA,* **René Noordhoek.** (r.noordhoek@knmi.nl), *KNMI, P.O. Box 201, 3730 AE De Bilt, The Netherlands,* **Johanna Tamminen,** (johanna.tamminen@fmi.fi), *FMI, P.O. Box 503, Fin-00101 Helsinki, Finland, and the* **OMI Science Team**

The Eos-Aura Ozone Monitoring Instrument (OMI), a Dutch-Finnish contribution to the NASA EOS-Aura satellite, was launched on 15 July 2004.

Scientific Questions

OMI is designed to improve our understanding of stratospheric chemistry, air quality (AQ), and climate change. The scientific objectives of OMI are [1]:

- to monitor the ozone layer and UV-B at the surface,
- to study the sources and distribution of trace gases that

affect global air quality, and

- to quantify the contribution of tropospheric ozone and aerosols to climate change.

OMI measures several trace gases (O_3, NO_2, SO_2, HCHO, BrO & OClO) related to air quality and chemistry. In addition, OMI measures aerosol absorption, cloud scattering layer mean pressure, and UV irradiance at the surface. The high spatial resolution of OMI allows one to see urban scale features and to find more cloud-free scenes than previous backscatter measurements (e.g. TOMS, SBUV, GOME, and SCIAMACHY). OMI is providing some of these data in near-real time to operational agencies in Europe and the United States.

Instrument Description

OMI is a nadir-viewing, imaging spectrometer that measures the solar radiation backscattered by the Earth's atmosphere and surface from 270 nm to 500 nm, with ~0.5 nm bandpass and up to 3 samples per bandpass. The instrument is insensitive to the polarization of the incoming radiation. OMI's two-dimensional CCD detectors, combined with a 114° viewing angle perpendicular to the flight direction, translate to a 2600 km wide swath on the Earth surface. This enables OMI to provide daily global coverage. In the normal operation mode, the OMI pixel size is typically 15 km × 30 km. See references [2, 3, 4] for a detailed description of instrument design and performance, data processing, and calibration approach.

Retrieval Description

OMI algorithms rely on experience gained from TOMS, SBUV, GOME and SCIAMACHY. Algorithms [5] were developed, and continue to be improved with close collaboration between science team members in Europe and the United States.

Ozone Profiles The OMI profile algorithm [5] is based on the optimal estimation technique [7]. It uses new approaches to calculate the required radiances and Jacobians in an efficient manner and to correct for rotational Raman scattering. This algorithm should be able to provide more accurate total O_3 estimates than the two algorithms discussed above, for it uses a broader range of OMI wavelengths.

Tropospheric Ozone. OMI ozone data are retrieved using both the TOMS (version 8) technique developed by NASA [5] and a DOAS (Differential Optical Absorption Spectroscopy) technique developed by KNMI [5, 6]. Tropospheric column ozone is currently being produced by subtracting stratospheric ozone column derived from the Microwave Limb Sounding (MLS) instrument on Aura from the OMI total ozone column [8]. The "cloud slicing" technique developed for TOMS [9], which is more robust and less sensitive to instrumental effects, has been used to remove bias between MLS and OMI and to validate the results.

Trace gases. NO_2, SO_2, BrO, and HCHO column densities are retrieved [5] by first fitting the spectroscopic features in the measured radiances to get slant columns. The slant column is converted into the vertical column using an air mass factor (AMF) which is calculated with a radiative transfer model and assumed vertical profile of the trace gas.

For SO_2, we currently use the Band Residual Difference algorithm [10] that uses four wavelengths corresponding to maxima and minima in the SO_2 absorption cross-

Table 13. Overview of OMI tropospheric chemistry data products.

Retrieved quantity [Unit]		Nadir Horizontal resolution (km)[a]	Vertical resolution[a]	Accuracy Abs::Rel[b]	Algorithm reference
Ozone Profile [ppmv]		13 × 48	6 km[c]	10%::10%	[5]
Tropospheric Column Ozone [DU[d]]		52 × 48[e]	Column[e]	25%::10%	[8, 9]
Aerosol Optical Thickness[f]		13 × 24	Column	0.1::0.05 or 30%::10%	[5]
SO_2 [molecules/cm^2]	non-volcanic	13 × 24	Column	$3x10^{16}$::2 10^{16} or 50%::20%	[10]
	Volcanic	13 × 24	Column	30%::20%	
NO_2 [molecules/cm$_2$]	Background	13 × 24	Column	$2x10^{14}$::$2x10^{14}$	[5, 11,12]
	polluted	13 × 24	Column	30%::20%	
HCHO [molecules/cm^2]		13 × 24	Column	35%::25%	[5]
BrO [molecules/cm^2]		13 × 24	Column	25%::25%	[5]

[a]All products have Daily Global coverage under daylight conditions, except when indicated otherwise: see notes (e) and (f)

[b]Absolute accuracy is given at the horizontal and vertical resolution indicated in the second and third columns, and represents the root sum of square of all (1σ) errors, including forward model, inverse model, and instrument errors, calculated over the covered area, as indicated in the 2nd column. Relative accuracy represents a component of the absolute error that varies at the measurements temporal resolution (once/day). When multiple values are given the larger value applies. These values reflect the ultimate goals for the accuracy of the OMI data products.

[c]Ozone profile: vertical resolution is the 20-45 km altitude range; [d]1 DU= 2.687 × 10^{16} molecules/cm^2;

[e]Tropospheric Ozone column in the latitude range of 60°S – 60°N; [f]Aerosol products are limited to cloud-free pixels.

Scientific Highlight – OMI

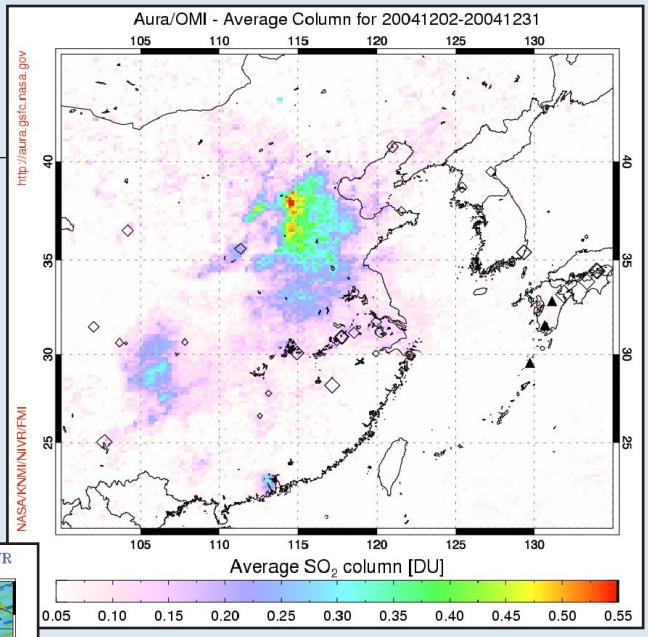

Figure 18. Average SO_2 column amount measured by OMI over eastern Asia in December 2004. Several SO_2 source regions in China can be identified. The principal source of SO_2 emissions in China is coal-fired power plants. Diamonds indicate the locations of copper smelters. (Courtesy of N.A. Krotkov, NASA-GSFC)

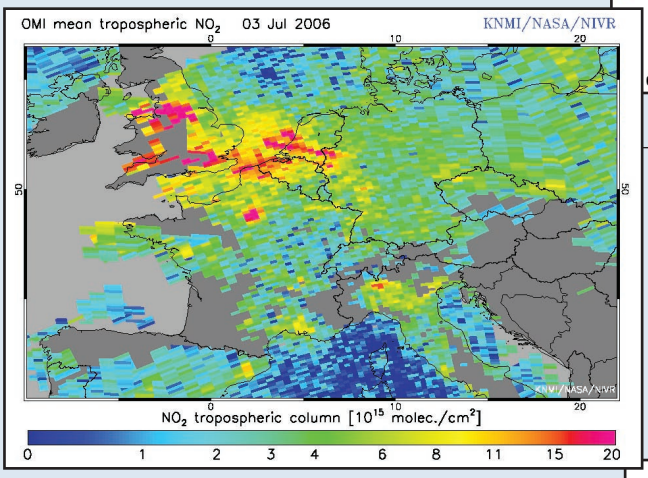

Figure 19. Near Real Time (NRT) measurements of tropospheric NO_2 over central Europe made by OMI on 3 July 2006. Grey areas are cloudy regions (effective cloud fraction > 20%). NRT measurements of this and other regions are available within 3 hours after observation at the TEMIS web site:http://www.temis.nl/airpollution/no2.html. (Courtesy of Henk Eskes, Ronald van der A, Pepijn Veefkind [KNMI], and Folkert Boersma [Harvard])

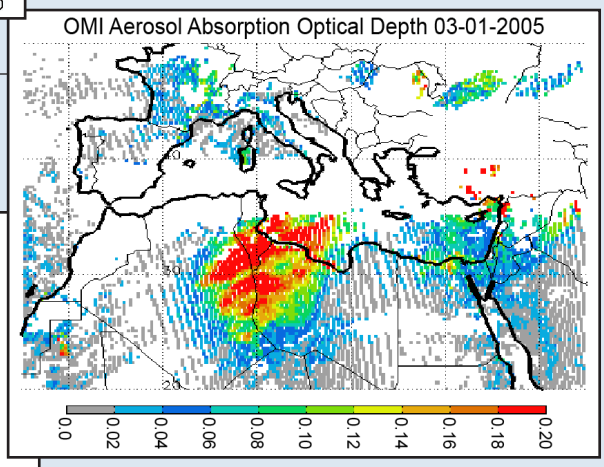

Figure 20. Absorption Optical Depth (388 nm) from OMI observations for a Saharan dust outbreak (March, 2005). (Courtesy of Omar Torres, NASA-GSFC and UMBC JCET)

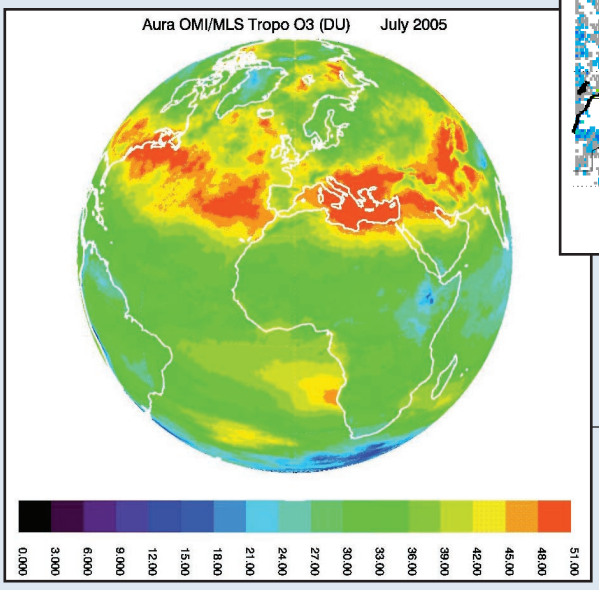

Figure 21. Tropospheric ozone columns inferred as a residual of TOMS total ozone columns and UARS MLS stratospheric ozone columns.

section. This algorithm provides observations of SO_2 in both volcanic and polluted regions with better precision than in previous instruments (see Fig. 18).

For NO_2 [11, 12], stratosphere NO_2 columns are estimated from the column data by first removing data over polluted areas and spatially filtering the rest of the data. OMI-derived tropospheric NO_2 columns track NO_2 pollution near the surface, which is an important precursor of urban smog (Fig. 19).

Aerosols. Using the TOMS UV algorithm [15], we are currently deriving aerosol index (AI) and aerosol absorption optical thickness (AAOT) from OMI (Fig. 20). Although the two quantities are closely related, quantitative estimates of AAOT can be made only in relatively cloud-free scenes, while AI is useful for tracking long-range transport of volcanic ash, smoke and dust over clouds and snow/ice, and through mixed cloudy scenes. An advanced multi wavelength UV-VIS algorithm [5], which focuses on aerosol optical thickness and aerosol types, is currently under development.

Two types of cloud parameters are needed for the retrieval of OMI products. An effective (radiative) cloud fraction is estimated for each pixel from the measured reflectances, and cloud scattering layer mean pressure is obtained from absorption by O_2-O_2 [5, 13] and the rotational Raman scattering [5, 14].

Retrieval characteristics

Table I lists the details on the resolution and the goals for accuracy of the OMI data products. Note that validation is currently ongoing for most products. Information on validation results, data quality and a list of known problems and limitations is given in the README files and in additional documents at the GES-DISC data center.

Data availability

Four OMI products are currently publicly available (http://disc.gsfc.nasa.gov/Aura/OMI/): TOMS and DOAS total ozone columns, cloud related products from the rotational Raman scattering, and the O_2-O_2 algorithms, column and tropospheric NO_2, AOD, SO_2, HCHO, OClO and BrO. OMI level 1b, AOD, and UVB have been provisionally released. They are available from the Aura Data Validation Center (http://avdc.gsfc.nasa.gov/) to NASA and ESA selected validation team members. In 2007 a reprocessing effort will lead to a new collection of OMI products, which will be released by the end of the year. More information can be found at the OMI (http://www.knmi.nl/omi) and TOMS (http://toms.gsfc.nasa.gov/) sites. OMI near real time products will also be produced. Some of them are already available at: http://www.temis.nl.

References

[1] Levelt, P. F. et al., 2006, Science Objectives of the Ozone Monitoring Instrument, *IEEE Trans. Geo. Rem. Sens., 44* (5), 1199-1208, doi:10.1109/TGRS.2006.872336.

[2] Levelt, P.F. et al., 2006, The Ozone Monitoring Instrument, *IEEE Trans. Geo. Rem. Sens., 44* (5), 1093-1101, doi:10.1109/TGRS.2006.872333.

[3] Dobber, M. R. et al., 2006, Ozone Monitoring Instrument Calibration, *IEEE Trans. Geo. Rem. Sens., 44* (5), 1209-1238, doi:10.1109/TGRS.2006.869987.

[4] van den Oord, G.H.J. et al., 2006, OMI Level0 to 1b Processing and Operational Aspects, *IEEE Trans. Geo. Rem. Sens., 44* (5), 1380-1397, doi:10.1109/TGRS.2006.872935.

[5] EOS-AURA OMI Algorithm Theoretical Basis Documents (2002), available on EOS web site at: http://eospso.gsfc.nasa.gov/eos_homepage/for_scientists/atbd/

[6] Veefkind, J. P., et al.,2006, Total Ozone from the Ozone Monitoring Instrument (OMI) Using the DOAS technique, *IEEE Trans. Geo. Rem. Sens., 44* (5), 1239-1244, doi:10.1109/TGRS.2006.871204.

[7] Rodgers, C.D., 2000, Inverse Methods For Atmospheric Sounding: Theory and Practice, Series on Atmosphere, Oceanic and Planetary Physics, vol. 2, F.W. Taylor, Ed., Singapore: World Scientific Publishing Co. Pte. Ltd.

[8] Ziemke, J. R., S. Chandra, B.N. Duncan, L. Froidevaux, P.K. Bhartia, P. Levelt and J. Waters, 2006, Tropospheric ozone determined from Aura OMI and MLS: Evaluation of measurements and comparison with the Global Modeling Initiative's Chemical Tracer Model, *J. Geophys. Res., 111,* D19303, doi:10.1029/2006JD007089.

[9] Ziemke, J.R., S. Chandra, P.K. Bhartia, 2005, A 25-year data record of atmospheric ozone in the Pacific from Total Ozone Mapping Spectrometer (TOMS) cloud slicing: Implications for ozone trends in the stratosphere and troposphere, *J. Geophys. Res., 110,* D15105, doi:10.1029/2004JD005687.

[10] Krotkov, N. A., S.A. Carn, A.J. Krueger, P.K. Bhartia, and Kai Yang, 2006, Band Residual Difference Algorithm for Retrieval of SO_2 From the AURA Ozone Monitoring Instrument (OMI), *IEEE Trans. Geo. Rem. Sens., 44* (5), 1259-1266, doi:10.1109/TGRS.2005.861932.

[11] Bucsela, E.J. et al., 2006, Algorithm for NO_2 Vertical Column Retrieval From the Ozone Monitoring Instrument, *IEEE Trans. Geo. Rem. Sens., 44* (5), 1245-1258, doi:10.1109/TGRS.2006.863715.

[12] Boersma, K. F., H.J. Eskes and E.J. Brinksma, 2004, Error analyses for tropospheric NO_2 retrieval from space, *J. Geophys. Res., 109,* D04311, doi:10.1029/2003JD003962.

[13] Acarreta, J.R., J.F. de Haan, and P. Stammes, 2004, Cloud pressure retrieval using the O_2-O_2 absorption band at 477 nm. *J. Geophys. Res., 109,* D5, D05204. doi: 10.1029/2003JD003915.

[14] Joiner, J. and A.P. Vasilkov, 2006, First Results From the OMI Rotational Raman Scattering Cloud Pressure Algorithm, *IEEE Trans. Geo. Rem. Sens., 44* (5), 1272-1282, doi:10.1109/TGRS.2005.861385.

[15] Torres, O., P. K. Bhartia, A. Sinyuk, E. J. Welton, B. Holben, 2005, Total Ozone Mapping Spectrometer measurements of aerosol absorption from space: Comparison to SAFARI 2000 ground-based observations, *J. Geophys. Res., 110,* D10S18, doi:10.1029/2004JD004611.

TES / Aura

Contributed by **Reinhard Beer** (Reinhard.Beer@jpl.nasa.gov), *Jet Propulsion Laboratory, M/S 183-601, 4800 Oak Grove Drive, Pasadena, CA 91109 USA*

The Tropospheric Emission Spectrometer (TES) was launched onboard the AURA satellite on July 15, 2004.

Scientific Questions

Investigation of global tropospheric chemistry with especial emphasis on the sources, sinks and transport of ozone and carbon monoxide.

Instrument Description

Sun-synchronous, 705 km orbit, 16-day repeat period (233 orbits), 13:45 equator crossing LMST (ascending node).

Design lifetime 5+ years.

1-D (16 pixels) imaging infrared Fourier Transform spectrometer. Spot sampling (72/orbit)

Spectral coverage 650 – 3050 cm^{-1} (3.3 – 15.4 µm).

Spectral resolution 0.1 cm^{-1} downlooking, 0.025 cm^{-1} limbviewing (apodized).

Retrieval Description

TES is a Fourier transform infrared emission spectrometer with high spectral resolution (0.1 cm^{-1}) and coverage over a wide spectral range (650 - 3050 cm^{-1}) [1]. The TES nadir footprint is 5 x 8 km and has 71 observations per orbit (spaced approximately 175 km apart) and 16 orbits per day. TES retrievals use an optimal estimation approach

Scientific Highlight – TES

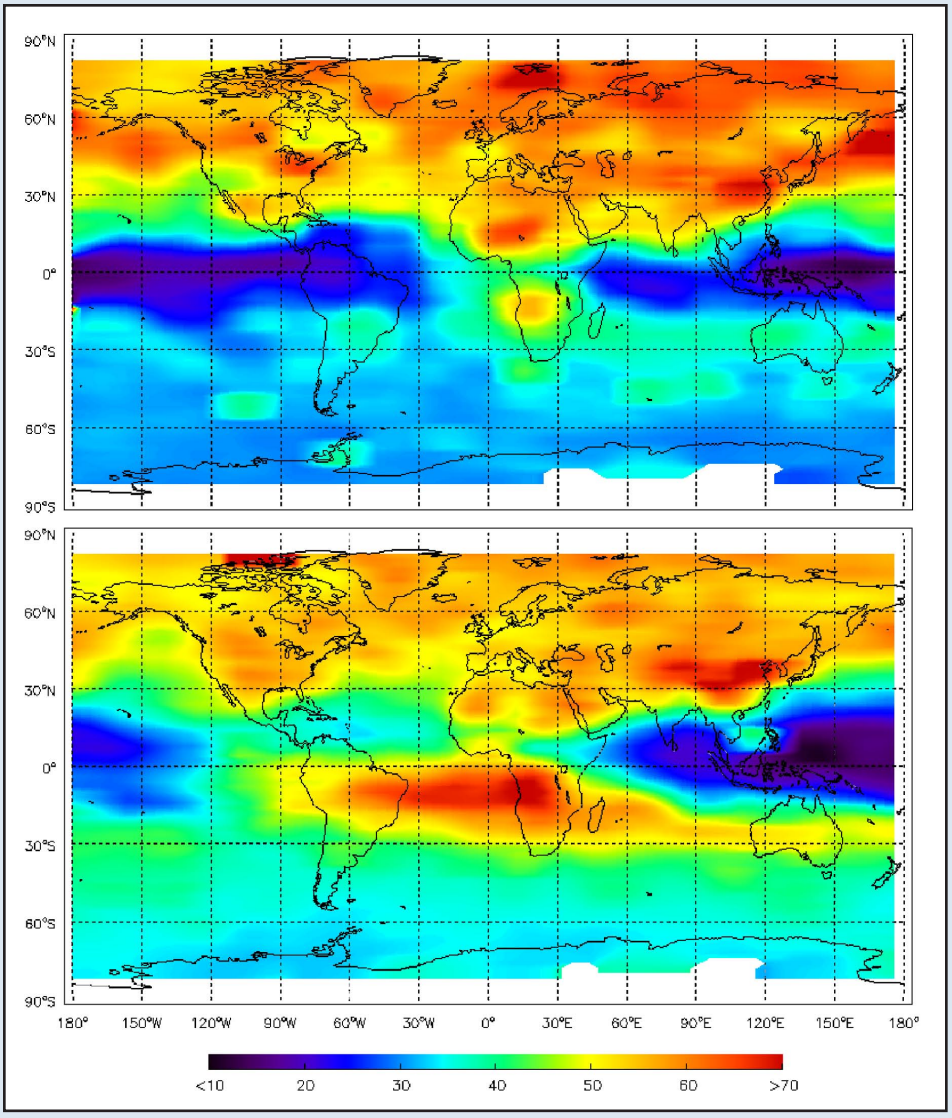

Figure 22. Monthly mean ozone concentrations (ppb) at the 681 hPa pressure level for May (top) and September (bottom) 2005. Note the consistently higher O_3 concentrations in the more populous and industrialized northern hemisphere and the signatures of biomass burning in Africa (May and September) and South America (September) [TES beta release data].

Table 14. Overview of TES tropospheric chemistry data products.

Retrieved quantity	Horizontal resolution	Vertical resolution (km)	Typical accuracy	Typical precision	Reference of retrieval algorithm	Validation reference
H_2O	N, L	3.6	80 ppm	26 ppm	[8]	[9]
O_3	N, L	7.8	9 ppb	3 ppb	"	"
CO	N, L	7.9	12 ppb	6 ppb	"	"
HNO_3	L	2.2	70 ppt	13 ppt	"	"

N = Nadir, 5 x 8 km; L = Limb, 20 x ~120 km

following Rodgers (2000; [2]). The spectral windows and algorithmic details used for TES retrievals of atmospheric state parameters, with corresponding error estimates, are described in Worden et al. (2004; [3]) and Bowman et al. (2002, 2006; [4,5]). Kulawik et al. (2006a; [6]) show how individual TES profiles are characterized for errors and vertical information. The TES retrievals are performed for both cloudy and clear scenes. A cloud top pressure and spectrally dependent effective optical depth are estimated along with the gas species (Kulawik et al., 2006b; [7]). In the current operational retrievals, there may be a cloud initial guess refinement step, depending on comparisons of the brightness temperatures. Following this possible step, temperature, water vapor, and ozone are retrieved simultaneously using spectral windows in the 670 - 900 cm^{-1} , 990-1070 cm^{-1}, and 1172 - 1315 cm^{-1} regions. The temperature information in this step comes from line widths and the CO_2, O_3, and H_2O vmr's. In subsequent steps, HDO and H_2O are jointly retrieved, followed by methane (using the 1292 - 1307 cm^{-1} spectral region) and then carbon monoxide. The TES standard product includes profile estimate, along with diagnostic information such as the total error covariance and averaging kernel.

Data accessibility

Go to http://eosweb.larc.nasa.gov

References

[1] Beer, R., T.A. Glavich, and D.M. Rider, 2001, Tropospheric emission spectrometer for the Earth Observing System's Aura Satellite, *Applied Optics, 40* (15), 2356-2367.

[2] Rodgers, C.D., 2000, Inverse methods for atmospheric sounding: Theory and practice, *World Scientific,* Singapore.

[3] Worden, J., S.S. Kulawik, M.W. Shephard, S.A. Clough, H. Worden, K. Bowman, and A. Goldman, 2004, Predicted errors of tropospheric emission spectrometer nadir retrievals from spectral window selection, *J. Geophys. Res., 109* (D9).

[4] Bowman, K.W., J. Worden, T. Steck, H.M. Worden, S. Clough, and C. Rodgers, 2002, Capturing time and vertical variability of tropospheric ozone: A study using TES nadir retrievals, *J. Geophys. Res., 107* (D23).

[5] Bowman, K.W., C.D. Rodgers, S.S. Kulawik, J. Worden, E. Sarkissian, G. Osterman, T. Steck, M. Lou, A. Eldering, M. Shephard, H. Worden, M. Lampel, S. Clough, P. Brown, C. Rinsland, M. Gunson, and R. Beer, 2006, Tropospheric emission spectrometer: Retrieval method and error analysis, *IEEE Transactions on Geoscience and Remote Sensing, 44* (5), 1297-1307.

[6] Kulawik, S.S., H. Worden, G. Osterman, M. Luo, R. Beer, D.E. Kinnison, K.W. Bowman, J.

[7] Kulawik, S.S., G. Osterman, D.B.A. Jones, and K.W. Bowman, 2006b, Calculation of altitude-dependent Tikhonov constraints for TES nadir retrievals, *IEEE Transactions on Geoscience and Remote Sensing, 44* (5), 1334-1342.

[8] Level 2 Algorithm Theoretical Basis Document, Version 1.16, JPL D-16474, June 27, 2002; available from the TES web site: http://tes.jpl.nasa.gov

[9] Validation Report, Version 1.0, August 15, 2005; available from the TES web site: http://tes.jpl.nasa.gov

PARASOL / PARASOL

Contributed by **Didier Tanré** (didier.tanre@univ-lille1.fr), *Laboratoire d'Optique Atmospherique, U.S.T. de Lille/ CNRS, Bat. P5, 59655 - Villeneuve d'Ascq cedex, France,* **Anne Liferman** (anne.lifermann@cnes.fr), *Centre National d'Etudes Spatiales, C.S.T., 18 avenue Ed. Belin, 31401 - Toulouse Cedex, France, and* **the PARASOL Team.**

PARASOL was launched on December, 18, 2004 and has been routinely acquiring data since March 2005. The PARASOL design lifetime is two years. PARASOL flies at an altitude of 705 km in a sun-synchronous orbit with 1:30 pm ascending node. The PARASOL (Polarization and Anisotropy of Reflectances for Atmospheric Science coupled with Observations from a Lidar) payload is largely based on the POLDER instrument [1] and is the second in the CNES's Myriade (Centre National d'Études Spatiales) line of microsatellites.

Scientific Questions

The Parasol mission will contribute to a better knowledge of the optical, physical and radiative properties of clouds and aerosols, to the estimate of the cloud and aerosol radiative forcing and to the understanding of the aerosol indirect effect.

Instrument Description

The Parasol payload consists of a digital camera with a 274x242-pixel CCD detector array, wide-field telecentric optics and a rotating filter wheel enabling measurements in 9 spectral channels from blue (0.443 µm) through to near-infrared (1.020µm) and in several polarization directions. Polarization measurements are performed at 0.490µm, 0.670µm and 0.865µm. The bandwith is between 20nm and 40nm depending on the spectral band. Because it acquires a sequence of images every 20 seconds, the instrument can view ground targets from different angles, ±51° along track and ±43° across track.

Retrieval Description

Data collected by Parasol allow us to derive, over the sea where the surface is dark, the total aerosol optical thickness and the fraction of fine particles within the accumulation mode. The Ångström coefficient, an indicator of particle size, is also deduced from the spectral optical thickness. Moreover, when the viewing geometry is suitable, PARASOL can discriminate large spherical marine aerosols from non-spherical desert aerosols, retrieve the effective radius of the accumulation and coarse modes, and provide an estimate of the real part of the refractive index. Over land, where the total radiance cannot be used because of highly reflective surfaces, the polarized

Table 15. Overview of PARASOL tropospheric chemistry data products.

Retrieved quantity	Horizontal[a] resolution (km)	Vertical[b] resolution	Typical accuracy	Reference(s) of retrieval algorithm	Validation reference(s)
τ_{tot}*	16 x 18 km^2	N/A	$\pm 0.05\tau \pm 0.05$	[2] Deuzé et al., 1999	[3] Goloub et al., 1999
r_{eff}*	16 x 18 km^2	N/A	Fine: 0.05µm Coarse: 0.5µm	[4] Herman et al., 2005	/
m_r*	16 x 18 km^2	N/A	0.10	[4] Herman et al., 2005	/
α*	16 x 18 km^2	N/A	0.3-0.5	[2] Deuzé et al., 1999	[3] Goloub et al., 1999
τ_{fine}*	16 x 18 km^2	N/A	TBD	[4] Herman et al., 2005	/
$\tau_{c,ns}$*	16 x 18 km^2	N/A	TBD	[4] Herman et al., 2005	/
τ_{fine}**	16 x 18 km^2	N/A	TBD	[5] Deuzé et al., 2001	[6] Goloub et al., 2000

*Over ocean, **Over land

τ_{tot} = Total aerosol optical thickness
τ_{fine} = Optical thickness of the aerosol fine mode
$\tau_{c,ns}$ = Optical thickness for large nonspherical aerosols
m_r = Real part of the refractive index of the aerosol fine mode
r_{eff} = Effective radius of the aerosol size distribution
α = Angstrom exponent for total aerosol optical thickness

Scientific Highlight – PARASOL

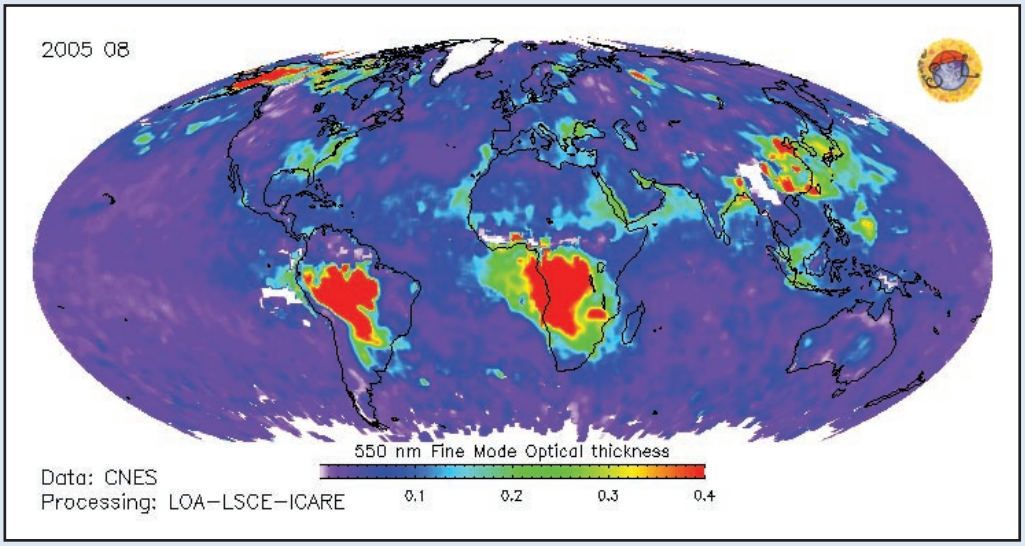

Figure 23. Aerosol optical thickness at 0.55µm of the accumulation mode observed by PARASOL in August 2005 (Courtesy of J.L. Deuzé).

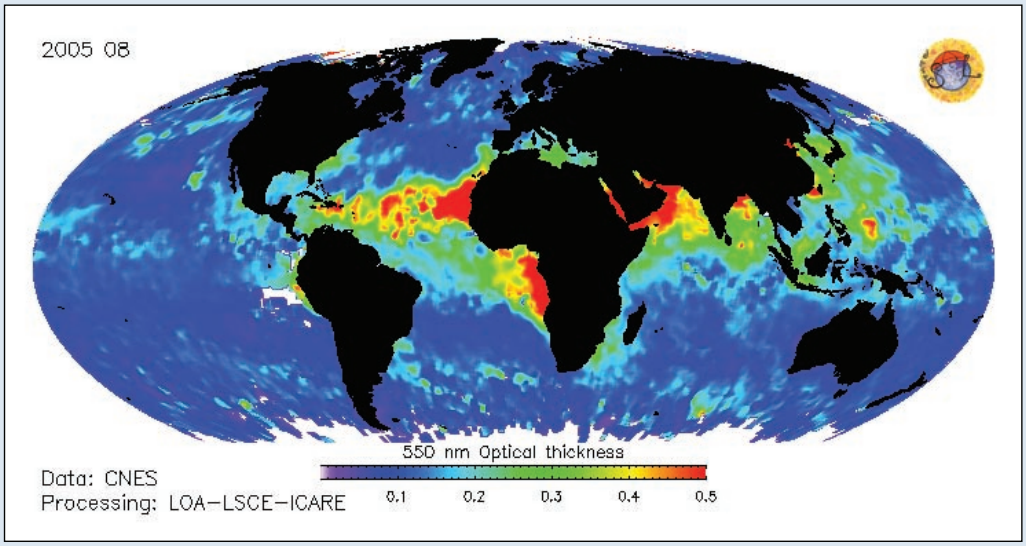

Figure 24. Total aerosol optical thickness at 0.55µm of the accumulation mode observed by PARASOL in August 2005 (Courtesy of J.L. Deuzé).

radiance, which is only sensitive to small particles, allows us to derive the optical thickness of the fine mode.

PARASOL also can detect clouds, determine their optical thickness, thermodynamic phase and altitude, and estimate the reflected solar flux. Measuring polarization allows us to clearly identify the cloud phase because liquid droplets and ice have a strong specific angular signature. For liquid water clouds, an original method that analyses polarized radiances is used, when the cloud field is uniform, for determining the droplet radius at the top of the cloud. The cloud level pressure (or altitude) is derived using polarization in the blue (at 0.443µm wavelength) and by measuring oxygen absorption in the red (~0.763µm wavelength). The cloud water content is derived from visible (0.67µm wavelength) reflectance measurements. PARASOL determines the column-integrated water vapor content from the contrast in absorption between the 0.910 µm and 0.865µm bands.

All the retrievals are based on the plane-parallel assumption. Ocean reflectance is modeled based on the wind speed estimate. The land polarized reflectances are derived from NDVI (normalized difference vegetative index) and ecosystem maps. A bimodal aerosol size distribution is assumed, with fine and coarse modes. The cloud droplet size distribution is fixed over land (9µm) and ocean (11µm). We use the Inhomogeneous Hexagonal Monocrystal (IHM) model for ice clouds.

The Parasol mission will take advantage of the other instruments in the A-Train formation, which mainly include the CERES and MODIS radiometers on the Aqua satellite, the OMI on AURA, the CALIOP lidar on CALIPSO and the radar on CLOUDSAT. The 5 satellites cross the equator one at a time, a few minutes apart, at around 1.30 pm local time, Although each mission is fully autonomous and consistent by itself, their combination provides the opportunity to derive new parameters as well as to put additional constraints on the inversions.

Acknowledgments

The PARASOL instrument was financed by the French Space Agency (CNES). Funding for science activities was provided by the Centre National de la Recherche Scientifique (CNRS), the Conseil Régional du Nord-Pas de Calais, the Fonds Européen de Développement Régional (FEDER) and the Délégation Régionale à la Recherche et à la Technologie du Nord-Pas de Calais.

Data accessibility

Level 1: http://parasol-polder.cnes.fr/

Level 2 & 3: http://www-icare.univ-lille1.fr/

References

[1] Deschamps, P.Y., F.M. Bréon, M. Leroy, A. Podaire, G. Sèze and A. Bricaud, The POLDER mission: Instrument characteristics and scientific objectives, *IEEE Trans.Geosci. Rem. Sens. 32,* 598-615, 1994.

[2] Deuzé, J.L., M. Herman, P. Goloub, D. Tanré, A. Marchand, 1999, Characterization of aerosols over ocean from POLDER/ADEOS-1, *Geophys. Res. Lett., 26,* 1421-1424.

[3] Goloub, P., D. Tanré, J.L. Deuzé, M. Herman, A. Marchand, F.M. Bréon, 1999, Validation of the first algorithm applied for deriving the aerosol properties over the ocean using the POLDER/ADEOS measurements, *IEEE Transactions on Geoscience and Remote Sensing, 37,* 1586-1596.

[4] Herman, M., J. L. Deuzé, A. Marchand, B. Roger, P. Lallart, 2005, Aerosol remote sensing from POLDER/ADEOS over the ocean: Improved retrieval using a nonspherical particle model, *J. Geophys. Res., 110,* D10S02.

[5] Deuzé, J. L., F. M. Bréon, C. Devaux, P. Goloub, M. Herman, B. Lafrance, F. Maignan, A. Marchand, G. Perry, D. Tanré, 2001, Remote Sensing of aerosols over land surfaces from POLDER/ADEOS-1 polarized measurements, *J. Geophys. Res., 106,* 4913-4926.

[6] Goloub, P. and O. Arino, 2000, Verification of the consistency of POLDER aerosol index over land with ASTR-2 fire product, *Geophys. Res. Lett., 27,* 899-902.

CALIOP / CALIPSO

Contributed by **David Winker** (david.m.winker@nasa.gov), *NASA Langley Research Center, Hampton, VA 23681-0001, USA*

The Cloud-Aerosol Lidar and Infrared Pathfinder Satellite Observations (CALIPSO) was launched on 28 April 2006 for a planned 3-year mission. CALIPSO is flying in formation with the Aqua, Aura, CloudSat, and Parasol satellites as part of the Afternoon Constellation or A-train. The constellation flies in a sun-synchronous orbit with an orbit inclination of 98°. CALIPSO flies about 2 minutes behind the Aqua satellite, with an equator crossing time of about 1:30 PM. The CALIPSO payload

Table 16. Overview of primary CALIOP tropospheric chemistry data products

Retrieved Quantity	Vertical Coverage	Horizontal resolution	Vertical resolution	Typical Accuracy	Retrieval references
Aerosol layer heights	0-30 km	5 km	30-360 m	60 m	[2] Vaughan, et al., 2004 ; [3] Liu et al., 2004
Aerosol backscatter profiles	0-30 km	40 km	120-360 m	20%	[2] Vaughan, et al., 2004 [7] Hostetler et al., 2006
Aerosol extinction profiles	0-30 km	40 km	120-360 m	40%	[2] Vaughan, et al., 2004 [7] Hostetler et al., 2006

Scientific Highlight – CALIPSO

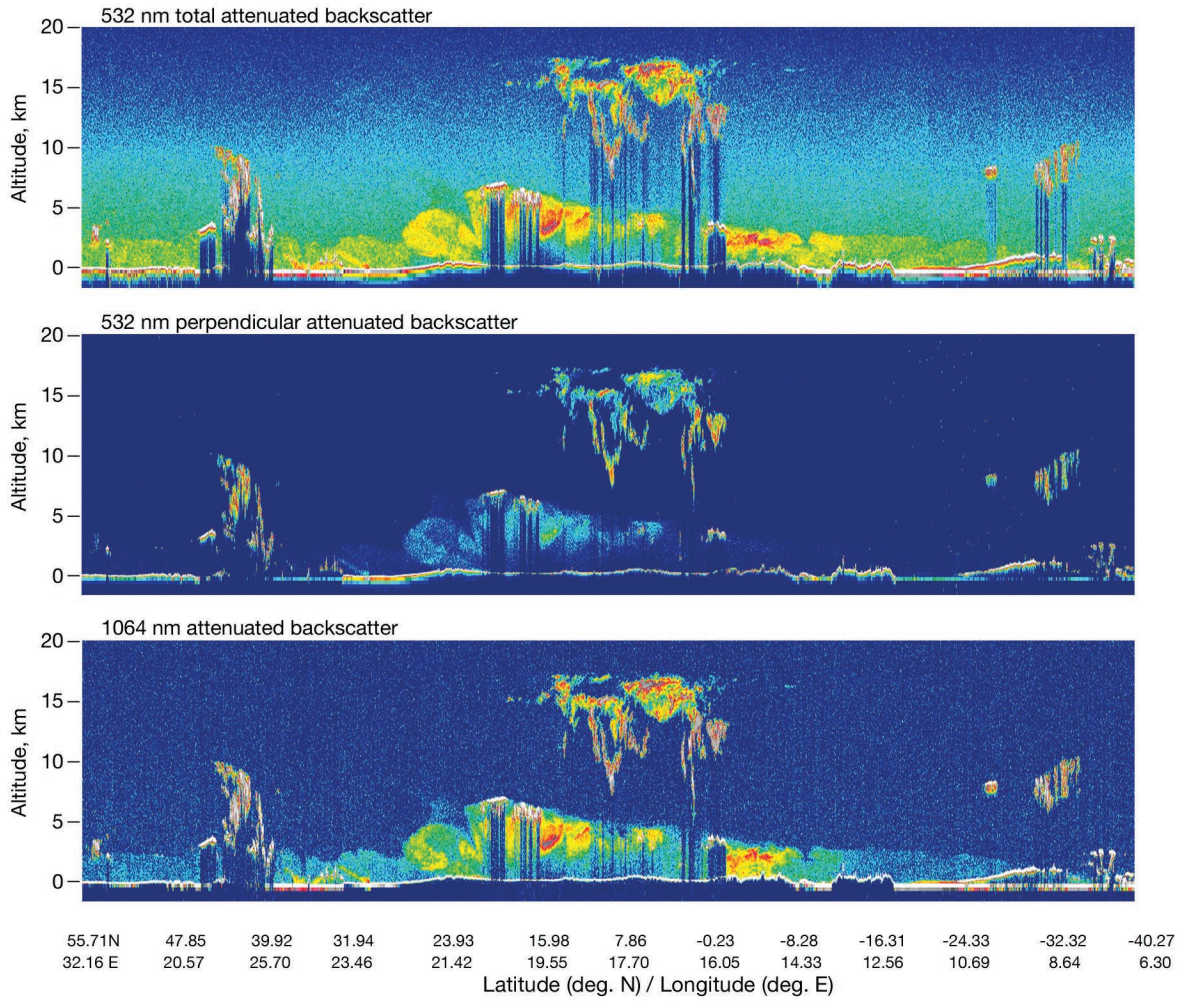

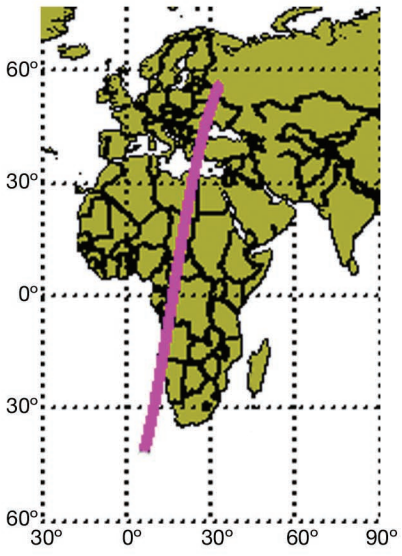

Figure 25. Cross-sections of attenuated backscatter observed by CALIPSO on June 9, 2006 across eastern Europe and Africa. The upper and lower panels display total attenuated backscatter at wavelengths of 532 nm and 1064 nm, respectively. The middle panel displays the orthogonal component at 532 nm. This example illustrates the rich complexity of changing aerosol structure and properties observed by CALIPSO in the presence of mid and high altitude cloud.

consists of three instruments: the Cloud-Aerosol LIdar with Orthogonal Polarization (CALIOP, sounds like "calliope"); the Infrared Imaging Radiometer (IIR) and the Wide Field Camera (WFC).

Scientific Questions

The CALIPSO lidar provides vertically-resolved information on aerosols and clouds, and will be used to address the following scientific questions:

- What are the effects of clouds and aerosols on radiative fluxes at the surface and within the atmosphere?
- How do aerosols modify cloud properties and processes?
- What are the pathways for intercontinental transport of air pollution?
- What are the most important feedback processes involving clouds, radiation, and climate?

Instrument/Satellite Description

CALIOP is a nadir-pointing instrument which provides information on the vertical distribution of aerosols and clouds as well as their optical and physical properties. CALIOP is built around a diode-pumped Nd:YAG laser producing linearly-polarized pulses of light at 1064 nm and 532 nm. The atmospheric return is collected by a 1-meter telescope, which feeds a three-channel receiver measuring the backscattered intensity at 1064 nm and the two orthogonal components of the 532 nm return (parallel and perpendicular to the polarization plane of the transmitted beam).

The IIR provides calibrated radiances at 8.65 µm, 10.6 µm, and 12.05 µm. over a 64 km swath centered on the lidar footprint. A rotating filter wheel provides the spectral measurements. The IIR is built around an Infrared Sensor Module, developed for the IASI instrument. Use of a microbolometer detector array in a non-scanning, staring configuration allows a simple and compact design to perform measurements at a 1 km resolution with a NETD better than 0.3 K (at 210 K) in all spectral bands.

The WFC is a modified star tracker camera, with a single channel covering the 620 nm to 670 nm spectral region providing images of a 61 km swath with a spatial resolution of 125 meters.

Retrieval Description

An adaptive threshold technique [1, 2] is used to locate cloud and aerosol layers. Cloud/aerosol discrimination is performed using the magnitude and spectral variation of the lidar backscatter [3]. Cloud ice/water phase is determined from the magnitude of the lidar depolarization. Cloud and aerosol extinction profiles are computed using standard iterative retrieval technique [4] and using a transmittance constraint when available [5].

Layer height data from CALIOP and visible reflectances from the WFC are used to constrain the standard retrieval [6] of cirrus emissivity and particle size from IIR data.

Data Accessibility

Data are available from the NASA Langley Atmospheric Science Data Center (ASDC) DAAC via on-line web orders (http://eosweb.larc.nasa.gov).

References

[1] Winker, D. M., and M. A. Vaughan, 1994, Vertical distribution of clouds over Hampton, Virginia observed by lidar under the ECLIPS and FIRE ETO programs. *Atmos. Res., 34,* 117-133.

[2] Vaughan, M., S. Young, D. Winker, K. Powell, A. Omar, Z. Liu, Y. Hu, and C. Hostetler, 2004, Fully automated analysis of space-based lidar data: an overview of the CALIPSO retrieval algorithms and data products. *Proc. SPIE, 5575,* 16-30.

[3] Liu, Z., M. A. Vaughan, D. M. Winker, C. A. Hostetler, L. R. Poole, D. L. Hlavka, W. D. Hart, and M. J. McGill, 2004, Use of probability distribution functions for discriminating between clouds and aerosols in lidar backscatter data, *J. Geophys. Res., 109,* doi:10.1029/2004JD004732.

[4] Gambling, D., and K. Bartusek, 1972, Lidar observations of tropospheric aerosols. Atmos. Environ, 6, 181-190.

[5] Young, S.A., Cutten, D.R., Lynch, M. J., and Davies, J. E., 1993, Lidar-Derived Variations in the Backscatter-to-Extinction Ratio in Southern Hemisphere Coastal Maritime Aerosols, *Atmos. Envi., 27A,* 1541-1551.

[6] Parol, F., Buriez, J. C., Brogniez, G., and Fouquart, Y., 1991, Information content of AVHRR Channels 4 and 5 with respect to effective radius of cirrus cloud particles, *J. Appl, Meeorol., 30,* 973-984.

[7] Hostetler, C. A., Z. Liu, J. Reagan, M. Vaughan, D. Winker, M. Osborn, W. H. Hunt, K. A. Powell, and C. Trepte, CALIPSO Calibration and Level 1 Data Products, PC-SCI-201, Release 1.0, April 7, 2006 (http://www-calipso.larc.nasa.gov)

[8] Winker, D. M., J. Pelon, and M. P. McCormick, 2003, The CALIPSO mission: Spaceborne lidar for observation of aerosols and clouds. *Proc. SPIE 4893,* 1-11.

[9] Winker, D. M., W. H. Hunt, and C. A. Hostetler, 2004, Status and Performance of the CALIOP Lidar. *Proc. SPIE 5575,* 8-15.

[10] Winker, D. M., 2005, Space-based lidar for observation of aerosols and clouds. In Laser Remote Sensing, T. Fujii and T. Fukuchi, eds. (Taylor and Francis, New York, NY, 2005) pp. 803-815.

GOME-2 / MetOp

Contributed by **Michael Eisinger** (michael.eisinger@uni-essen.de), *Universität Essen, Schwanhildenhöhe 2, 45141 Essen, Germany*

The Second Global Ozone Monitoring Experiment (GOME-2) is one of the instruments embarked on the MetOp satellite series of polar orbiting operational satellites for meteorology and climate monitoring. It is an enhanced version of the Global Ozone Monitoring Experiment (GOME) operating in-orbit since 1995 on the ERS-2 satellite. Like its predecessor, GOME-2 is a nadir-scanning double spectrometer covering the 240-790 nm wavelength range. From the observed earth radiances a large number of geophysical parameters can be derived. Primary target parameters are total column densities and vertical profiles of ozone. Furthermore, column densities of several other traces gases (NO_2, BrO, SO_2, HCHO, OClO) and information on aerosols, clouds, UV fields, and polarisation can be retrieved. GOME-2 is planned to be operational between 2006 and 2020.

Scientific Questions

- Long-term monitoring of global ozone layer and trace gases relevant for stratospheric ozone.
- How does the ozone layer recover in response to the Montreal protocol measures?
- Long-term monitoring of global tropospheric pollution from anthropogenic and natural sources (industry, biomass burning, volcanoes …). What are the locations, magnitudes and trends of significant emissions?
- Provision of lower stratospheric wind information (contained in ozone fields) to numerical weather prediction models in near-real time.

Instrument Description

GOME-2 is a nadir-scanning UV/VIS grating spectrometer covering the wavelength range 240-790 nm in four main channels (FPA 1-4) and 300-800 nm in two orthogonal polarisation channels (PMD s and p). Each of the six channels employs a 1024-element Reticon linear photodiode array cooled to about 235 K; the polarisation channels use only a subset of 279 spectral elements which are further co-added into 15 spectral bands. Main channels have a spectral resolution (FWHM) of 0.26-0.51 nm sampled at 0.12-0.21 nm (the lower numbers refer to FPA 1 and 2, covering 240-400 nm). GOME-2 is scanning in 6 s intervals (4.5 s forward scan, 1.5 s back scan) at a default swath width of 1920 km. The scan speed is adjusted across the swath such that all forward scan groundpixels have the same size (80x40 km^2 across/along track for the default integration time of 187.5 ms). Polarisation channels are spatially oversampling the main channels by a factor of 8 (ground pixel size 10 x 40 km^2). GOME-2 has three onboard calibration sources: LEDs, a spectral lamp (PtCrNeAr), and a white lamp (Halogen Tungsten). The sun is viewed once per day via a Quartz quasi-volume diffuser. GOME-2 is generating data at a rate of 400 kbit/s or 300 MB/orbit.

The first GOME-2 model was launched aboard MetOp-A on 19 Oct 2006. MetOp is flying in a sun-synchronous near-circular polar orbit with a mean local solar time of 09:30 h at descending node crossing. GOME-2 has a design lifetime of 5 years. Two more models have already been built and will be launched aboard MetOp-B (2011) and MetOp-C (2015).

Retrieval Description

Operational level 2 products as produced by the members of the Ozone Monitoring Satellite Application Facility (O3MSAF) are summarised in the table below. Horizontal resolution is 80 x 40 km^2 unless specified otherwise. Typical accuracy and precision values for trace gas vertical columns are specified as ranges where the low (high) number corresponds to a typical high (low) total column. In addition, effective cloud fraction, cloud top height, and fractional polarisation for each ground pixel will be provided in the operational level 1 products.

Table 17. Overview of GOME-2 tropospheric data products.

Retrieved quantity	Vertical resolution	Typical accuracy (1σ)	Typical precision (1σ)	Remarks
Ozone				
Ozone profiles	6 to 8 independent layers (2 in the troposphere)	Stratosphere: < 10 % Troposphere: < 30 %		640x40 km^2 grid
Trace gas total columns				
NO_2	N/A	5…20 %	5…20 %	
BrO		20…50 %	10…50 %	
SO_2		50…100 %	50…100 %	Precision 5…30 % for volcanic SO_2
HCHO		50…100 %	20…50 %	
Aerosols				
Absorbing Aerosol Indicator	N/A	Not specified		
Aerosol Optical Depth		< 20 %		
Aerosol type		N/A		Desert dust/smoke/volcanic ash

Data accessibility

Local real-time GOME-2 raw data broadcast from MetOp in its High Resolution Picture Transmission (HRPT) data stream can be received by authorised users equipped with an AHRPT reception station, and data decryption information available from EUMETSAT user services.

Global near-real time (NRT) products will be distributed via EUMETSAT's data distribution system EUMETCAST targeted to Europe and some areas in Africa. Users require a PC with a Digital Video Broadcast (DVB) card connected to a satellite antenna, together with client software obtainable from EUMETSAT user services.

NRT products will be available within 2h 15min from sensing for level 1 products, and within 3h from sensing for level 2 products.

Archived products from the EUMETSAT Unified Meteorological Archive and Retrieval Facility (UMARF) will be available on request. Archived products from the EUMETSAT Unified Meteorological Archive and Retrieval Facility (UMARF) will be available on request.

References

GOME-2 Products Guide, EUM.OPS-EPS.MAN.05.0005, available online at http://www.eumetsat.int/idcplg?IdcService=SS_GET_PAGE&nodeId=550&l=en

The EUMETSAT webpage www.eumetsat.int is the primary source of documentation, tools and status information on EPS/MetOp. In particular see http://www.eumetsat.int/idcplg?IdcService=SS_GET_PAGE&nodeId=447&l=en for information on MetOp and NOAA services.

IASI / MetOp

Contributed by **Cathy Clerbaux** (ccl@aero.jussieu.fr), *Service d'Aéronomie, IPSL, Universite Pierre et Marie Curie, Boîte 102, 4, Place Jussieu, 75252 Paris CEDEX 05, France,* **Claude Camy-Peyret** (camy@ccr.jussieu.fr), *LPMAA, Université Pierre et Marie Curie, Case 76, 4, Place Jussieu, F-75252 Paris CEDEX 05, France,* **Peter Schluessel** (peter.schluessel@eumetsat.int), *Am Kavalleriesand 31 - 64295 Darmstadt, Germany, and* **Thierry Phulpin** (Thierry.phulpin@cnes.fr), *Centre National d'Etudes Spatiales 18, av Edouard Belin, 31400 Toulouse, France.*

IASI, the Infrared Atmospheric Sounding Interferometer, is a new tropospheric remote sensing instrument that will be carried for a period of 14 years on the MetOp-A, B, and C weather satellites deployed as part of the EUMETSAT Polar System. The first METOP was successfully launched on October 19, 2006. IASI is a joint undertaking of the French space agency CNES (Centre National d'Etudes Spatiales) and EUMETSAT, the European Organisation for the Exploitation of Meteorological Satellites, with CNES managing the instrumental development and EUMETSAT operating the instrument in orbit.

Scientific Questions

The IASI mission will provide improved infrared sounding capabilities for the temperature profiles in the troposphere and lower stratosphere, moisture profiles in the troposphere, as well as measuring some of the chemical components that play a key role in climate issues, global change and atmospheric chemistry (CO_2, CH_4, N_2O, CO, O_3, HNO_3).

Instrument Description

The instrument consists of a Fourier transform spectrometer associated with an imaging system, designed to measure the infrared spectrum emitted by the Earth in the thermal infrared using a nadir geometry. The instrument is providing spectra of high radiometric quality at 0.5 cm^{-1} resolution (apodised), from 645 to 2760 cm^{-1}.

The MetOp polar orbit (at ~800 km) is slightly slanted at a 98.7° inclination to the equator, and the Earth will pass beneath the satellite ground track at 09:30 in the morning. The time to complete an orbit is about 101 minutes, which implies that MetOp will make a little more than 14 revolutions a day.

The IASI instrument field of view is sampled by a matrix of 2 × 2 circular pixels of 12 km diameter each (see Fig. 26). Measurements will be taken every 50 km at nadir, with broad horizontal coverage due to its ability to scan across track with a swath width of ± 1100 km.

Retrieval Description

The number of geophysical parameters retrieved from the measurements depends on cloud conditions, which also determine the set-up of the retrieval scheme.

The first retrieval uses statistical methods, based on a linear EOF (Empirical Orthogonal Function) regression

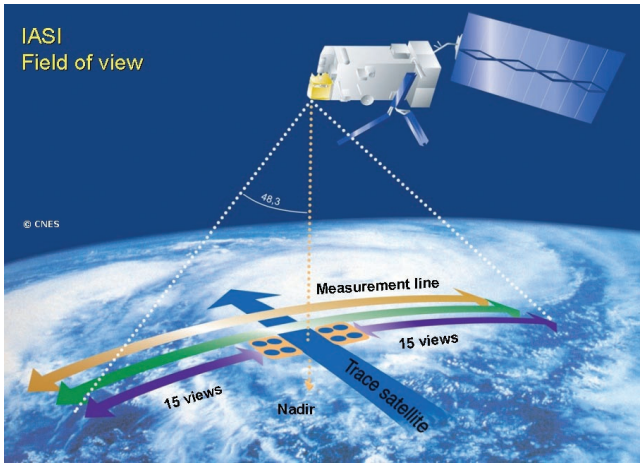

Figure 26. The IASI system will measure the spectrum of infrared radiation emitted by the Earth from a low altitude sun-synchronous orbit, with a swath width of 2200 km and a horizontal resolution of 50 × 50 km, so that the global atmosphere is observed twice per day.

Table 18. Overview of IASI tropospheric chemistry data products.

Retrieved quantity	Horizontal resolution (km)	Vertical resolution (km)	Typical accuracy[a]	Reference(s) of retrieval algorithm
Temperature	12 for 1 pixel 50 for 4 pixels	1 km (tropo)	1K	*Operational product* [1] Schluessel et al., 2005
Water vapour	12 for 1 pixel 50 for 4 pixels	1-2 km (tropo)	10%	*Operational product* [1] Schluessel et al., 2005
Ozone	12 for 1 pixel 50 for 4 pixels	Total column 0-6 ;0-12 ;0-16	2% 30%, 15%, 9%	*Operational product* [2] Turquety et al, 2004
CO	12 for 1 pixel 50 for 4 pixels	Total column[b]	5-10%	*Operational product* [2] Turquety et al, 2004
CH_4	12 for 1 pixel 50 for 4 pixels	Total column[b]	3%	*Operational product* [2] Turquety et al, 2004
N_2O	12 for 1 pixel 50 for 4 pixels	Total column	5%	*Operational product* [3] Lubrano et al., 2004
HNO_3	12 for 1 pixel 50 for 4 pixels	Total column[b]	NA	*Research product* [7] Wespes et al., 2007
CO_2	500[c]	Total column	1%[c]	*Research product* [4] Chedin et al., 2003
CFC-11, CFC-12	200	Total column	NA	*Research product* [5] Coheur et al., 2003

[a] The accuracy are provided for a 50 km horizontal resolution (averaged of 4 pixels) and for cloud-free conditions

[b] Coarse profiles will be tentatively retrieved (research products) [c] For 500 km × 500 km and 15 days in time

or a nonlinear artificial neural network (ANN) [1]. For temperature and water vapour profiles, ozone columns of tropospheric layers, surface temperature, and surface emissivity, the entire IASI spectrum is used to calculate principal component scores, which enter the linear regression retrieval.

Likewise, the principal component scores can be entered into a feed-forward ANN to retrieve temperature and water-vapour profiles. Up to 500 principal component scores are used in the regression or the ANN retrievals. The retrieval of trace-gas columns is done using an ANN with a set of selected IASI radiances [2], sensitive to the particular trace gases, together with the previously derived temperature profile. The selection between linear regression and ANN, the number of principal component scores, as well as all weights and regression coefficients are configurable.

The results from the first retrieval may constitute the final product or may serve as input to the final, iterative retrieval; the choice depends on the configuration setting and on quality of the first retrieval results. The final retrieval is a simultaneous iterative retrieval, seeking the maximum aposteriori probability solution for the minimisation of a cost function using the Levenberg–Marquardt method. The cost function aims at minimising the difference between measured and simulated radiance vectors, subject to a constraint given either by climatology, the ATOVS Level 2 product, or NWP (numerical weather

Scientific Highlight

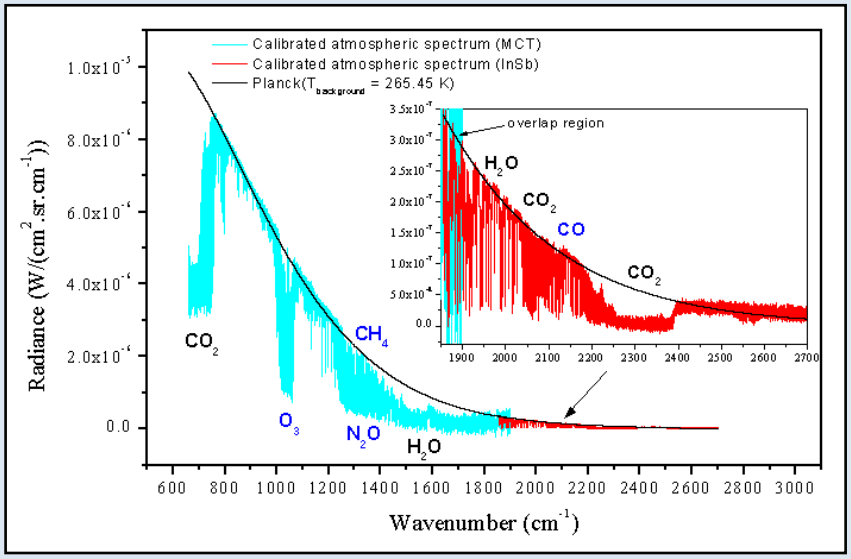

Figure 27. Spectra recorded during an IASI-balloon flight (above Sweden in March 2001) to measure the O_3 profile as well as CH_4, N_2O and CO total columns [6]. These data are obtained by combining the radiances recorded by two detectors (MCT and InSb).

prediction) forecast.

Several scientific groups will be involved in the validation of IASI products by comparison with correlative measurements from ground based, aircraft or balloon instruments (see Fig. 27 as an example).

Data accessibility

More information can be found at:

http://smsc.cnes.fr/IASI/index.htm

http://www.eumetsat.int/

The IASI Science Plan can be found at:

http://smsc.cnes.fr/IASI/IASI_Science_Plan_Issue1_released_version.pdf

Acknowledgments

The work relative to trace gas retrieval is undertaken in the framework of the ISSWG (IASI Sounding Science Working Group) activities under the auspices of EUMETSAT and CNES.

References

[1] Schlüssel, P., T. H. Hultberg, P. L. Phillips, T. August, X. Calbet, 2005,The operational IASI Level 2 processor, *Adv. Space Res., 36,* 982-988.

[2] Turquety, S., J. Hadji-Lazaro, C. Clerbaux, D. A. Hauglustaine, S. A. Clough, V. Cassé, P. Schlüssel and G. Mégie, 2004, Operational trace gas retrieval algorithm for the Infrared Atmospheric Sounding Interferometer, *J. Geophys. Res., 109,* D21301, doi:10.1029/2004JD004821.

[3] Lubrano, M., G. Masiello, M. Matricardi, C;Serio and V. Cuomo, 2004, Retrieving N_2O from nadir-viewing infrared spectrometers, *Tellus, 56B,* 249-261.

[4] Chedin, A., R. Saunders, A. Hollingsworth, N. Scott, M. Matricardi, J. Etcheto, C. Clerbaux, R. Armante and C. Crevoisier, 2004, The feasibility of monitoring CO_2 from high-resolution infrared sounders, *J. Geophys. Res., 108* (D2), doi:10.1029/2001JD001443.

[5] Coheur, P.-F., C. Clerbaux and R. Colin, 2003, Spectroscopic measurements of halocarbons and hydrohalocarbons by satellite-borne remote sensors, *J. Geophys. Res, 108* (D4), doi:10.1029/2002JD002649.

[6] Y. Té, P. Jeseck, C. Camy-Peyret, S. Payan, G. Perron and G. Aubertin, 2002, Balloon borne calibrated spectrometer for atmospheric nadir sounding, *Appl. Optics, 41,* 6431 6441.

[7] Wespes, C., D. Hurtmans, H. Herbin, B. Barret, S. Turquety, J. Hadji Lazaro, C. Clerbaux and P.-F. Coheur, 2007, Satellite measurements of nitric acid global distributions in the troposphere and the stratosphere, *J. Geophys. Res.,* in press.

OCO / OCO

Contributed by **David Crisp** (David.Crisp@jpl.nasa.gov)*, Jet Propulsion Laboratory, M/S 183-501, 4800 Oak Grove Drive, Pasadena, CA 91109 USA*

The Orbiting Carbon Observatory (OCO) mission is currently scheduled for launch from Vandenberg Air Force Base in California in late 2008. During its 2-year nominal mission, OCO will fly in the Earth Observing System (EOS) Afternoon Constellation (A-Train). OCO will fly 4 minutes ahead of the EOS Aqua platform sharing the same ground track. This 705 km altitude, circular, sun-synchronous orbit has a 1:26 PM equator crossing time and provides near global coverage with a 16-day global repeat cycle.

Scientific Questions

The primary goal of OCO is to retrieve accurate, high-resolution estimates of the column-averaged CO_2 dry air mole fraction over the globe. Secondary products will include surface pressure, surface-weighted estimates of the column-averaged water vapor and atmospheric temperature, and the vertical distribution and optical depth of optically-thin clouds and aerosols.

Carbon dioxide (CO_2) is the principle man-made greenhouse gas. Comparisons of precise, ground-based CO_2measurements with CO_2 emission rates from fossil fuel combustion and other human activities indicate that only about half of the carbon dioxide (CO_2) that has been emitted into the atmosphere over the past 40 years has remained there; the rest has apparently been absorbed by the land biosphere or oceans. Measurements also indicate that the atmospheric CO_2 buildup varies dramatically from year to year in response to smoothly increasing emission rates. While the exiting ground based network provides precise global constraints on the CO_2 buildup, it does not have the spatial resolution and coverage needed to identify the nature or geographic distribution of the natural sinks responsible for absorbing this CO_2 or the processes that control their efficiency from year to year.

NASA's Orbiting Carbon Observatory (OCO) is an Earth System Science Pathfinder (ESSP) mission that is currently under development to address this problem. OCO will make space-based measurements of atmospheric carbon dioxide (CO_2) with the precision, resolution, and coverage needed to characterize the geographic distribution of CO_2 sources and sinks and quantify their variability over the seasonal cycle. These measurements will improve our understanding of the nature and processes that regulate atmospheric CO_2 enabling more reliable forecasts of CO_2 buildup and its impact on climate change.

Instrument Description

OCO carries a single instrument that incorporates three high resolution grating spectrometers designed to measure the absorption of reflected sunlight by CO_2 and molecular oxygen (O_2) bands at near-infrared wavelengths. Spatially resolved high resolution ($\lambda/\Delta\lambda$~21,000) spectra collected in the CO_2 bands near 1.61 and 2.06 μm provide surface-weighted estimates of the CO_2 column abundance. Bore-sighted high resolution ($\lambda/\Delta\lambda$~18,000) spectra in the 0.76

Table 19. Overview of OCO tropospheric chemistry data products.

Retrieved quantity	Horizontal resolution (km)	Vertical resolution	Typical accuracy	Typical precision	Reference(s) of retrieval algorithm	Validation reference(s)
X_{CO2}	3-10 square km	Total-column	<2%/sounding <0.3% on regional scales	0.3%	[3] Kuang et al. 2002. [1] Boesch et al. 2006	[4] Crisp et al. 2004. [5] Washenfelder et al. 2006.

μm O_2 A-band provide precise estimates of surface pressure as well as constraints on clouds, aerosols, and the surface. The CO_2 and O_2 soundings are analyzed to yield estimates of the column-averaged CO_2dry air mole fraction, X_{CO2}. A sampling rate of 12 to 24 soundings/second yields a small surface footprint (<3 km^2 at nadir) that helps to minimize biases associated with spatial variations in clouds and surface topography and provides thousands of soundings on regional scales each month. A comprehensive ground-based validation system is used to assess random errors and minimize biases in the X_{CO2} product to ensure precisions of 0.3 to 0.5% (1 to 2 ppm) on regional scales (1000 km by 1000 km) at monthly intervals.

OCO will collect science observations in Nadir, Glint, and Target modes. Nadir soundings provide the highest spatial resolution and are expected to return more useable soundings in regions that are partially cloudy or have significant surface topography. In Glint mode, the spacecraft will point the instrument toward the bright "glint" spot, where sunlight is specularly reflected from the surface. Glint measurements are expected to provide much higher signal to noise ratios over the ocean and other dark surfaces. OCO will switch from Nadir to Glint modes on alternate 16-day global ground track repeat cycles so that the entire Earth is mapped in both modes on roughly monthly time scales. Finally, Target mode will be used to observe specific stationary surface targets as the satellite flies overhead. Target passes will be conducted over one OCO calibration site each day, on average.

Retrieval Description

The raw radiance spectra (Level 0) collected by OCO will first be processed to yield radiometrically calibrated, geolocated spectral radiances within the O_2 and CO_2 bands (Level 1). The bore-sighted spectra for each coincident CO_2 / O_2 sounding will then be processed to estimate the column averaged CO_2 dry air mole fraction, X_{CO2} (Level 2). Other Level 2 data products to be retrieved from each sounding include the surface pressure, surface-weighted estimates of the column-averaged water vapor and atmospheric temperature, and the vertical distribution and optical depth of optically-thin clouds and aerosols. These quantities will be compared to results retrieved over the ground based validation sites to yield regional-scale constraints on the space-based X_{CO2} product over the sunlit hemisphere on monthly intervals.

The OCO retrieval algorithm incorporates a forward model for generating atmospheric radiance spectra, an instrument model that simulates the instrument response, and an inverse model for refining the atmospheric state vector. The forward model is based on a spectrum-resolving (line-by-line) multiple scattering model designed to generate high resolution synthetic spectra in scattering and absorbing atmospheres (c.f. Boesch 2006; [1]). The instrument model simulates the wavelength-dependent radiometric performance, the spectral dispersion, instrument line shape, scattered light, and other instrument properties that affect the measured spectra. The inverse model uses optimal estimation theory [2] to simultaneously retrieve CO_2 and O_2 columns as well as other state properties to produce an improved fit to the observed spectra [1, 3].

A comprehensive ground-based validation system will be used to assess random errors and regional scale biases in the space-based X_{CO2} product [4]. The NOAA CMDL CO_2 data serves as the standard. This standard is based on in situ measurements of the CO_2 from flasks, tall towers, and aircraft. To link these point measurements to the space based measurements of the CO_2 column, the OCO validation program will use independently calibrated column data from ground-based, solar-looking, Fourier Transform Spectrometers (FTS's) that observe CO_2 and O_2 in the same spectral bands used by OCO. A series of these systems are currently being installed as part of the Total Column Carbon Network (TCCN). The OCO Project is contributing to this network by installing two new FTS's at the Department of Energy Atmospheric Radiation Monitoring (ARM) sites near Darwin Australia and in Oklahoma, and upgrading at least 4 existing FTS facilities from the Network for Detection of Stratospheric Change (NDSC).

No measurements from other satellites are needed to process the OCO measurements. However, spatially coincident measurements of

Figure 28. Illustration of the OCO spacecraft over the Earth.

water vapor and atmospheric temperature could simplify the X_{CO2} retrieval process and facilitate the validation of the OCO products. Similarly, near-simultaneous measurements of clouds and aerosol profile by CloudSat and CALYPSO would also be of use in the X_{CO2} retrieval process, if they are available.

Data accessibility

Six months after the start of routine science operations, Level 0 and Level 1 data products will start to be delivered to the NASA Distributed Active Archive Center (DAAC) within 6 months of acquisition by the ground station, and will be accessible to the science community. Beginning 9 months after the start of routine science operations, an exploratory Level 2 data product will be delivered to the NASA DAAC. Higher level products, including gridded maps of CO_2 sources and sinks will be delivered to the DAAC as they are developed and validated. In addition, the OCO mission was recently selected as a Third Party Mission by the European Space Agency (ESA). All OCO data products deposited in the NASA DAAC will immediately be mirrored by ESA to facilitate access by the European science community.

References

[1] Boesch, H., G. C. Toon, B. Sen, R. Washenfelder, P. O. Wennberg, M. Buchwitz, R. de Beek, J. P. Burrows, D. Crisp, M. Christi, B. Connor, V. Natraj, and Y. Yung, 2007, Space-based Near-infrared CO_2 Retrievals: Testing the OCO Retrieval and Validation Concept Using SCIAMACHY, Measurements over Park Falls, Wisconsin, *J. Geophys. Res., 111,* D23302, doi:10.1029/2006JD007080.

[2] Rodgers, C. D., 2000, Inverse methods for atmospheric sounding: theory and practice, World Science Publishing, Singapore.

[3] Kuang, Z.M., J. Margolis, G. Toon, D. Crisp, Y. Yung, Spaceborne measurements of atmospheric CO_2 by high-resolution NIR spectrometry of reflected sunlight, *Geophys. Res. Lett., 29* (15), art. no. 1716.

[4] Crisp, D., R. M. Atlas, F.-M. Breon, L. R. Brown, J. P. Burrows, P. Ciais, B. J. Connor, S. C. Doney, I. Y. Fung, D. J. Jacob, C. E. Miller, D. O'Brien, S. Pawson, J. T. Randerson, P. Rayner, R. J. Salawitch, S. P. Sander, B. Sen, G. L. Stephens, P. P. Tans, G. C. Toon, P. O. Wennberg, S. C. Wofsy, Y. L. Yung, Z. Kuang, B. Chudasama, G. Sprague, B. Weiss, R. Pollock, D. Kenyon, S. Schroll, 2004, The Orbiting Carbon Observatory (OCO) Mission, *Adv. Space. Res., 34* (4), 700-709.

[5] Washenfelder, R.A., G.C. Toon, J.F. Blavier, Z. Yang, N.T. Allen, P.O. Wennberg, S.A. Vay, D.M. Matross, and B.C. Daube, 2006, Carbon dioxide column abundances at the Wisconsin Tall Tower site, *J. Geophys. Res., 111,* D22305, doi:10.1029/2006JD007154.

Announcements

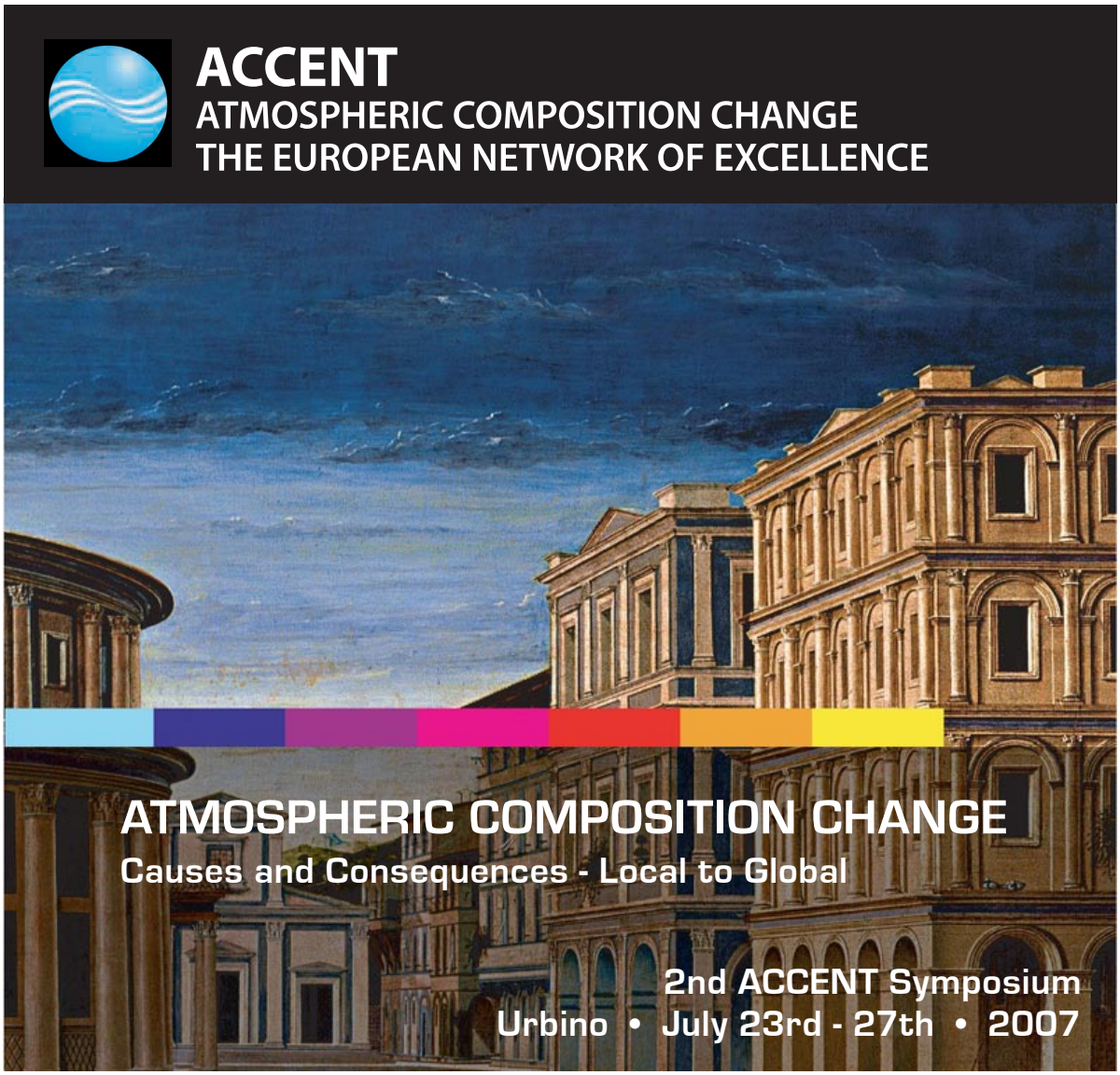

The beautiful Renaissance town of Urbino, declared a world heritage site by UNESCO in 1998, has the privilege to host the Second International Symposium of ACCENT, the European Network of Excellence in Atmospheric Composition Change, which will be held from July 23 -27, 2007.
The primary focus of the conference will be on the relevance of atmospheric composition change and on societal issues as climate change, ecosystems, air quality, and human health. Further topics that will be discussed include: measuring atmospheric composition change, training and education, and synthesis of scientific results for policy makers and the general public.

For more information, please visit:
www.accent-network.org/2nd-symposium/

Please help us keep our mailing list up to date by sending your revised contact information:

IGAC Core Project Office
NOAA-PMEL
7600 Sand Point Way
Seattle, WA 98115-6349 USA

email: igac.seattle@noaa.gov

IGACtivities Newsletter

Editor: Sarah Doherty
Production manager: Ho Ching Lee
Newsletter formatting: Beth Tully
IGAC logo: Linda Kubrick

Published by IGAC Core Project Office
RESEARCH CENTER FOR ENVIRONMENTAL CHANGE
ACADEMIA SINICA
128 Academia Rd. Sec. 2
P.O. Box 1-55 NanKang
Taipei, 11529 Taiwan

中華郵政台北誌字第 137 號執照登記為雜誌交寄
發行人：劉紹臣
發行所：中央研究院環境變遷研究中心
發行地址：台北市 115 南港區研究院路二段 128 號 1-55 號信箱

IGAC was initiated by the Commission on Atmospheric Chemistry and Global Pollution (CACGP) and is a Core Project of the International Geosphere-Biosphere Programme (IGBP). The IGAC Seattle Core Project Office is currently supported by the National Science Foundation (NSF), National Aeronautics and Space Administration (NASA), and National Oceanic and Atmospheric Administration (NOAA). The IGAC Taipei Core Project Office is funded by Academia Sinica, Taipei. The Rome Core Project Office is supported by the Italian National Research Council and by the European Commission Network of Excellence ACCENT. Any opinions, findings and conclusions, or recommendations expressed in this newsletter are those of the individual author(s) and do not necessarily reflect the views of the responsible funding agencies.

IGACtivities Newsletter

Taipei TAIWAN
R.O.C.
POSTAGE PAID
NEWSLETTER
LICENCE NO.N285

國內
郵資已付
台北郵局許可證
台北字第 285 號

IGAC Core Project Office
RESEARCH CENTER FOR ENVIRONMENTAL CHANGE
ACADEMIA SINICA
128 Academia Rd. Sect. 2
P.O. Box 1-55 NanKang
Taipei, 11529 Taiwan

Printed on Recycled Paper
Please Recycle after Use!